INFORMATION TO USERS

This manuscript has been reproduced from the microfilm master. UMI films the text directly from the original or copy submitted. Thus, some thesis and dissertation copies are in typewriter face, while others may be from any type of computer printer.

The quality of this reproduction is dependent upon the quality of the copy submitted. Broken or indistinct print, colored or poor quality illustrations and photographs, print bleedthrough, substandard margins, and improper alignment can adversely affect reproduction.

In the unlikely event that the author did not send UMI a complete manuscript and there are missing pages, these will be noted. Also, if unauthorized copyright material had to be removed, a note will indicate the deletion.

Oversize materials (e.g., maps, drawings, charts) are reproduced by sectioning the original, beginning at the upper left-hand corner and continuing from left to right in equal sections with small overlaps.

Photographs included in the original manuscript have been reproduced xerographically in this copy. Higher quality 6" x 9" black and white photographic prints are available for any photographs or illustrations appearing in this copy for an additional charge. Contact UMI directly to order.

Bell & Howell Information and Learning
300 North Zeeb Road, Ann Arbor, MI 48106-1346 USA

UMI®
800-521-0600

MOLECULAR ANALYSIS OF HTLV-I TAX INTERACTIONS WITH THE NF-κB AND IκBα TRANSCRIPTION FACTORS

by

LOUISA PETROPOULOS

A Thesis submitted to the Faculty of Graduate Studies and Research in partial fulfillment of the requirements for the degree of
Doctor of Philosophy

Department of Microbiology and Immunology
McGill University, Montreal
June 1998

Ευχαριστω την μανα μου και την αδελφη μου Σωτηρια
Με πολυ αγαπη,
Λουιζα

ABSTRACT

The human T cell leukemia virus type I (HTLV-I), the etiological agent of adult T cell leukemia is the first human retrovirus linked to malignancy. The viral protein Tax, is essential for HTLV-I gene transactivation and responsible for oncogenic transformation. Tax is capable of indirectly transactivating numerous growth regulatory genes through interactions with host transcription factors. One of the targets of the Tax protein is the NF-κB/IκB family of transcriptional regulators. In HTLV-I Tax expressing cells, the maintenance of NF-κB activity is essential for cellular transformation. Previous studies demonstrated that Tax activated NF-κB through binding to the Rel homology domain of NF-κB. The objective of this work was to elucidate the mechanism by which Tax transactivates NF-κB. We addressed the specificity and function of Tax interaction with members of the NF-κB/IκBα family and demonstrated that: 1) Tax increased IκBα degradation, resulting in the induction of NF-κB DNA binding activity; 2) Tax enhanced NF-κB binding to DNA 40 to 100 fold by increasing NF-κB dimer formation which was detected in the absence of DNA; 3) Tax interacted with all NF-κB DNA binding subunits and with IκBα *in vitro* ; 4) Tax physically associated with IκBα *in vivo;* and 5) Tax and IκBα had antagonistic effects on NF-κB binding and gene activity. These results suggested that Tax interaction with IκBα interferes with the formation of NF-κB-IκBα complexes and may play a role in targeting IκBα for degradation. To further characterize the interactions between Tax and IκB, co-immunoprecipitation experiments were performed that identified a complex in HTLV-I infected cells comprising Tax-IκBα and the HsN3 subunit of the 26S proteasome. Metabolic labeling and protein turnover studies indicate that Tax targets IκBα to the proteasome for degradation in a stimulus independent manner. The Tax-IκBα-proteasome interaction may play a small but significant role in the constitutive turnover of IκBα and NF-κB constitutive activity.

Résumé

Le virus HTLV-I (Human T-cell Leukemia Virus type I) est l'agent éthiologique de l'ATL (Adult T cell leukemia) et représente le premier rétrovirus qui a été identifié comme induisant des tumeurs chez l'homme. La protéine virale Tax est indispensable à la transactivation des gènes de HTLV-I et est responsable de la transformation oncogénique des cellules. Tax est capable de transactiver de manière indirecte, par interaction avec des protéines de la cellule hôte, de nombreux gènes impliqués dans la prolifération cellulaire. La famille de protéines régulatrices de la transcription NF-κB/IκB est une des cibles de Tax. Dans les cellules exprimant Tax, le maintien du taux des protéines NF-κB est requis pour la transformation des cellules. Des études antérieures ont démontré que Tax active NF-κB en se fixant à son domaine d'homologie Rel. Le but de ce travail a été de tenter d'élucider le mécanisme par lequel Tax transactive NF-κB. Nous avons déterminé la spécificité et la fonction de l'interaction entre Tax et les membres de la famille NF-κB/IκBα et nous avons pu démontrer que : 1) Tax induit la dégradation de IκBα, ce qui conduit a l'induction de la fixation de NF-κB à l'ADN ; 2) Tax augmente le taux de fixation de NF-κB à l'ADN de 40 à 100 fois en induisant la formation de dimères NF-κB, détectée en absence d'ADN ; 3) Tax est capable d'interagir avec toutes les sous-unités de NF-κB qui se lient à l'ADN ainsi qu'avec IκBα *in vitro* ; 4) Tax s'associe physiquement à IκBα *in vivo* ; 5) Tax et IκB ont des effets antagonistes sur la fixation de NF-κB à l'ADN et l'activation des gènes. Ces résultats suggèrent que l'interaction entre Tax et IκBα interfère avec la formation des complexes NF-κB/IκBα et Tax pourrait diriger IκBα vers la dégradation. Afin de poursuivre la caractérisation des interactions entre Tax et IκBα, nous avons effectué des expériences de co-immunoprécipitation qui nous ont permis d'indentifier un complexe comprenant Tax-IκBα ainsi que la sous-unité HsN3 du proteasome 26S. Des études de marquage métabolique ont démontré que Tax dirige IκBα vers le protéasome pour etre dégradé et ceçi en reponse à une stimulation. L'interaction entre Tax, IκBα et le protéasome pourrait jouer un rôle mineur mais significatif dans le temps de demi-vie de IκBα et l'activité constitutive de NF-κB.

Acknowledgments

I would like to express my gratitute to my supervisor Dr. John Hiscott for allowing me to work in his lab and for his support during the course of my Ph.D studies.

I would like to thank Dr. Rongtuan Lin who is not only a brilliant scientist but also a wonderful mentor, guide and friend. It has been a great pleasure to work in the company of Dr. Lin whose unmatched scientific mind, abilities and love for his work has served as my inspiration to keep on going.

I would like to thank Hannah Nguyen for riding the peaks and valleys with me. Thanks a million for all your "Ben non" and trying to keep me grounded. Your friendship and support over the years has meant a lot to me. One thing I have finally figured out is : $A\infty = \emptyset$. Miss ya Nut!

I would also like to thank Carm DeLuca for making my time in the lab fun. I must say thanks for all the times you looked out for me when getting in and out of trouble. Think the coast is clear? In your dreams B^3!

I am grateful for Michele Algarte for the french translation of the abstract.

Finally, I would like to thank all of the people in the lab, past and present, who have made it a fun place to be.

Preface

In accordance with the Guidelines for Thesis Preparation, the candidate has chosen to present the results of the thesis in the classical form. A general introduction is presented in chapter 1 and appears in part in the following review article:

1. Hiscott J., **Petropoulos L.** and Lacoste J. Molecular Intractions between HTLV-I Tax protein and the NF-κB/IκB transcription complex. *Virology*. **214** (1995) 3-11.

The materials and methods used in this thesis are presented in chapter 2. The results are described in chapters 3 to 6 and appear in part in the following articles, in the same order:

2. Lacoste J., **Petropoulos L.**, Pepin N., Hiscott J. Constitutive phosphorylation and turnover of IκBα in HTLV-1 infected and Tax expressing T cells. *J. Virology*. **69** (1995) 564-569.

3. **Petropoulos L.**, Lin R. and Hiscott J. Human T Cell Leukemia Virus Type I Tax protein increases NF-κB dimer formation and antagonizes the inhibitory activity of the IκBα regulatory protein. *Virology*. **225** (1996) 52-64.

4. **Petropoulos L.** and Hiscott J. Differential interactions between HTLV-I Tax protein IκBα is dependent on phosphorylation state. *Virology*. (in press).

The work presented in chapter 3 was shared by the other co-authors. Figures 12 and 13 were done by Normand Pepin and Judith Lacoste.

Table of Contents

List of Figures and Tables

List of Figures Page

List of Tables

List of Abbreviations

aa	amino acid
AD-I	Acidic Domain I
AD-II	Acidic Domain II
ANK	ankyrin repeats
ATL	Adult T cell Leukemia
AZT	zidovudine
bZIP	basic domain of the leucine zipper motif
CAT	chloramphenicol acetyltransferase
CBP	CREB Binding Protein
CNS	central nervous system
CRE	CREB Responsive Element
CREB	cAMP Responsive Element Binding protein
DBD	DNA binding domain
DIM	dimerization region
EMSA	electrophoretic mobility shift assay
HAM	HTLV-I Associated Myelopathy
HLA	human leukocyte antigen
HTLV-I	human T cell leukemia virus type I
ICSAT	interferon consensus sequence binding protein in adult T cell leukemia or activated T cells
IKK	IκBα kinase complex
IL-2	Interleukin 2
IFNα	Interferon alpha
IRF	Interferon Regulatory Factor
LPS	lipopolysaccharide
LTR	Long Terminal Repeat
MHC I	Major Histocompatability Complex type I
MEKK	Mek kinase 1
NAC	N-Acetylcysteine
NF-κB	Nuclear Factor of the kappa light chain in B cells
NLS	nuclear localization signal
PDTC	pyrrolidinedithiocarbamate
PEST	Pro, Glu/Asp, Ser, and Thr
PMA	phorbol 12-myristate 13-acetate
PMSF	phenylmethylsulfonyl fluoride
RHD	Rel homology domain
SRD	signal response domain
SRF	serum response factor
TNFα	tumor necrosis factor alpha
TSP	Tropical Spastic Paraparesis

CHAPTER 1

GENERAL INTRODUCTION

The human T cell leukemia virus type I (HTLV-I) has the dubious honor of being the first human oncoretrovirus to be discovered in 1980 by Robert Gallo (145). HTLV-I was isolated from cell cultures obtained from an Afro-American patient with a lymphoproliferative disease originally considered a cutaneous T cell lymphoma and later characterized as adult T cell leukemia/lymphoma (ATL) (145). Interestingly, another disease with a very different pathophysiology from ATL was soon linked to HTLV-I as the causative agent. This neurodegenerative HTLV-I associated myelopathy (HAM) and tropical spastic paraparesis (TSP) (57,137,138).

1. Adult T cell leukemogenesis

Endemic in southwestern Japan, the West Indies, Central Africa, the Caribbean basin and southeastern USA, ATL is an aggressive and fatal leukemia/lymphoma of mature $CD4^+$ T helper lymphocytes. In Jamaica, 67% of all T cell lymphoma incidents are ATL, representing the majority of non-Hodgkin lymphomas (72). The lifetime risk of developing ATL in individuals infected with HTLV-I is low, at 1-5% and with a mean age of 43 years. The majority of HTLV-I infected individuals are asymptomatic carriers (66,162,184). In these individuals, polyclonaly integrated viral sequences are detected (86,196). Of individuals that do develop ATL, the disease state is classified into 4 subgroups, acute, chronic, lymphoma and smoldering. The acute type ATL is the predominant clinical subtype, followed by lymphoma, chronic and smoldering subtypes (86,162,184). One study found the median survival of all ATL subtypes to be 20 weeks; for acute type, 13 weeks; lymphoma type, 20 weeks; and the chronic type, 25 weeks (162,184). Individuals with chronic/smoldering ATL feature normal white cell counts, prominent skin lesions (resulting from cutaneous infiltration by malignant lymphocytes) and modest bone marrow and visceral involvement (162,184). Chronic/smoldering ATL is a less aggressive form of ATL that eventually progresses to acute ATL, a highly aggressive disease with a very poor prognosis. This stage is

characterized by elevated white blood cell counts, presence of morphologically abnormal lymphocytes, hypercalcemia, skin lesions as well as important visceropathy (162,184). Leukemic cells are represented by one dominant clone, carrying a single rearrangement of the T-cell antigen receptor β gene (131). Monoclonal or oligoclonal patterns of proviral insertion are detected in leukemic cells derived from patients with chronic/smoldering or acute ATL (86,162,196).

Although HTLV-I preferentially targets and transforms $CD4^+$ T cells, it also infects many other cell types *in vivo* and *in vitro*, including T cells, B cells and monocytes (136). Typical ATL display chromosomal breaks and karyotypic abnormalities that are often indicative of the degree of disease severity (86,155,196). Another characteristic feature of ATL leukemic cells is elevated expression of the interleukin 2 receptor (IL-2R) (82,116,196). Tumor cell growth however, does not require expression of IL-2R (196).

There is limited HTLV-I gene expression in ATL patients (92,153), and since the proviral genome is often deleted (153), it appears that continued viral expression is not required for maintenance of the transformed phenotype. The resulting low virus titers in infected individuals explains why transmission of HTLV-I is possible only through the transfer of living infected cells, via milk, blood and sexual contact (31,78,127,197).

2. HTLV-I Associated Myelopathy/ Tropical Spastic Paraparesis (HAM/TSP)

HTLV-I has been associated with a number of other pathologies, including tropical spastic paraparesis/HTLV-I-associated myelopathy (TSP/HAM). As with ATL, the geographical distribution of TSP/HAM is the same as that of HTLV-I. TSP/HAM is a chronic neurodegenerative syndrome and affected individuals suffer progressive

demyelination of motor neurons of the spinal cord, leading to myelopathy (58,137). Multiple sclerosis, a similar but more severe pathology and Polymyositis, an inflammatory muscle disorder, have also been associated with HTLV-I infection (83,105,124).

3. The HTLV-I Retrovirus

HTLV-I linked diseases are associated with very high viral loads. As much as 20% of peripheral blood mononuclear (PBMC) cells can be infected (147). Remarkably, unlike the human immunodeficiency virus (HIV) the HTLV retroviruses are genetically very stable. Genetic analysis of HTLV-I virus isolates from ATL patients and TSP/HAM patients reveals that even geographically widely dispersed viruses are less than 10% divergent at the nucleic acid level (45,143). HTLV-I is responsible for ATL and TSP/HAM, yet patients are found to develop either ATL or TSP/HAM and sometimes both. What factor(s) determines the direction of pathogenesis?

HTLV-I genetic variations alone cannot account for disease progression. Rather, it now appears that the genetic makeup of the individual plays and important role in the susceptibility to HTLV-I disease. Immunological studies point to a correlation between immune responsiveness and pathogenesis (45,187). Individuals who develop TSP/HAM have a high occurrence of HLA haplotypes Cw7, B7 and DR1 (45,187). Conversely, individuals who develop ATL or were asymptomatic carriers, were HLA-A26, B61 and DR69. How does the HLA of an individual contribute to the disease state?

Interestingly, particular HLA haplotypes have been associated with a strong immunogenic response against HTLV-I. HTLV-I infected T cells express a variety of

T cell epitopes that are recognized in the context of class I and class II HLA antigens (184).

Peripheral blood lymphocytes from asymptomatic HTLV-I carriers of different HLA haplotypes when incubated with HTLV-I viral antigens, two categories of T cell proliferative responses were found, high T cell proliferative responders and low T cell proliferative responders. The T cells that produced a strong proliferative response in the presence of HTLV-I antigens were of the haplotypes HLA-DRB1, DQB1, 0101, 0501,1502-0601 (187). The low responders were DRB1, DQB1, 1501-0602 and 0901-0303 (45,187). Thus, the immune response mounted against HTLV-I viral antigens depends on the genetic predisposition of the individual. Individuals with the HLA haplotypes that result in a high immune response are predisposed to develop TSP/HAM, while those resulting in a low T cell response remain asymptotic or develop ATL.

Most of the epitopes are represented by HTLV-I viral antigens but some are autoantigens induced by HTLV-I e.g. gp34, CNS antigen and antigens of unknown specificity (165). All of these are strongly recognized by autologous T cells to induce polyclonal proliferative responses of T cells and cytotoxic T cells (166). To explain how a strong immune response would result in the development of TSP/HAM, various models have been proposed. The direct infection model proposes that HTLV-I infected $CD4^+$ T cells and CNS cells express viral antigens that activate a cytotoxic immune response, destroying infected cells. In the case of TSP/HAM, myelopathy is the result of the destruction of neuronal cells. The autoimmune model suggests that HTLV-I activates autoreactive T lymphocytes, allowing them to migrate to the CNS, where they recognize their target antigens presented on the CNS constituent cells. HTLV-I infected patients have been found to display other autoimmune-like diseases, supporting this concept. In the bystander damage mechanism, infected $CD4^+$ T cells

enter the CNS (165). Specific antigen recognition by the infected cells induces their proliferation, expanding the pool of cells presenting antigen. The continuous stimulation and proliferation of immunocompetent cells leads to inflammation resulting in tissue damage (165). Thus, since HTLV-I has a wide range of cell type infectivity, the HTLV-I associated TSP/HAM may be a result of a HTLV-I versus host immunoreaction (165).

4. Treatment of ATL

The standard chemotheraputic regimens that have proven to be highly successful in the treatment of malignant leukemias and lymphomas have failed miserably in the treatment of HTLV-I associated ATL. Despite the fact that only 2- 5% of HTLV-I infected individuals develop ATL worldwide, this translates into 15-25 million people developing and dying of ATL.

Different combination regimens of conventional chemotherapy have produced a 4 year survival rate of below 5%. Therefore, new alternative treatments are needed in the treatment of ATL, particularly in the acute and lymphomatous forms.

A combination therapy of zidovudine and IFNα induced a rapid remission response within 1 month with a maximum response reached after several months. A synergistic response between IFNα and AZT was suggested since individual administration of the compounds had little effect on reducing the number of circulating leukemic cells. Therefore, the use of high doses of both agents is required (61,77). Despite initial success, the IFNα/AZT combination therapy does not appear to be a cure since relapses occurred when patients in remission were taken off the treatment. Cross-resistance with cytotoxic chemotherapy does not seem to occur, as suggested by the high response rate observed in patients for whom all other forms of cytotoxic

chemotherapy had previously failed. In addition a good response to chemotherapy was observed in patients following relapse after IFNα/AZT treatment (77).

The mechanism of action of the combination of AZT and IFNα remain unclear. IFNα is known to act at an immunological level by inducing an antiviral state in cells. On the other hand, most ATL cells do not express the HTLV-I genome and therefore do not undergo any reverse transcription. As such, the role of AZT in ATL remains to be elucidated. Interestingly AZT has been shown to suppress transformation of normal peripheral blood lymphocytes that were cocultured with HTLV-I transformed cell lines (77).

4.1. The development of a vaccine

The development of a successful vaccine against HTLV-I would represent the first human retroviral vaccine and the first vaccine against a human leukemia. However, is such a vaccine feasible? A significant advantage in the search for a vaccine against HTLV-I-compared the other important retrovirus of the century, HIV-is attributed to the HTLV's genomic stability.

Animal models have demonstrated that a successful oncoretroviral vaccine can be developed. Inactivated or attenuated live virus vaccines appear to be the most efficient in protecting from viral infection and/or disease development. In addition, vaccines that induce the best levels of protection are ones that protect through neutralizing antibodies and by cell-mediated immunity. Therefore, the aim would be to induce both neutralizing antibodies and cell mediated immunity by incorporating both *env* and *gag* genes.

5. Genomic structure

Cell tropism of a retrovirus is primarily determined at two stages of the virus cycle: adsorption-penetration, and proviral transcription (130). The mechanism of *in vivo* $CD4^+$ T cell tropism of HTLV-I has not been determined. Studies of binding of HTLV-I to cell lines or primary cells and pseudotype interference assays indicate that the viral receptor is present on many mammalian lymphoid cell lines and appears to be up-regulated by mitogenic activation of primary human peripheral blood mononuclear cells (PBMCs) (130). Therefore, unlike HIV-1 cell tropism, which is primarily determined by the presence of the viral receptor, cell tropism of HTLV-I is most likely determined at the post penetration stage of the virus life cycle (130). One study demonstrated that the HTLV-I LTR directs different rates of virus transcription and viral production in primary $CD4^+$ and $CD8^+$ cells (130). Increased levels of viral mRNA and protein are due to an enhanced rate of transcription in $CD4^+$ T cells however; other potential differences between the two cell types, such as transcriptional silencers in $CD8^+$ T cells, differential mRNA processing and virus maturation, may also contribute to differences in virus production (130).

The HTLV-I retrovirus contains the typical retrovial genes encoding Gag, Pol, and Env; but also in addition, HTLV contain other open reading frames (ORFs) in a portion of the genome termed the X region, located between the *env* gene and the 3' LTR (Figure 1). Expression of the various ORFs is achieved through frameshifting and differential splicing which produces unspliced, singly spliced, and multiply spliced mRNA (44).

5.1. The X region proteins

In HTLV-I, the X region is about 1.6 kb in size and contains 10 ORFs. To date, mRNAs expressing the x-I, x-II, x-III and x-IV ORFs have been described (44). A

Figure 1: Genomic Structure of HTLV-I. The viral structural and regulatory genes are flanked by the 5' and 3' LTRs containing the U3, R and U5 regions. The viral genes are represented by the overlapping colored boxes. Typical retroviral structural genes coding the group-specific antigen (gag), the protease (prt), the polymerase (pol) and the envelope (env) are found in the 5' region. In the 3' region, the pX region encodes the HTLV specific genes. These include genes essential for HTLV-I expression, tax and rex. The viral mRNA transcripts are represented below the viral genome. The unspliced transcript encodes the structural proteins of the gag, prt, and pol. The singly spliced transcript encodes the envelope proteins (gp46 and p21). Finally, a double splicing of the mRNA results in the synthesis of Tax and Rex.

HTLV-I Genome

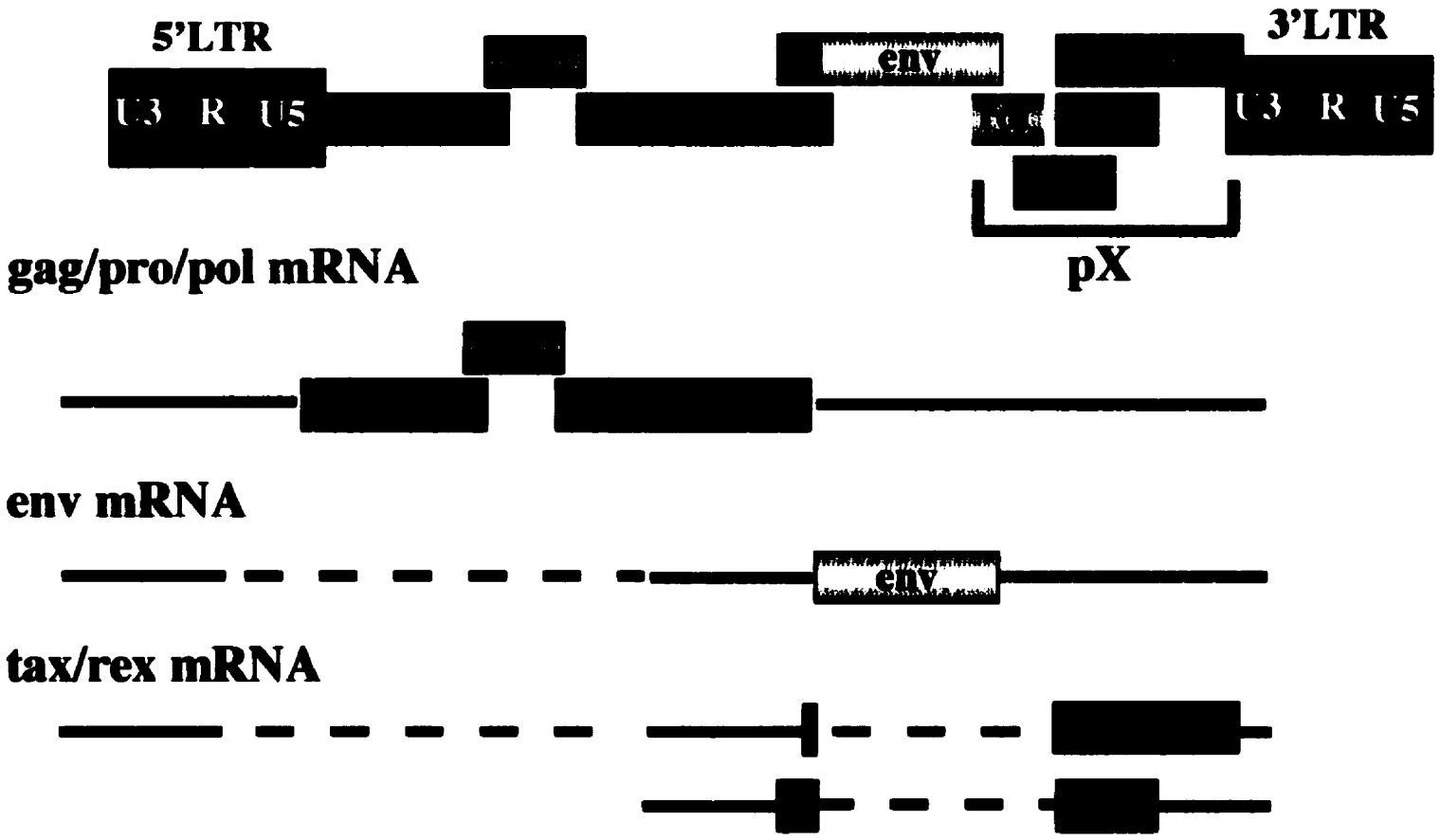

singly spliced mRNA consisting of the noncoding exon 1 linked to a specific acceptor located at nucleotide (nt) 6383 in the x-I ORF encodes a 99 aa protein termed $p12^{I}$. The essential regulatory proteins Tax and Rex are encoded by overlapping ORFs in a doubly spliced mRNA consisting of exon 1 linked to exons 2 and 3. Exon 2 encodes the N-terminal 20 aa of Rex and the initiator methionine of Tax; exon 3 contains the x-III and x-IV ORFs; encoding the remainder of Rex and Tax, respectively (Figure 1).

$p12^{I}$ protein

The $p12^{I}$ protein is a very hydrophobic protein localized to the cellular endomembranes and perinuclear regions of the cell. It has been implicated in cellular transformation in murine fibroblasts and is able to potentiate focus-forming ability of the E5 oncoprotein of bovine papillomavirus type 1 (51). Interestingly, in transfected HeLa cells, $p12^{I}$ binds to both the β and γ_c chains of the IL-2R, and this interaction interferes with the trafficking of these receptor chains to the cell surface. This type of interaction would seem to mimic that of other viral proteins; including E5 and gp55 protein of the spleen focus-forming virus (SFFV) (51). It is possible that the binding of $p12^{I}$ to IL-2R β and γ_c induces the activation of this signaling pathway, but this remains to be demonstrated (51).

The x-II ORF is expressed from a multiply spliced mRNA containing exons 1 and exon 2. Within x-II, two proteins are encoded, rof ($p13^{II}$) and tof ($p30^{II}$) (Figure 1). Both are phosphoproteins with a nuclear localization however, their function remains a mystery.

Rex

Rex (p27) is a phosphoprotein found predominately in the cell nucleolus, whose function is thought to be regulated by its nucleolar localization and phosphorylation

(1,2). Rex activates expression of the unspliced and singly spliced mRNAs encoding *gag/pro/pol* and *env* via direct interaction with a cis-acting RNA element termed the Rex-responsive element (RXRE), present in the 3' LTR. In fact, dephosphorylation of Rex results in the decrease of accumulation of unspliced viral mRNA (48,68).

Tax

Tax is a 40 kDa protein that regulates HTLV-I replication by activating the unique 21-base pair (bp) repeats present within the U3 region of the viral LTR (Figure 2). This protein also has the ability to stimulate a wide array of cellular genes; some of which are involved in the activation and proliferation of T cells. Tax does not bind directly to DNA but rather activates transcription by modulating the function of various host transcription factors. In the case of the HTLV-I promoter, the three unique 21 bp repeats present within the LTR are referred to as the Tax response elements (TREs) (Figure 2). Within the TREs, DNA consensus sequence binding sites for host transcription factors of the CREB/ATF family are found. Tax indirectly associates with the Tax response elements (TREs) present in the 21 bp repeats by directly binding to members of the CREB/ATF family of transcription factors.

Tax localizes to the nuclei of HTLV-I-infected cells, mediated via an N-terminal, atypical nuclear localization sequence (164). Mutagenesis studies (161,163) demonstrated that distinct amino acid residues of Tax were required for transactivation of the CREB and NF-κB pathways (Figure 3). Mutation of a region located between amino acid 315 and 325 abrogated CREB-mediated Tax transactivation without affecting NF-κB-mediated transactivation (Figure 3). Conversely, scattered mutations in Tax between amino acids 113 to 258 resulted in intact CREB but deficient NF-κB-mediated transactivation, demonstrating that Tax transactivation occurred via distinct regions of the viral protein that targeted specific

Figure 2: Upstream control elements in the HTLV-I LTR. The transcriptional enhancer region (U3) contains binding sites for three Tax Responsive Element-1 (TRE-1) regions and one TRE-2 region. The TREs contain several consensus binding sites for the host cellular transcription factors of the ATF/CREB family.

Upstream control elements in the HTLV-I LTR

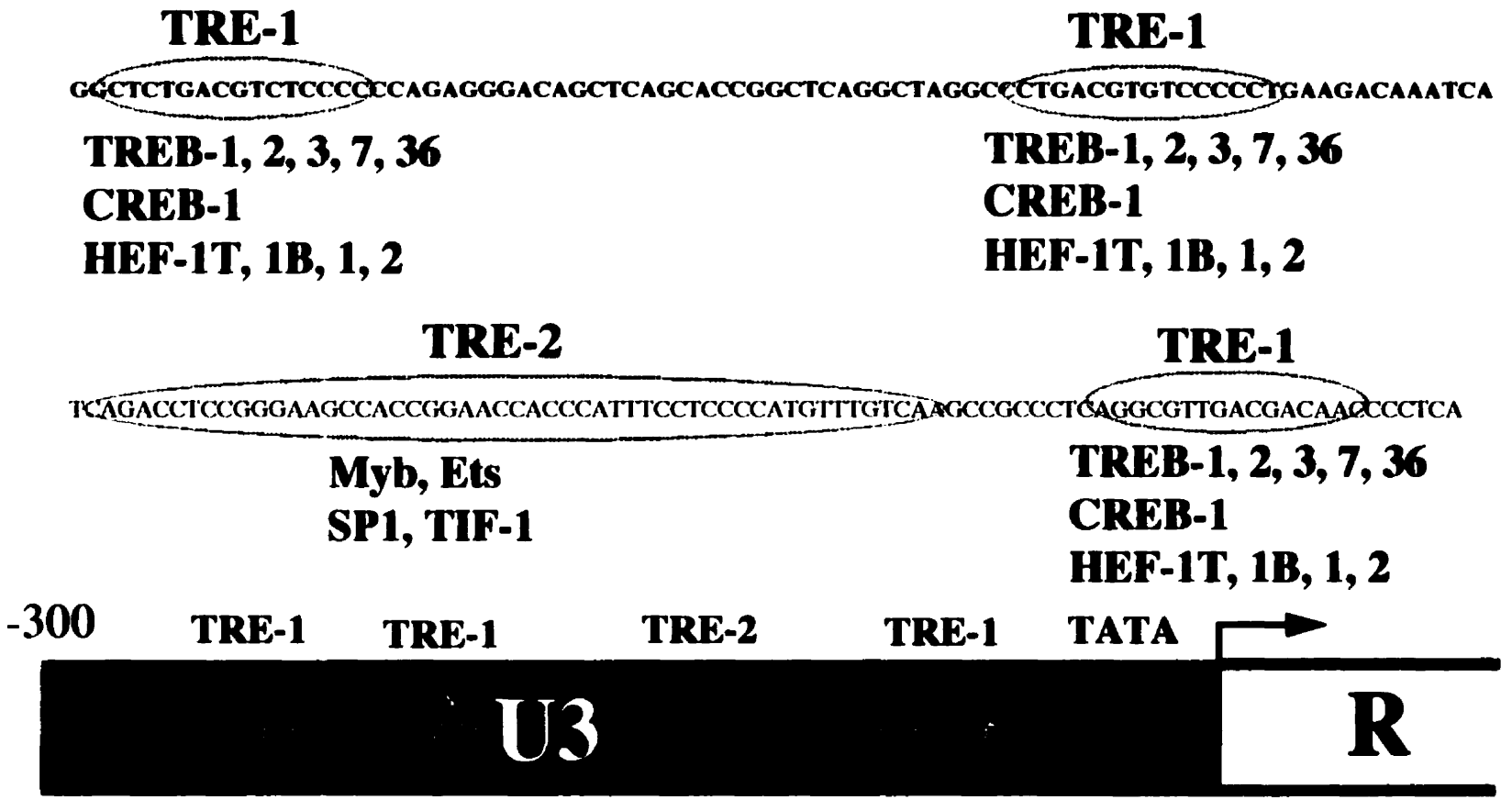

Figure 3: Schematic of the Tax protein. Tax is a 40 kDa protein containing two transcriptional activation domains, AD-I and AD-II. An atypical nuclear localization signal (NLS) is located in the 2-59aa N-terminal region of the protein. The NLS contains a zinc (Zn) finger motif. The function of a cluster of cysteine residues (C) found within the molecule, remains unknown. Interspersed within the molecule are residues important for CREB mediated activity (3aa, 315aa, 317aa, 319aa and 325aa) or NF-κB mediated activity (113aa, 130aa, 160aa, 258aa).

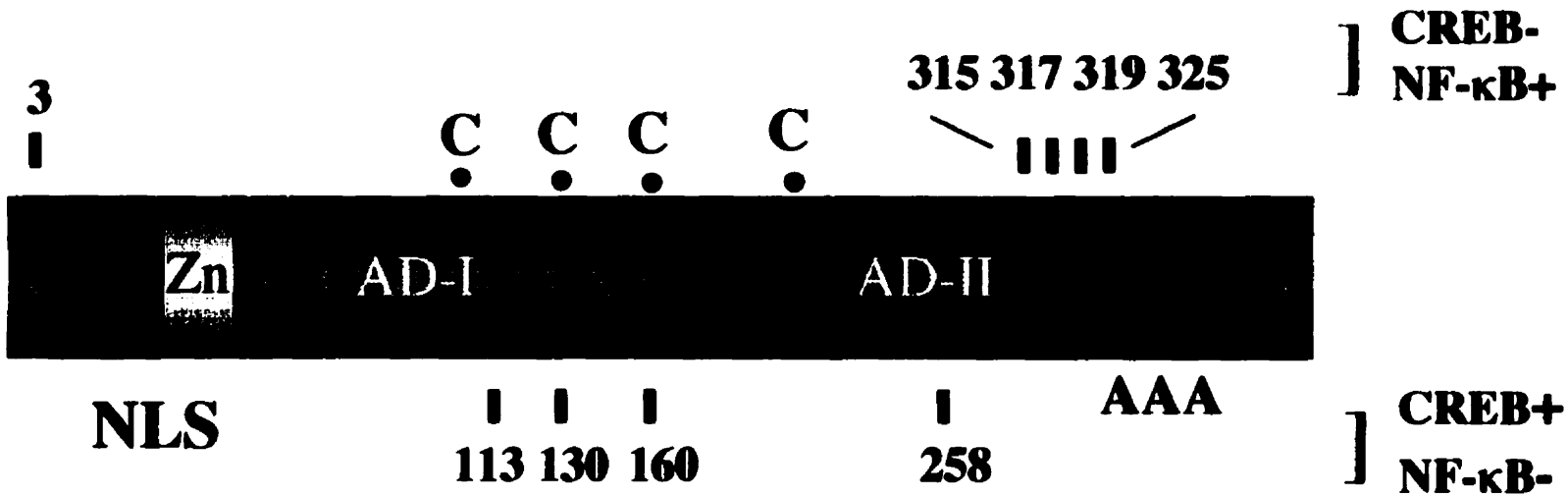
3
C C C C
315 317 319 325
CREB-
NF-κB+
Zn
AD-I
AD-II
NLS
113 130 160
258
AAA
CREB+
NF-κB-

transcription factors (161,163) (Figure 3) The transactivation phenotype of Tax mutants such as M22 ($CREB^-/NF\text{-}\kappa B^+$) and M47($CREB^+/NF\text{-}\kappa B^-$) have served as valuable reagents in the dissection of Tax-host transcription factor interaction (163). Mutational analysis however, failed to define discrete functional domains mediating Tax transactivation, indicating that about 95% of the protein was indispensable for this activity. Chimeric proteins fusing Tax to a Gal4 DNA binding domain identified a transactivation function of Tax that was separable into two overlapping stretches AD-I (aa2-255) and AD-II (aa227-337), both of which were required for the formation of a functional activation domain (183). Using a similar assay (a Gal4-Tax fusion protein and a responsive promoter containing Gal4 consensus binding sites), Semmes and Jeang determined that activation by the Gal4-Tax fusion was "squelched" by coexpression of wild type Tax protein *in trans*. Tax mutants containing changes in amino acids 289 to 322 failed to inhibit Gal4-Tax activation (160). Furthermore, the 289-322aa domain of Tax fused to Gal4 was able to activate a core promoter, indicating that this region defines a modular activation domain that contacts an essential transcription factor (160).

Tax is synthesized and secreted by infected host cells. Interestingly, secreted Tax was found to exert a proliferative effect on neighboring uninfected cells (111,117). These cells were found to have internalized Tax and directed it to the nucleus (117). Therefore, it appears that exogenous Tax protein can act as a cytokine, taken up by several cell types, via an as-yet, unknown mechanism.

6. Road to cellular transformation

The precise mechanism by which HTLV-I transforms human T cells remains unclear, but the transactivator Tax appears to play the central role in leukemogenesis. Tax expression has been shown to transform cell lines and primary T cells *in vitro* (39,118,176). Also, transgenic mice expressing Tax develop nonlymphoid tumors *in vivo* (71,128).

6.1. T cell activation and proliferation

Growth factors are necessary to carry T cells from the late G1 to S phase of the cell cycle. Tax appears to act as a mitogen by inducing the expression of early mitogen genes and of the L-2Rα chain, a component of the high-affinity IL-2R. In addition, Tax transactivates IL-2 gene expression and triggers an autocrine/paracrine mechanism, which may lead to T cell proliferation (51).

6.2. IL-2 autocrine loop

T cell activation requires the presence of two signals, one originating from interaction of the CD3-T cell receptor (TCR) complex with appropriate peptide antigen in the context of MHC, and the other provided by costimulatory molecules, in particular B7-1 and B7-2 (51). Productive infection of $CD4^+$ T cells by HTLV-I causes a state of T cell activation that has escaped this normal control. Events marking the transition from normal to transformed T cells, include the transition from IL-2 dependence to IL-2 independence (51). HTLV-I Tax expressing cells are initially IL-2 dependent but become IL-2 independent over a period of time in culture. Furthermore, a direct correlation between IL-2 independence and JAK/STAT activation was observed. Specifically, the JAK3, STAT5 proteins were constitutively phosphorylated on tyrosine, and the STAT proteins were present in the nucleus and able to bind DNA

(51). In fact, the IL-2R chains, JAK3 and STAT5 could be coimmunoprecipitated. Abnormal expression of several intracellular protein tyrosine kinases of the *src* family, including an upregulation of *lyn* and downregulation of *lck* has been seen in Tax expressing cells. Transcription of lck is blocked in the IL-2-independent, HTLV-I transformed T cell lines or Tax expressing cells but not in the IL-2 -dependent cells (104).

6.3. Tax induces G1 to S phase transition in the cell cycle

The long latency period in the development of ATL lends to the speculation that the increased HTLV-I mediated T cell proliferation would allow for the accumulation of genetic changes which would result in leukemogenesis. The tumor suppresser gene p53 would seem to be the likely candidate for alteration in HTLV-I induced transformation, since this gene is frequently mutated in several other types of tumors. However, genetic analysis of the p53 gene in DNA from uncultured ATL cells and infected T cell lines revealed that p53 mutation is rare. Surprisingly, high p53 protein expression has been found in HTLV-I infected T cell lines and in uncultured ATL cells. Stabilization of p53 protein was also demonstrated in the majority of HTLV-I infected cells (144). However, the stabilization of p53 protein did not translate into cell cycle arrest. Instead Tax expression was found to inactivate p53 mediated transactivation (144). Tax inhibited p53 function by interfering with the activity of the N-terminal activation domain (amino acids 1-52) (122,144). Impairment of the p53 transactivating function was more evident in IL-2-independent than in IL-2-dependent HTLV-I infected cells (144), although an explanation for the differences has not been found.

Tax plays a role in cell cycle progression by direct interference of the function of the cell cycle inhibitor, $p16^{INK}$ (112,175). The $p16^{INK}$ protein remains bound to the CDK4 kinase, keeping the kinase inactive. When Cyclin D is available, it displaces $p16^{INK}$

and forms a CDK4/Cyclin D heterodimer. When bound to Cyclin D, the CDK4 kinase is active and phosphorylates its substrate, the retinoblastoma (Rb) protein. Unphosphorylated Rb is complexed to the E2F transcription factor, sequestering E2F in a non-binding form and preventing E2F mediated transcription. The phosphorylated Rb releases E2F, freeing E2F to activate transcription. The $p16^{INK}$ protein contains an ankyrin motif through which Tax binding occurs, immobilizing $p16^{INK}$ and preventing its ability to repress CDK4 kinase activity (112,175).

7. Tax physically associates with cellular transcription factors

The activation of the HTLV-I LTR and cellular transcription occurs in the absence of *de novo* protein synthesis. Rather, Tax mediated transcription utilizes preexisting cellular transcription factors. Direct interaction has been observed with members of the extensive bZIP family of transcription factors which include the cyclic AMP-responsive factors CREB/ATF, the serum response factor (SRF) and AP-1 (23,52,53,171,172,200,201,204). Other transcription factors include the Ets and NF-κB/Rel families (27,126,172,174,189).

The CREB/ATF transcription factors are essential for HTLV-I LTR transcription. Tax has been found to enhance CREB/ATF mediated transcription . *In vitro*, Tax was shown to enhance dimerization of CREB by interaction with the basic region of the leucine zipper (bZIP) domain. The CREB/ATF transcription proteins bind to and transactivate DNA as dimers therefore, the enhancement of CREB dimer formation by Tax favors CREB mediated transcription. *In vivo*, Tax transactivates the HTLV-I CREB site directly but cellular CRE requires phosphorylated CREB and the co-activator CBP. Phosphorylated CREB dimers can recruit CBP and only the CREB-CBP heterotrimer transactivates through the CRE DNA binding site. Tax is able to bind and facilitate recruitment of CBP to the phosphorylated CREB complex (100,168).

7.1. NF-κB proteins are targets for Tax trans-activation.

One of the important targets of interaction for Tax protein is the NF-κB/IκB transcription complex. NF-κB DNA binding activity is constitutively elevated in HTLV-I infected cells and is thought to contribute to the transformed phenotype (202). Significantly, inhibition of NF-κB activity by antisense RNA in cells derived from Tax transgenic animals results in loss of the transformed phenotype (91).

The NF-κB/Rel transcription factors are a family of dimer-forming proteins that bind to the consensus DNA sequence 5'-GGGANNYYCC-3', found in the promoter regions of cellular genes implicated in immunoregulatory and inflammatory processes, including cytokines, cell surface receptors, adhesion molecules and acute phase proteins (reviewed in (10,70). Structurally, all DNA binding members of the family (NF-κB1 p50, NF-κB2 p52, RelA (p65), c-Rel and RelB) share an amino terminal *rel* homology domain (RHD). The N-terminal half of the RHD forms a motif (Arg-X-X-Arg-X-Arg-X-X-Cys) unique to the NF-κB/Rel family and is essential for DNA binding (Figure 4) (95,180). The C-terminal region of the RHD is responsible for dimerization between the NF-κB/Rel family members (reviewed in 10,70). Homo- and heterodimer formation among the DNA binding members of the NF-κB family permit a range of differential transcriptional activities that may stimulate or inhibit gene expression (108,141). Adjacent to the C-terminal region of the RHD is a nuclear localization signal (NLS) (Arg-Lys-Arg-Gln-Lys and Lys Arg-Lys-Arg) which permits the translocation of NF-κB/Rel proteins to the nucleus for transcriptional transactivation (Figure 4) (29,55,63,64). The crystal structure of a p50 homodimer bound to DNA identified the DNA binding domain (DBD) of the RHD as containing a recognition loop which interacts with the major groove of DNA leaving the C-terminal region free for dimerization; forming a pattern that resembles immunoglobulin-like modules (125).

Figure 4: The NF-κB/Rel family members. All NF-κB proteins share the Rel homology domain (RHD)  . Within the RHD is the DNA binding domain (DBD) and a region essential for NF-κB dimer formation (DIM). The NF-κB1/p105 and NF-κB2/p100 contain a long c-terminal domain with seven ankyrin repeats  and a PEST region  . Cleavage of the C-terminal region of p105 and p100 occurs at a site near a flexible glycine-rich hinge (to generate the transcription factors NF-κB1/p50 and NF-κB2/p52, respectively. All NF-κB/Rel members contain a nuclear localization signal flanking the 3' region of the RHD  . c-Rel, p65, and v-Rel contain transcriptional transactivation ability, mediated through transactivation domains I and II. The c-Rel member contains a unique cytoplasmic anchorage domain (C).

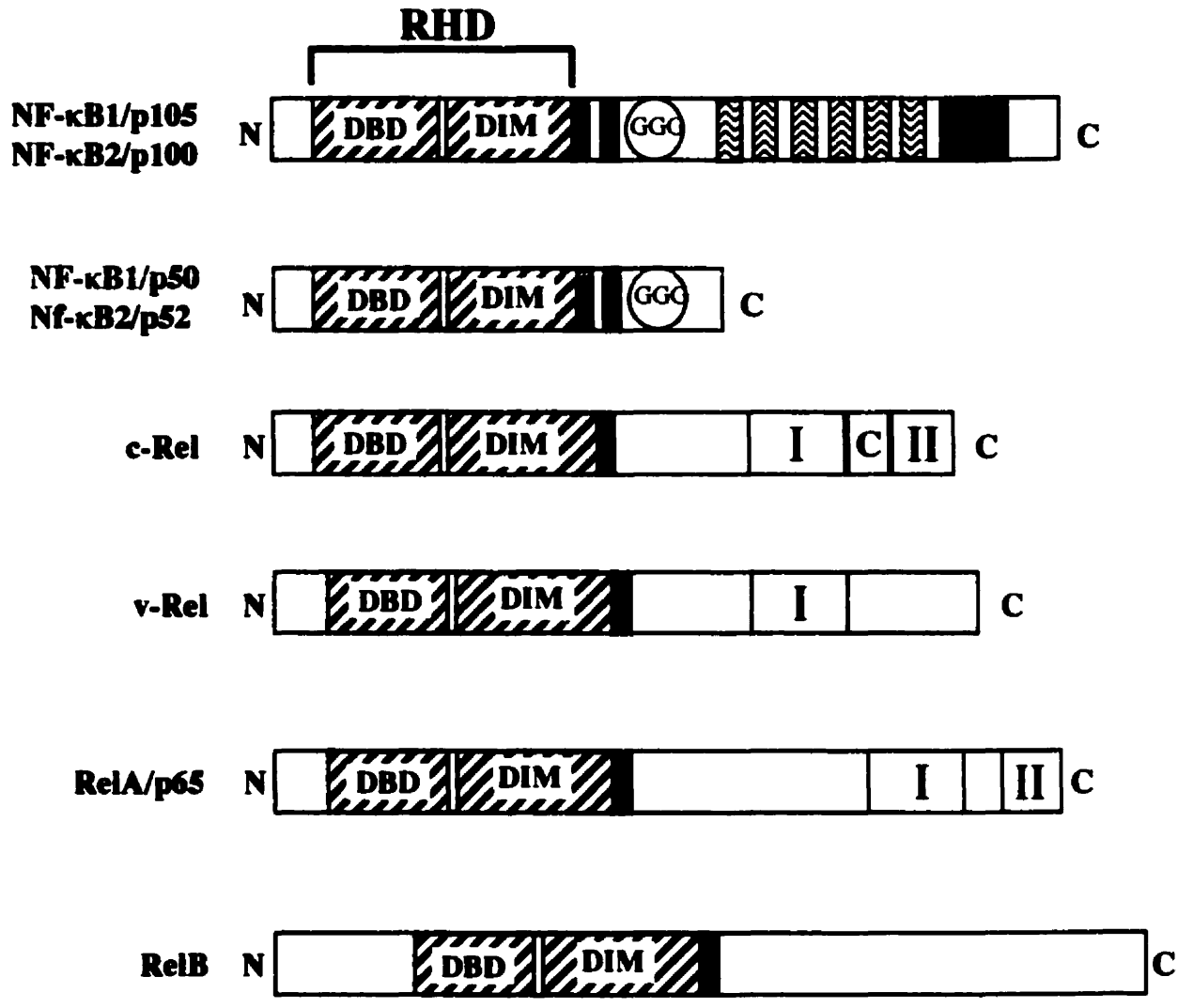
RHD
NF-κB1/p105
NF-κB2/p100
N
DBD
DIM
GGC
C
NF-κB1/p50
Nf-κB2/p52
N
DBD
DIM
GGC
C
c-Rel
N
DBD
DIM
I
C
II
C
v-Rel
N
DBD
DIM
I
C
RelA/p65
N
DBD
DIM
I
II
C
RelB
N
DBD
DIM
C

NF-κB1/p105 and NF-κB2/p100 are non-DNA binding NF-κB/Rel family members. The N-terminal regions of NF-κB1/p105 and NF-κB2/p100 contain the RHD, their C-terminal regions contain seven ankyrin repeats (114). A glycine rich region divides the two functional domains and allows sufficient structural flexibility for the C-terminal to fold back and interact with the RHD (Figure 4). This physical interaction masks the DNA binding domain and nuclear localization signal of NF-κB/Rel proteins, thereby preventing nuclear translocation (19,21). Partial proteolysis of NF-κB1/p105 and NF-κB2/p100 generate the transcriptionally active NF-κB subunits p50 and p52, respectively (reviewed by (34,69,70,149). The partial proteolysis generating p50 and p52, arise by a ubiquitin dependent proteolytic degradation of the C-terminus up to a site adjacent to the glycine rich hinge (Figure 4)

Cellular stimulation by multiple inducers (cytokines, virus infection, mitogens, radical oxygen intermediates) leads to the phosphorylation, ubiquitination and subsequent degradation of IκBα. IκBα loss permits NF-κB/Rel dimer translocation to the nucleus and target gene activation (Figure 5) (19,62). Degradation and resynthesis of IκBα appear to be general mechanisms determining the rapid but transient activation of gene activity by NF-κB(20,38,169). Activated p65 and c-Rel proteins in turn induce *de novo* IκBα RNA expression, thus completing an autoregulatory loop that ultimately restores the cytoplasmic pool of latent NF-κB/IκB (Figure 5) (20,38,102,169). NF-κB/Rel activity is also regulated at the transcriptional level, conferred by the presence of NF-κB sites in the promoters of NF-κB1(p105 and p50), c-*rel*, MAD-3(IκBα) and NF-κB2 genes (47,73,102,170).

Changes in the balance of NF-κB subunits available in a particular cell may alter the pattern of gene expression and, by implication, contribute to oncogenic transformation.

Figure 5: The NF-κB/IκBα activation pathway. NF-κB/Rel dimers are sequestered in the cytoplasm by IκBα (step 1). Activators of NF-κB (LPS, TNF, virus infection, PMA and many others) trigger a signal transduction pathway (step 2) which results in the phosphorylation of IκBα by IKK (IκBα Kinase) (step 3). Phosphorylation of IκBα results in a structural change in the IκBα molecule (step 4). Following phosphorylation, IκBα is ubiquitinated (step 5) and the complex is targeted to the proteasome for degradation (step 6). The IκBα protein is degraded thus freeing the NF-κB dimer for translocation to the nucleus (step 7). Once in the nucleus, NF-κB transactivates genes involved in the immune response (step 8). Also, NF-κB activates the transcription of its own inhibitor, IκBα. The newly synthesized IκBα once again binds to free NF-κB (step 9), terminating NF-κB transactivation.

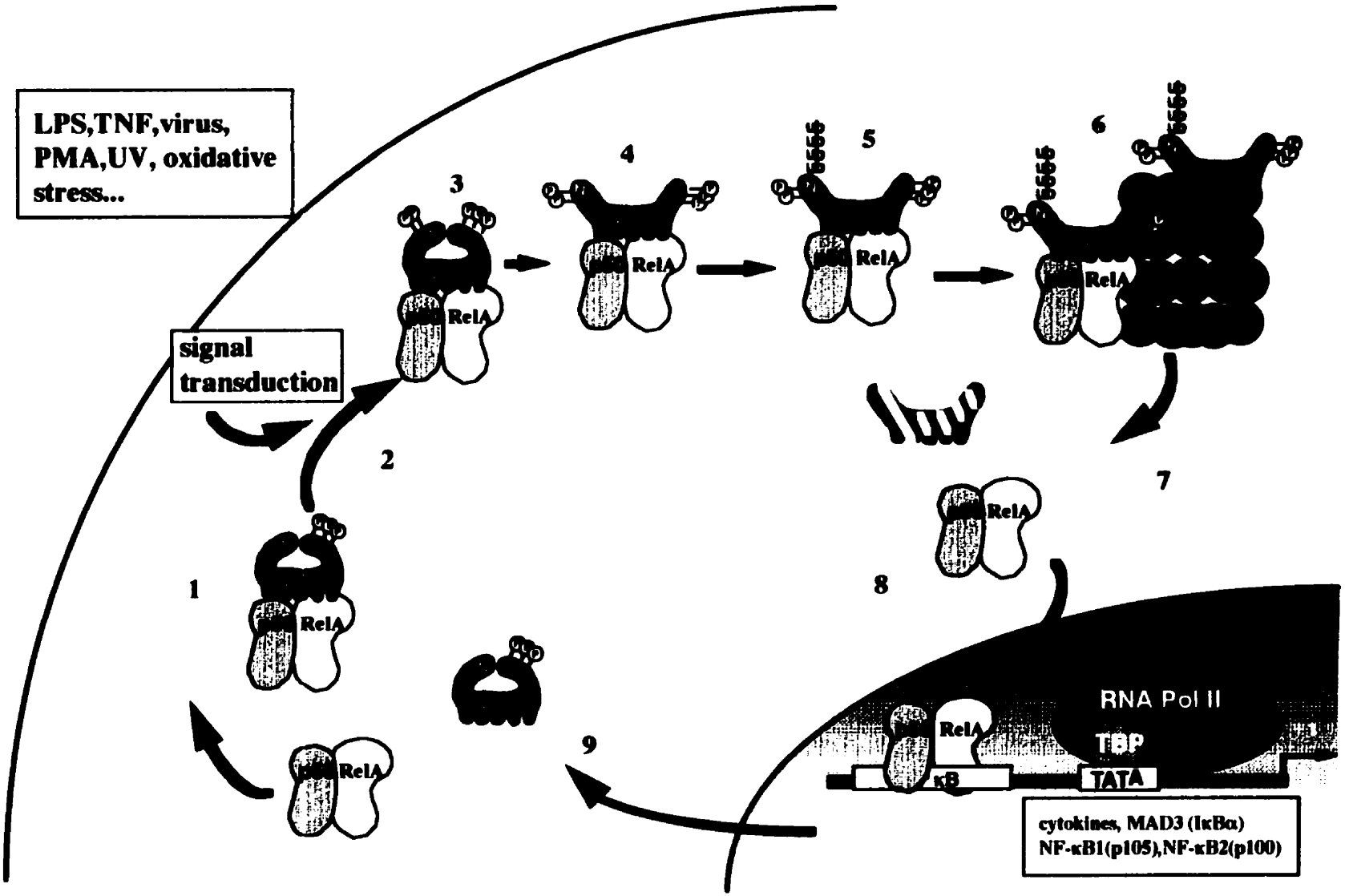
LPS,TNF,virus,
PMA,UV, oxidative
stress...
signal
transduction
1
2
3
4
5
6
7
8
9
RelA
RNA Pol II
TBP
TATA
κB
cytokines, MAD3 (IκBα)
NF-κB1(p105),NF-κB2(p100)

Several lines of evidence have demonstrated the involvement of NF-κB/*rel* in leukemogenic transformation. 1) v-*rel* is the oncogenic derivative of *c-rel* and is found in the virulent avian reticuloendotheliosis virus (REV-T). REV-T transforms and immortalizes avian T and B lymphocytes, as well as monocytes (30). v-*rel* has been shown to bind to NF-κB sites and inhibit the ability of NF-κB to stimulate target genes. Current evidence indicates that v-*rel* represents a dominant negative repressor that functions by overcoming the action of c-*rel*, its normal cellular counterpart (13). 2) Chromosomal translocations have been identified in human B cell lymphoma and chronic lymphocytic leukemia (CLL) that alter the structure and/or function of NF-κB2, (originally identified as lyt-10) in the t(10;14) chromosomal translocation (129,157), c-Rel (the t(2;2) translocation in the RC-K8 lymphoma line (113) and the IκB molecule *bcl* 3) the t(14;19) translocation in CLL (135).

Overexpression of IκBα antisense RNA, but not IκBγ antisense RNA decreased the steady state levels of IκBα, altered NF-κB DNA binding and gene activity and induced malignant transformation as measured by saturation density, growth in soft agar and tumorgenicity in nude mice. In contrast, overexpression of IκBα resulted in decreased saturation density, a flattened cellular morphology and decreased NF-κB dependent reporter gene activity. These results indicated that overexpression of an IκBα antisense RNA may disrupt the NF-κB/IκB autoregulatory loop, leading to cellular transformation and raise the possibility that IκBα may represent a potential growth suppresser activity (16).

7.2. Physical interactions between Tax and NF-κB subunits.

A number of studies have recently focused on the physical associations between Tax and NF-κB/IκB subunits, often with seemingly contradictory results. Nonetheless, several points of consensus have now emerged. Using various assays, including co-

immunoprecipitation of labeled proteins from HTLV-I infected or Tax expressing T cells, *in vitro* affinity chromatography or co-transfection-immunofluorescence localization, it is clear that Tax interacts with high affinity with the NF-κB2 p100 precursor (27,90,101,126,170). Physical association is also detected with the NF-κB2 p52 product (27,90,139), indicating that Tax binds to NF-κB2 via interaction with the Rel homology domain. The exact binding domains within either protein have yet to be determined.

One consequence of Tax-NF-κB2 interactions is a distinct intracellular pattern of sequestration of Tax protein; in cells overexpressing NF-κB2 p100, Tax is localized predominantly to the cytoplasm (87,139) whereas in cells overexpressing nuclear NF-κB2 p52, Tax is exclusively localized to the nuclei of transfected cells (139). Thus, the transcription modulatory influence of Tax may be significantly influenced by cytoplasmic-nuclear partitioning associated with the NF-κB proteins. The sequestration of Tax by p100 further implies a role for p100 in the maintenance of HTLV-I latency observed in ATL (27).

Distinct multimeric complexes of NF-κB have also been described existing in the cytoplasm in association with the NF-κB2 p100 precursor (90,126,170). The presence of these complexes in the cytoplasm is dependent on the ankyrin repeat domains located in the COOH-terminal half of the p100. Using metabolically labeled extracts from transfected cells and co-immunoprecipitation, the presence of a complex consisting of p100-p50-RelA was demonstrated (90); interaction of p50-RelA heterodimers was dependent upon the COOH-terminal ankyrin repeat of p100. Tax expression produced an antagonistic effect on the cytoplasmic sequestration function of NF-κB2 p100, resulting in the release and nuclear translocation of p50-RelA dimers from the multimeric complex. A model to account for these observations proposes that

Tax exerts its effects through physical association with the NH_2-terminal Rel homology domain of NF-κB2 p100, which in turn interferes with the inhibitory function of the C-terminal ankyrin domain (90). There is however no evidence that the antagonistic effects of Tax on NF-κB2 p100 involves increased processing of the p100 precursor to its product p52 (27,101). The presence of a cytoplasmic, p100-containing NF-κB reservoir that is targeted by Tax provides a distinct mechanism, in addition to Tax-induced IκBα degradation, by which Tax may augment the levels of nuclear NF-κB observed in HTLV-I infected cells.

Previous studies have also demonstrated that Tax interacted physically with NF-κB1 p105, p50 and IκBγ (the 70 kDa protein derived from the carboxyl terminal portion of p105), through both the Rel homology domain and the ankyrin repeat motif of the precursor molecule (79,80,126,172). These interactions stimulated nuclear translocation of NF-κB. The site of Tax binding within NF-κB1 p50 was localized between amino acids 140 and 341, the region of p50 required for dimerization and DNA binding (173). The physical interaction between Tax and p105 has been controversial since some groups were unable to co-immunoprecipitate Tax and p105 complexes from HTLV-I infected and Tax transfected cells (27,101,167). However, recent experiments have demonstrated that both Tax-p100 and Tax-p105 complexes can be immunoprecipitated from cells, although the affinity of Tax for p100 was determined to be about fivefold higher than the affinity of Tax for p105 (126). Tax-IκBγ interactions were also documented in co-expression assays (80); the biological significance of Tax-IκBγ interactions is unclear, since IκBγ has not been observed in T cells or any other human cells (84). More recently interactions of Tax with RelA and c-Rel via the Rel homology domains have been described (174). Some of the interactions between Tax and NF-κB members described above were detected under "forced" conditions - i.e. using *in vitro* affinity assays or evaluating extracts from cells engineered to

overexpress individual or multiple proteins. It is therefore important to verify Tax-NF-κB interactions using several cell systems and relevant assays, particularly since the effects of Tax on NF-κB expression may be cell-line specific (126). These limitations notwithstanding, the evidence indicates that HTLV-I Tax physically interacts with NF-κB2 with high affinity, and likely with other DNA binding members with lower affinity, via the Rel homology domain. The relative accumulation and cell-type specific abundance of NF-κB proteins may also contribute to interactions *in vivo*.

7.3. Changes in the relative abundance of NF-κB subunits.

Constitutive Tax expression leads to sustained nuclear expression of both c-Rel and p52 and dysregulated NF-κB DNA binding activity (43,88,101,106,167). Preferential c-Rel induction by HTLV-I infection has been demonstrated at both the protein and RNA levels, indicating that the effect is at least partially regulated at the transcriptional level (43,106). Furthermore, Tax transcriptionally activated the c-Rel promoter in co-expression experiments, and this activation may be controlled at least in part by RelA autoregulation (106,167).

8. The IκB family

The IκB family is a growing family of NF-κB inhibitory proteins. The family includes, IκBα, IκBβ, IκBγ, IκBδ, IκBε, IκB-R, Bcl-3, cactus and the NF-κB precursor proteins p100 and p105 (Figure 6) (56,74,84,123,178,190,194). The IκB proteins are identified by their ability to bind to and inhibit NF-κB activity through an ankyrin structural motif. The ankyrin motif is present in multiple copies in the central region of the IκB proteins (Figure 6). Each ankyrin repeat contains 30-33 amino acids and the number of repeats present within the IκB members varies from three to seven (Figure 6). Since multiple NF-κB homodimers and heterodimers are present within a cell type, different IκB molecules can thus differentially bind to NF-κB complexes and regulate activity

Figure 6: The IκB family: The IκB family is presently composed of 8 members. All members of the IκB family have the ability to bind to the NF-κB/Rel proteins and contain ankyrin repeats  , which are found in multiple copies. A PEST sequence  is found in all members with the exception of IκBε. PEST sequences have been implicated in enhanced protein turnover as is for IκBα, but not always, as in the case of IκBβ. NF-κB1/p105 and NF-κB2/p100 are also NF-κB/Rel members ; their IκB-like C-terminal tails fold over to mask the DNA binding domain  , inhibiting DNA binding. IκBγ comprises the C-terminal region of NF-κB1/p105, generated by alternative mRNA splicing of *nfkb*1.

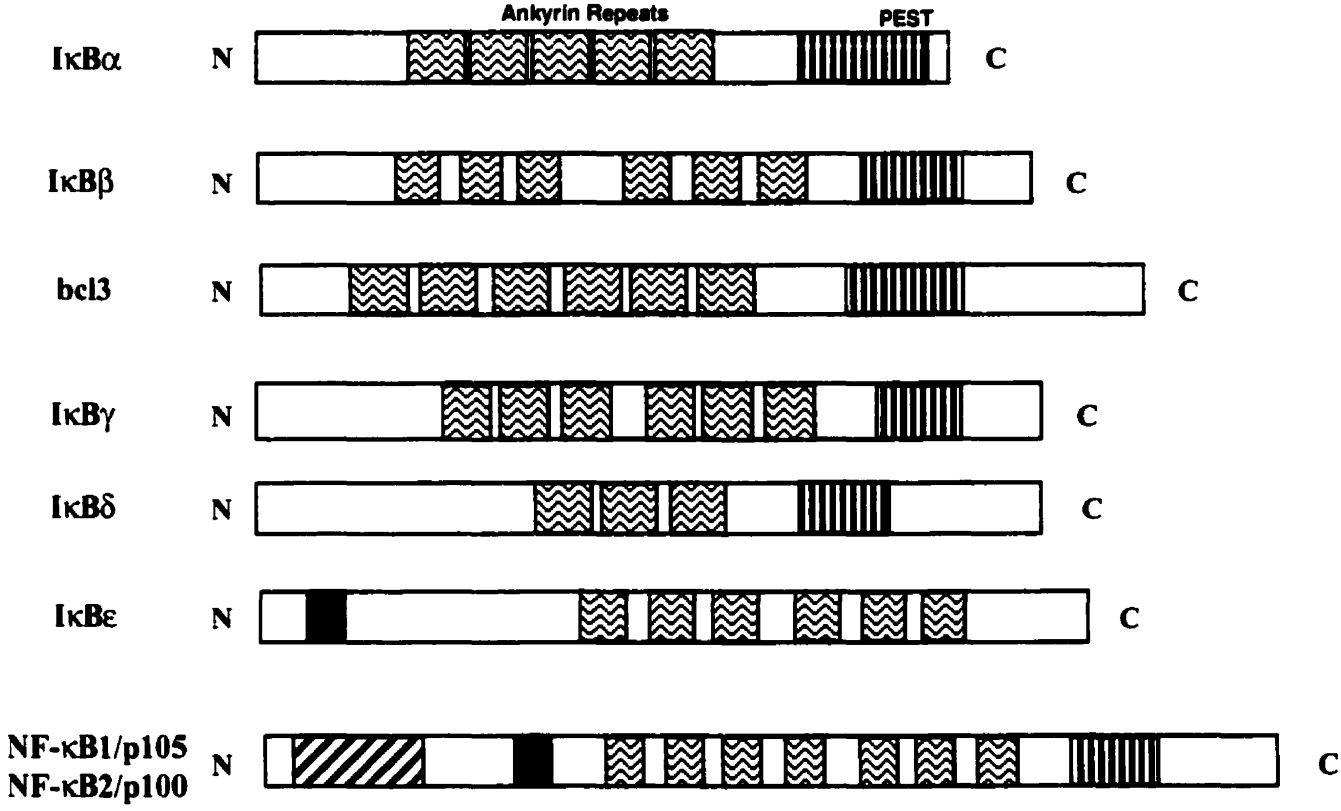
Ankyrin Repeats
PEST
IκBα
N
C
IκBβ
N
C
bcl3
N
C
IκBγ
N
C
IκBδ
N
C
IκBε
N
C
NF-κB1/p105
NF-κB2/p100
N
C

independently or coordinately. For example, IκBα and IκBβ preferentially bind to complexes containing p65 and c-Rel whereas IκBγ and bcl-3 inhibit homodimers of p50 and p52 (reviewed in 75). The NF-κB precursor proteins bind to p50, p65 and c-Rel and retain them in the cytoplasm. The ankyrin-containing C-terminal domains of p100 and p105 can fold back and interact with its own N-terminal Rel domain, including the NLS, and thus prevent nuclear translocation (75).

In addition to the ankyrin repeats, the IκB family of proteins contains a carboxy-terminal acidic region, termed the PEST region (proline, glutamic acid, serine and threonine). PEST sequences have been implicated in regulating the half-life of the protein. Although deletion of the PEST sequence has been shown to partially protect IκBα from induced degradation, no such degradation susceptibility has been attributed to PEST in the turnover of Cactus (24). Therefore, the role of PEST in the IκB proteins remains unclear.

Of the IκB family members, IκBα has been most extensively studied. Interestingly, IκBα transcription is activated by NF-κB itself. The newly synthesized IκBα will bind up and sequester any free cytoplasmic NF-κB (5). Furthermore, IκBα contains a novel nuclear localization sequence (NLS) which allows for its translocation to the nucleus and remove active NF-κB complexes from DNA (5). Nuclear localization of IκBα is mediated by the second ankyrin repeat, allowing IκBα to enter the nucleus and act as a postinduction repressor of NF-κB/Rel proteins (151) (Figure 7). A nuclear export signal (NES) present within IκBα allows for the nuclear export system to transport the nuclear NF-κB/IκBα complex out of the nucleus thereby terminating NF-κB mediated transcription (5).

Figure 7: Protein interactions regulating IκBα activity. The IκBα protein can structurally be divided into three segments, the Signal Response Domain, ankyrin repeat region and the PEST region. The Signal Response Domain, located in the N-terminal region of IκBα, is responsible for inducible degradation. Upon appropriate activation, the signal transduction pathway activates the IKK to specifically phosphorylate IκBα at Ser32 and Ser36. Phosphorylation is a prerequisite to ubiquitination at sites K21 and K22 by the ubiquitin conjugating enzyme pathway. This allows for signal induced proteasome mediated degradation. The ankyrin repeats are important for interaction with the NF-κB/Rel homology domain of NF-κB proteins. The PEST region is constitutively phosphorylated by casein kinase II at Ser283, Thr291 and Thr299 and important for the intrinsic stability of IκBα. A nuclear export signal (NES) is located and a nuclear localization signal (NLS) located within the ankyrin repeats, are important for exit and enty from and into the nucleus, respectively.

Protein Interactions Regulating Human IκBα Activity

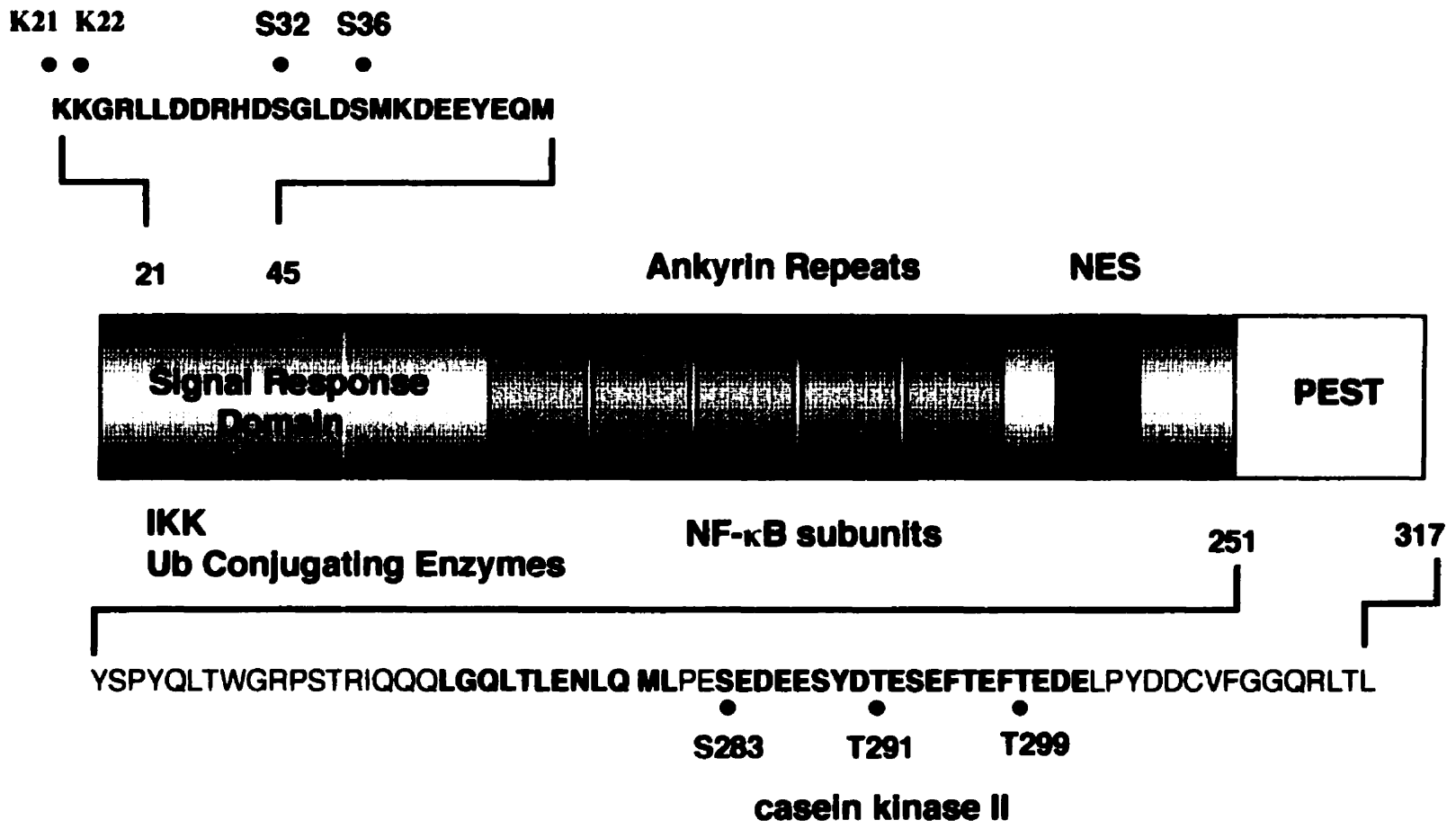

In vivo, IκBα knockout mice have been generated which appear to be normal at birth. However, soon after they exhibit severe runting, skin defects and extensive postnatal granulopoiesis and die by the eighth day. Tissue analysis from the IκBα knockout mice demonstrate differential effects depending on the tissue type. Hematopoietic cells show elevated levels of nuclear NF-κB and mRNAs of several genes regulated by NF-κB. On the other hand, embryonic fibroblasts show minimal constitutive NF-κB and normal signal-dependent NF-κB activity that could correspond to that of IκBβ degradation. The phenotypic abnormalities seen are likely due to the loss of IκBα protein since mice lacking both IκBα and the p50 subunit of NF-κB demonstrate a delayed onset of disease and death (22).

9. Mechanism of IκBα degradation

The NF-κB transcription factors are retained in the cytoplasm by IκBα, thus inhibiting NF-κB mediated transcription. Studies aimed at determining the mechanism of degradation of IκBα have demonstrated the existence of two pathways: 1) Signal induced degradation and 2) constitutive turnover of IκBα (Figure 8).

9.1. Signal induced degradation

Activating agents such as virus infection, cytokines (TNFα, IL-1), lipopolysaccharide (LPS) and phorbol esters induce the degradation of IκBα thereby releasing NF-κB/Rel dimers for nuclear translocation. Studies looking at the structural requirements for inducer mediated degradation of IκBα have demonstrated a signal response domain (SRD) located in the N-terminal region of IκBα. Multiple signaling pathways converge to induce activation of the NF-κB inducing kinase (NIK) which in turn activates the IκBα kinase complex (IKK). The IKK complex is composed of a heterodimer IKK-α and IKK-β and directly phosphorylates Serine 32 and Serine 36 within the SRD of IκBα (119,193,203). The N-terminal phosphorylation is an

essential prerequisite step to covalent attachment of ubiquitin at Lys-21 and Lys-22 (11). Once ubiquitinated the IκBα protein is marked for degradation by the ubiquitin-proteasome degradation system (11,156). The C-terminal 41 amino acid region of IκBα also plays a role in its inducible degradation but the mechanism for this remains unresolved (36).

9.2. Constitutive IκBα turnover

In vitro studies have demonstrated that the protein domains of IκBα involved in its induced breakdown are not required for basal turnover (93). Deletion of either the N-terminal SRD or the C-terminal PEST sequence does not alter the turnover of IκBα under non-induced conditions (93). Although it appears that basal turnover is a proteasome mediated event, phosphorylation nor ubiquitination is necessary (93).

Tax protein induced expression of NF-κB DNA binding activity in the nucleus of both HTLV-I infected or Tax-expressing human T cells is associated with increased phosphorylation and rapid proteolytic degradation of IκBα (88,99,167). The phosphorylated form of IκBα has been shown to remain complexed with NF-κB/Rel dimers in the cytoplasm and is subjected to rapid proteasome-mediated degradation while in association with NF-κB (3,46,49,110,182). Thus the viral Tax protein by indirectly mediating phosphorylation of IκBα may target IκBα for rapid degradation, leading to constitutive NF-κB DNA binding activity and aberrant gene expression.

Mutational analysis of IκBα demonstrated that mutations at serine 32 or serine 36 of IκBα generated a molecule that did not undergo signal induced phosphorylation or degradation, whereas mutation of other potential phosphoacceptor Ser, Thr and Tyr residues in the NH_2-terminal 89 residues of IκBα did not block signal induced

Figure 8: Inducible Degradation versus Constitutive Degradation of IκBα. Inducible IκBα degradation. In unstimulated cells, IκBα is found in a heterotrimer complex with NF-κB in the cytoplasm **(A)**. Activators, such as TNFα or virus infection **(B)**, result in the phosphorylation of IκBα by IKK **(C)**. The resulting net negative charge of the domains may modify IκBα structure, forcing the protein to adopt a new conformation **(D)** which can be recognized by the ubiquitin-conjugating enzymes, permitting ubiquitination of K21 and K22. Following ubiquitination **(E)**, IκBα is targeted to the proteasome for degradation **(F)**. With degradation of IκBα, the NLS of NF-κB dimer is exposed, allowing for translocation to the nucleus and binding to DNA **(G)**. **Constitutive IκBα degradation.** In unstimulated cells, free IκBα or complexed to NF-κB (1), is directly targeted to the proteasome for degradation (2).

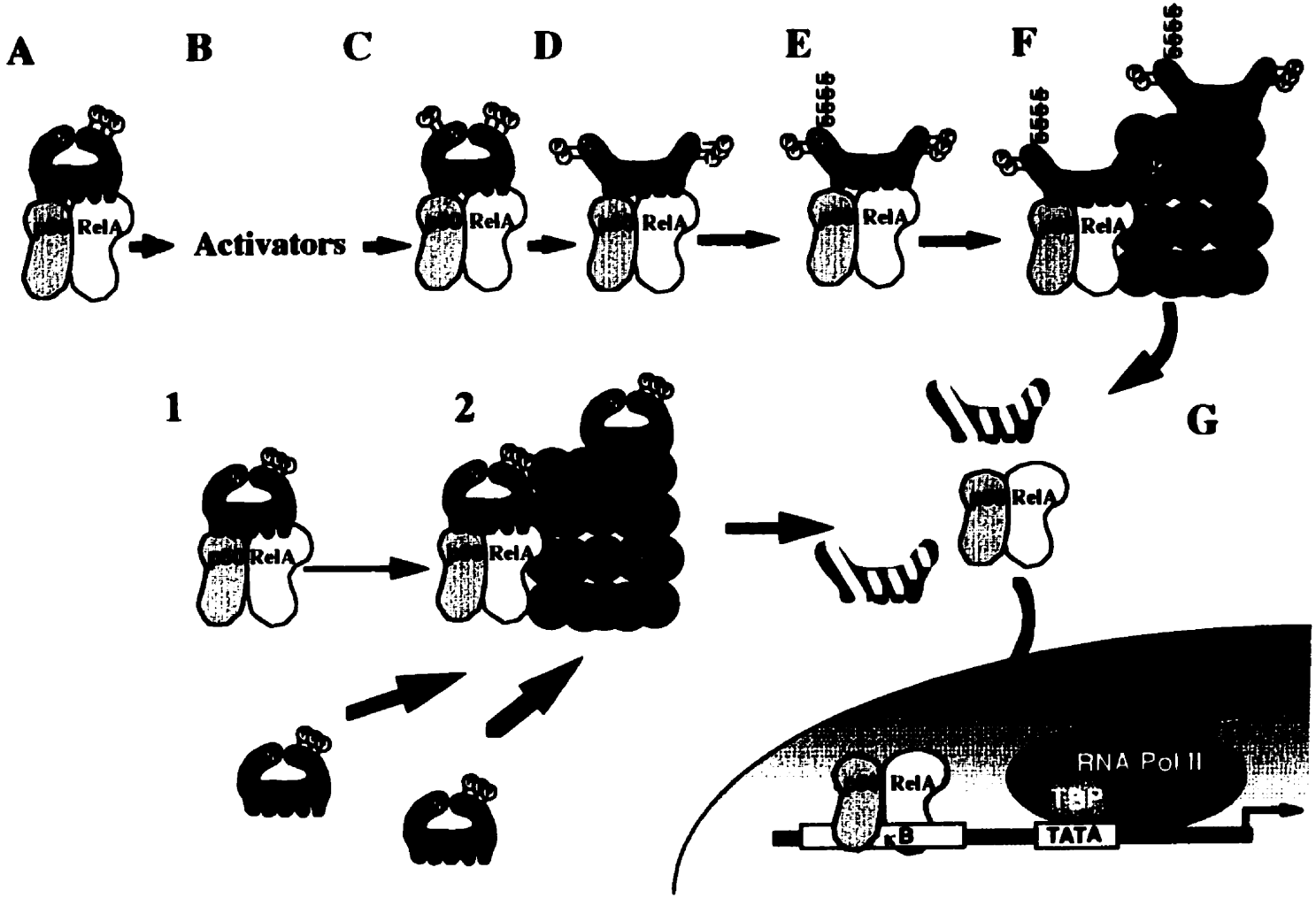
A
B
C
D
E
F
RelA
Activators
1
2
G
RNA Pol II
TBP
TATA
κB

phosphorylation or degradation of the protein (37) (Figure 8). Proteolysis of the inhibitor also required sequences at the carboxyl terminus of IκBα, since a mutant lacking the 41 C-terminal residues was not proteolyzed in response to inductive signals. These studies demonstrated that signal induced phosphorylation of IκBα at Ser 32 and/or Ser 36 was necessary for proteolysis of the inhibitor and for activation of NF-κB (37,181). Proteolysis of IκBα required additional COOH-terminal PEST sequences, a region rich in Pro Glu/Asp Ser and Thr residues often found in proteins that turn over rapidly (Figure 8).

Removal of the N-terminal 36 amino acids of IκBα, or specific point mutation of Ser-32 or Ser-36 blocked phosphorylation, degradative loss and functional release of IκBα from NF-κB as a consequence of Tax overexpression (35). These NH2-terminal alterations created transdominant repressors that escaped from Tax induced turnover and inhibited NF-κB activation. Introduction of a phosphoserine mimetic at aa32 and aa36 corrected the IκBα defect, indicating a causal relationship between phosphorylation and proteolytic degradation of the inhibitor (Figure 8). Tax may associate with and/or activate a host kinase that phosphorylates IκBα, or Tax may act upstream of the kinase(s) responsible for inducible IκBα phosphorylation. These studies thus define a signal response domain in IκBα that regulates inducible degradation of IκBα in response to a diverse range of NF-κB activators that include tumor necrosis factor, T cell activation signals and HTLV-I Tax protein (35,37).

10. Multiple mechanisms of Tax-mediated transactivation.

The observation that Tax interacts physically with NF-κB2(lyt-10) suggests that Tax may mediate its transforming potential at least in part via association with an NF-κB protein previously implicated in B and T cell leukemogenesis (50,129,157). In the B cell lymphoma associated chromosomal translocation t(10;14)(q24;q32), the amino-

terminal DNA binding domain of NF-κB2(lyt-10) is juxtaposed to the immunoglobulin Cα locus resulting in the generation of a NF-κB2-IgCα1 fusion protein. The t(10;14) chromosomal translocation produced a constitutively activated, DNA binding NF-κB2 molecule via loss of the ankyrin repeat-containing carboxy terminus and transcriptional deregulation of NF-κB2 caused by translocation into the transcriptionally active immunoglobulin locus (157). By analogy, HTLV-I, utilizing the Tax protein, may activate gene expression by interfacing with the NF-κB/*rel* signaling pathway at the level of the NF-κB2 protein.

It is not clear whether Tax remains associated with the NF-κB dimers translocating to the nucleus. However, other functions attributed to Tax suggest that it does. Tax enhanced the DNA binding activity of the ATF/CREB cellular proteins that bind to the HTLV-I 21-bp repeats (59). This activity was mediated through the DNA binding and dimerization domains of these proteins and did not require formation of stable Tax-containing complexes (52). Tax was also shown to increase the *in vitro* DNA binding activity of ATF/CREB proteins by stimulating dimerization, and thus facilitating the DNA binding reaction (188). Enhancement of dimerization and DNA binding may allow dimers containing at least one strong transcriptional activation domain (e.g. RelA or c-Rel) to efficiently activate transcription, perhaps without further involvement of Tax. The capacity of Tax protein to increase the binding of cellular transcription factors to DNA via an increase in dimerization represents a unique mechanism by which Tax may mediate its effects on gene expression.

The Tax transactivation function could play a direct role in stimulating transcription. Tax may associate with subunits such as p52 or p50, which are strong DNA binding proteins that lack a transactivation function. The resulting complexes would combine

both DNA binding and transactivation functions necessary to induce transcription (202).

11. Tax induction of the IRF-4

Interferons (IFNs) are a large family of multifunctional proteins involved in antiviral defense, cell growth regulation and immune activation (132). As such, extensive studies of the IFNs has lead to their successful application as therapeutic agents in a variety of diseases such as leukemia and multiple sclerosis (132). Upon viral infection, type I (IFN-α/β) or type II (IFNγ) IFNs are secreted by cells (132). Type I IFNs are produced by many cell types whereas type II is limited to T cells and natural killer cells (NK) (132). Secreted IFNs interact in an autocrine and paracrine manner to induce gene expression through the JAK-STAT pathway (132). By this mechanism the antiviral state is induced in uninfected cells which provides a primary means of defense.

The most important IFN inducible cellular genes identified to date are the Interferon Regulatory Factors (IRFs). Recently the IRF family has expanded to include 10 members; IRF-1, IRF-2, IRF-3, IRF-4, IRF-5, IRF-6, IRF-7, ICSBP, ISGF3γ, vIRF. The IRFs can be classified into three groups; 1) activators of gene expression (IRF-1, IRF-3 and ISGF3γ), 2) repressors (IRF-2 and ICSBP) and 3) both activator and repressor (IRF-4) (132). IRF expression is either constitutive and/or induced upon treatment with IFNs, cytokines or viral infection. Regulation of IRF activity is partially at the post-translational level, generally through structural modification induced by phosphorylation and by differential dimerization between IRF members. Studies characterizing IRF expressing cell lines and IRF knockout mice reveal that distinct roles can be attributed to each member of the IRF family (reviewed in (132).

11.1. IRF-4/ICSAT

Recently, IRF-4 (variously known as LSIRF, Pip and ISCAT), a new human lymphoid restricted IRF family member was isolated (195). IRF-4 is expressed in B cells and only in T cells activated by PMA/ionomycin or when HTLV-I Tax infected.

As all members of the IRF family, IRF-4 shares significant homology in the N-terminal 115 amino acids which comprise the DNA binding domain (DBD) (Figure 9). The C-terminal region functions as the transactivation domain. Within the C-terminal region, amino acids 138-450 are required for autoinhibition of DNA binding and is important for ternary complex formation with PU.1 and DNA (33).

In B cells, IRF-4 heterodimerizes with PU.1 to bind within $Igloo_{-4}$ enhancer, regulating λ light chain expression. PU.1 is an erythrocyte, macrophage and B cell specific protein related to the *ets* family of transcription factors (140). Proper expression of PU.1 is essential for hemopoetic development. Overexpression of PU.1 leads to immortilization and malignant transformation of erythrocytes whereas a PU.1 knockout results in a loss of B cell, T cell, granulocyte, and monocyte development (159). Three structural domains have been identified within the PU.1 protein: 1) the amino terminus contains the transcriptional activation domain, 2) a PEST domain is located in the central region (between amino acids 120 and 160) and 3) at the C-terminus (amino acids 161-260), the DNA-binding ETS domain. The PU.1-IRF-4 heterodimer binds to the λB sequence. However, while PU.1 can bind to its cognate site in the absence of IRF-4, IRF-4 binding to λB is PU.1 dependent. A two step-model for PU.1 mediated recruitment of IRF-4 to DNA has been proposed. First, in the absence of DNA, PU.1 binds to IRF-4 via the PU.1 ETS domain. This interaction does not require the PU.1 PEST domain or PU.1 phosphorylation and does not result in recruitment of IRF-4 to DNA (140). Second, phosphorylation of PU.1 at serine 148 induces a

Figure 9: The functional domains of Pip/IRF-4. IRF-4, as with all members of the IRF family share significant homology in the N-terminal 115aa which comprises the DNA binding domain (DBD). The IRF Association Domain (IAD) is a region first identified in ICSBP responsible for its interaction with IRF-1 and IRF-2; Two region of Pip responsible for autoinhibiton of DNA binding and ternary complex formation are shown: domain A is a separate functional domain whose fusion to a heterologous IRF DBD prevents DNA binding and association with PU.1 and DNA, whereas domain B is not a separable domain but is essential for this phenotype. Domain A also confers transactivation upon PU.1/Pip interaction.

Activator/Repressor

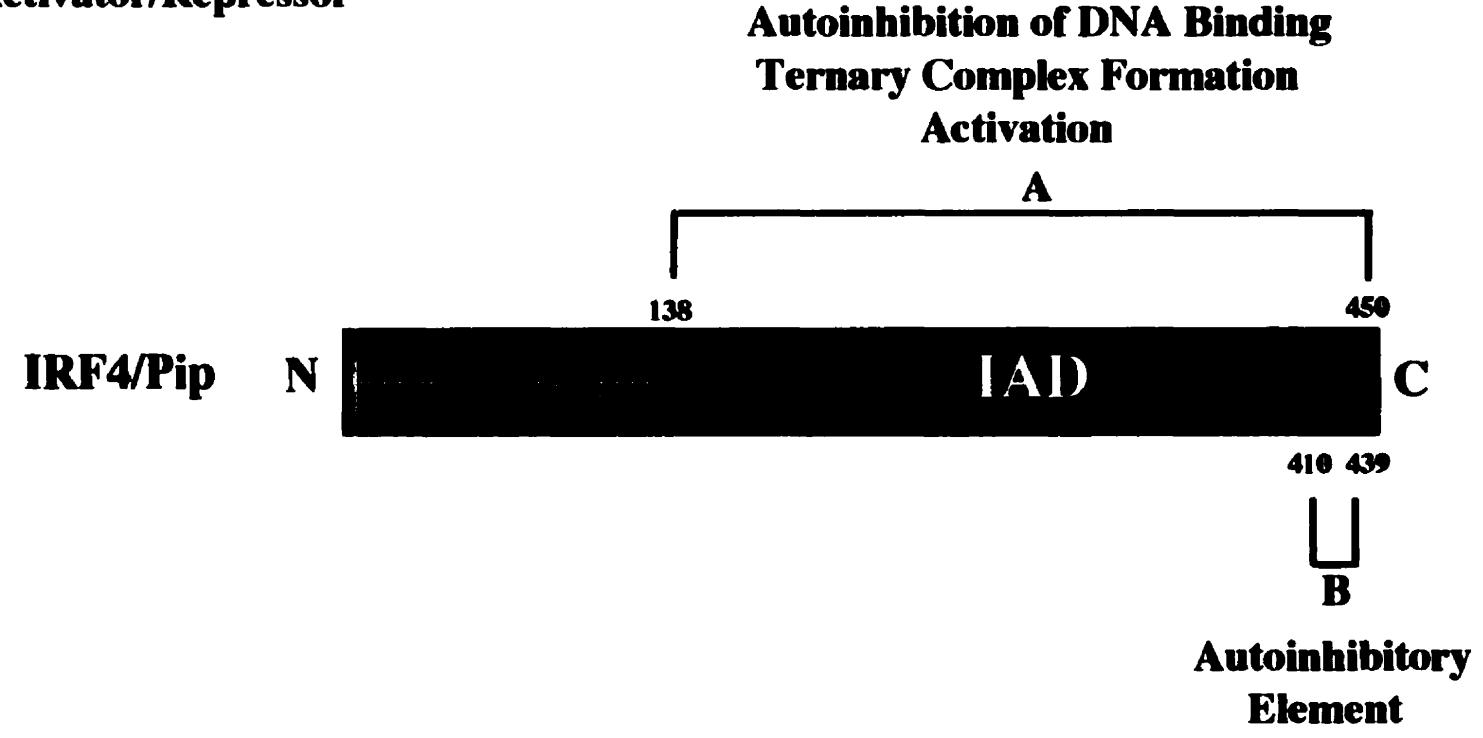

structural change in the PU.1 protein. This structural change may directly induce changes in IRF-4 that either exposes or alters the IRF-4 DNA-binding domain, enabling recruitment and binding of IRF-4 to DNA (140).

In resting T cells, IRF-4 is not expressed (25). Only upon stimulation with PMA and ionomycin is IRF-4 expression detected in T cells . Interestingly, T cells isolated from patients with ATL were shown to also express IRF-4. Moreover, Tax alone is capable of inducing IRF-4 expression (25). Since the oncogenic potential of HTLV-I resides with the transactivation capabilities of Tax, induction of IRF-4 expression by Tax may be an important cellular target implicated in HTLV-I induced leukemogenesis (132). Interestingly, IRF-4 knockout mice develop severe immunodeficiencies. While normal T cell and B cell distribution is observed at 4-5 weeks of age, the IRF-4 deficient mice soon develop severe lymphadenopathy (132). Both B cell and T cell activation is profoundly affected; serum immunoglobulin concentrations and antibody responses are reduced (132). In addition, cytotoxic and antitumor responses are absent in the IRF-4 deficient mice (132). Early T cell activation events such as calcium influx and the expression of activation markers CD25 and CD69 occur normally in IRF-4 deficient mice. Therefore, IRF-4 may function at a later step in T cell activation, possibly at the level of IL-2 production and/or IL-2 response since exogenous IL-2 does not induce T cell proliferation in these cells (132).

Unlike in B cells, the IRF-4 protein in T cells binds to the ISRE sequence. Binding to the ISRE results in repression of IFN α/β gene expression (195). Therefore, IRF-4 has a dichotomous function; in B cells, IRF-4 associates with PU.1 to activate transcription whereas in T cells IRF-4 can act alone in binding and repressing IFN α/β transcription.

Altogether, these results suggest a complicated mechanism of cellular transformation. The model emerging from these recent studies is that expression of the Tax protein in HTLV-I infected cells targets the NF-κB/IκB transcription complex, as well as other host proteins, at multiple regulatory levels. Tax mediates the induction of IκBα phosphorylation and rapid degradation, the formation of complexes between Tax and NF-κB2, as well as other family members, and indirectly mediates the transcriptional activation of c-Rel, NF-κB2 and IκBα genes by an autoregulatory mechanism. These molecular events culminate in constitutive nuclear NF-κB DNA binding activity composed of multiple heterodimers of c-Rel, NF-κB2 p52 and NF-κB1 p50 and transcriptional activation of NF-κB-regulated genes. In particular, induction of the IL-2 and IL-2Rα expression establishes a positive autostimulatory loop that initiates a polyclonal proliferation of $CD4^+$ T lymphocytes. This rapidly growing population presumably undergoes multiple mutational events (152) that, over a time period involving decades *in vivo*, favor the appearance of a leukemic population of T cells.

Specific Research Aims

HTLV-I infection initiates a multistep oncogenic process which ultimately results in the leukemic transformation of $CD4^+$ T cells. The HTLV-I Tax protein is essential for viral gene transcription and responsible for leukemogenesis. Tax mediated transcriptional activation occurs indirectly through interactions with cellular transcription factors. One of the cellular targets of Tax mediated transactivation is the NF-κB/Rel family of transcription factors. Evidence has indicated that sustained NF-κB/Rel activity is necessary for the maintenance of the transformed phenotype and constitutive NF-κB activity is observed in HTLV-I and Tax expressing cells. The overall objective of this work was to elucidate the molecular mechanisms by which Tax mediates constitutive NF-κB activity in HTLV-I infected cells. The following research aims were developed: The first aim was to examine the effect of Tax on the NF-κB inhibitory molecule IκBα. The results demonstrated a Tax induced degradation of IκBα through induction of the signal response pathway. Evidence indicated a direct interaction with members of the NF-κB/Rel family *in vivo*. The second aim was to investigate the effect of Tax-NF-κB interactions on NF-κB binding and transactivation. Direct Tax-NF-κB interactions demonstrated an increase in NF-κB dimer formation and enhanced DNA binding. In the process, a direct Tax-IκBα interaction was observed in Tax expressing cells. The third aim was to investigate the physiological role of a Tax-IκBα interaction. Evidence indicated that Tax preferentially interacted with N-terminally hypophosphorylated IκBα. IκBα was found to associate to one of the proteasome subunits in a Tax dependent manner. Finally, the constitutive turnover of IκBα was enhanced in the presence of Tax.

Chapter 2

Materials & Methods

1. Cell lines

1.1. Cell lines

Jurkat cells are $CD4^+/CD8^-$ human immature T helper lymphocytes. Although these cells are immortalized and continuously growing, they resemble normal resting T cells both in morphology and activation requirements. Therefore, through out the work presented in this thesis, they have been used as the normal control against which Tax expressing and HTLV-I infected T cells were compared. The MT-2 cell line is a human T cell line isolated from umbilical cord blood lymphocytes co-cultured with cells from ATL patients. These cells are transformed with and continuous producers of HTLV-I virions (121). The HTLV-I-transformed MT-4 cells are human T cells isolated from a patient with ATL. C8166-45 cells are human umbilical cord blood lymphocytes co-cultured with cells from ATL patients. The HTLV-I genome contained in these cells is largely deleted, and only the Tax and Rex viral proteins are expressed. 293 cells are human fibroblast cells, N-Tera-2 cells are human embryonal carcinoma and finally, NIH 3T3 cells are mouse fibroblast cells.

1.2. Cell Culture

293 cells were grown in alpha minimal essential medium containing 10% fetal calf serum. The T cell lines, Jurkat, MT-2, MT-4 and C8166 were grown in suspension in RPMI-1640 (GIBCO), with 10% fetal bovine serum. NIH 3T3 cells were grown in D-MEM containing 10% fetal bovine serum. All cell lines were supplemented with 2 mM /L-glutamine and gentamycin (10 μg/ml).

2. Cell Transfection

2.1. Lipofectamine transfection of NIH 3T3 cells

NIH 3T3 cells ($1x10^6$) were seeded into 10 cm plates prior to transfection. Appropriate amounts of DNA (see figure legends) and lipofectamine (Lipofectamine, GIBCO) were diluted in D-MEM (without serum), gently mixed together and incubated at room temperature 30 min to allow formation of complexes. Complexes were then diluted with 200 µl of D-MEM and added to subconfluent cells previously rinsed with D-MEM (without serum). Cells were exposed to DNA complexes for 5 hr and then, to terminate the reaction, fed with an equal volume of D-MEM 20% FBS for 18-24 hr at 37°C. Medium was then replaced with fresh, complete medium and the incubation was continued for an additional 24 h.

2.2. Electroporation of Jurkat cells

Jurkat cells (10^7/sample) were washed twice in RPMI without FCS or antibiotics. The cells were then resuspended at a concentration of 10^7 cells in a total volume of 380 µl of RPMI and transferred to a 0.4 cm cuvette. DNA (10 µg) was added to a final volume of 400 µl. Electroporation was done at 275V and at 960 µF. Following electroporation, the cells were cooled on ice for 10 minutes and then transferred to complete media (RPMI with 10% FBS).

2.3. Transfection by calcium phosphate of N-Tera-2 and 293 cells

Using the calcium phosphate method (109), N-Tera 2 cells (2×10^6 cells) were transfected with wild type Tax (10 µg) or with the Tax mutants M22 (NF-κB$^-$/CREB$^+$) or M47 (NF-κB$^+$/CREB$^-$) (163) and with 0-10 µg of IκBαΔ4 (18,107) for 48h. Cells were then harvested and used for CAT analysis or immunoprecipitations.

293 cells (2 x 10^6 cells) were transfected with ΔNIκBα with Tax (10 μg) or without Tax and allowed to incubate for 48h. Cells were then labeled for pulse chase analysis, harvested and extracts subjected to immunoprecipitations.

3. Recombinant DNA

3.1. Reporter gene constructs

The chloramphenicol acetyltransferase (CAT) gene was used as a reporter for transcriptional activity in transient expression assays. The SV1CAT plasmid contains the CAT gene under the control of the GC-rich SV40 promoter but lacks SV40 enhancer activity (122). The SV2CAT construct uses both the promoter and strong enhancer of SV40 to drive CAT gene expression. The HIV/CAT construct links the complete HIV-1 LTR (-350 to +80) to the CAT gene. The κB(3)/CAT (or HIV enh/CAT) construct was obtained by inserting three copies of the HIV-1 NF-κB enhancer into the enhancerless *Acc*I-*Sph*I-cleaved SV1CAT vector (Figure 10).

3.2 Constitutive expression vectors

Wild type and mutated human IκBα cDNAs were inserted downstream of the Simian virus-40 (SV40) promoter in the pSVK3 mammalian expression vector. The pHTat vector contains the Tax gene flanked by the 5' and 3' HTLV-I LTR. Both M22 (NF-κB$^-$/CREB$^+$) and M47 (NF-κB$^+$/CREB$^-$) mutant Tax are cloned in CMV promoter containing vectors. The proteasome subunits HC9 (pSGF-HC9) and HsN3 (pSGF-HsN3) which were a gift from Dr. Pierre Jalinot, contain an N-terminal Flag tag. The T7-tagged K21/22R transdominant mutant was a gift from Dr. D. Ballard.

Figure 10: Reporter gene constructs. The U3 and R regions of HIV-1 LTR are subdivided into the modulatory and negative regulatory elements, the enhancer (including two NF-κB sites), the core promoter and the TAR elements to which viral and cellular factors bind. HIV CAT reporter plasmids contain wild type or mutated version of the HIV LTR, linked to the CAT gene: all encode the TAR elelment.

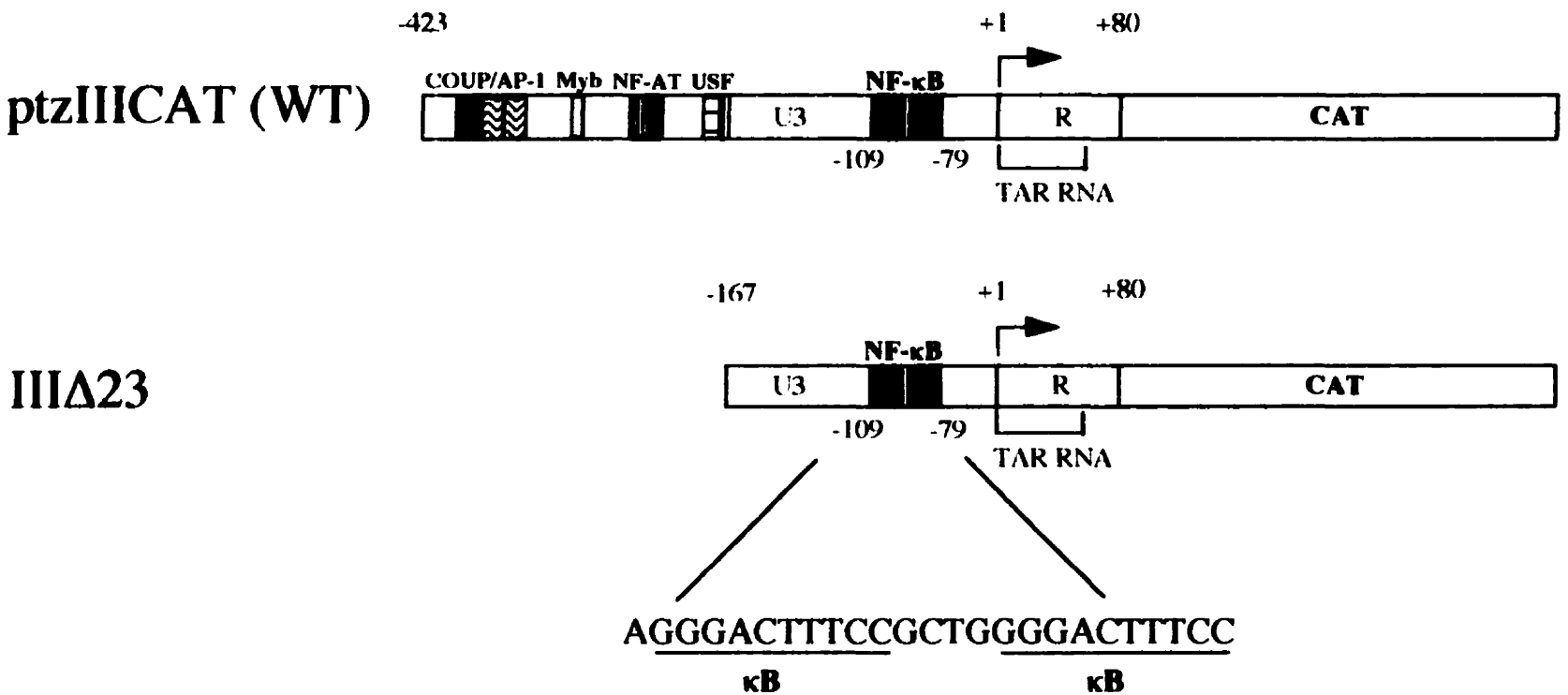
ptzIIICAT (WT)
-423
+1
+80
COUP/AP-1
Myb
NF-AT
USF
NF-κB
U3
R
CAT
-109
-79
TAR RNA
IIIΔ23
-167
+1
+80
NF-κB
U3
R
CAT
-109
-79
TAR RNA
AGGGACTTTCCGCTGGGGACTTTCC
κB
κB

3.3. Recombinant protein expression vectors

Plasmids for the expression of NF-κB-GST fusion proteins were produced by subcloning different NF-κB cDNAs into pGex-2T or pGex-3X vectors (Pharmacia) (101); p50, p65 and N'p65 (transactivation domain is deleted) were cloned into pGex-3X and p52 and IκBα were cloned into pGex-2T. The fragment containing the amino-terminal 55 amino acids (aa) of IκBα. (NIK) amplified by PCR with primer A (5'GATCGTCGACAGCTCGT CCGCGCATGTTC-3') and B (5'-GTCCGTCGACCTCGGTGAGCTGCTGCTTCC-3'), cut with Sal I blunt ended and cloned into the Sma I site of pGex-2T. The IκBα ankyrin (ANK) domain was amplified using primers C (5'-GTGAGAAT TCCCTCTGTGTCA-3') and D (5'-TTCAGGGATCCTGTAATGGCC-3'). The fragment was digested with Bam HI and Eco RI and cloned into pGex-2T. The C-terminal domain was sub cloned from pSVK3-IκBα using restriction sites Pvu II/Sal I and cloned into Sma I/ Sal I of pGex-4T-2. The full length IκBα was cloned into the Eco RI site of pGex-2T. c-Rel and Tax were polyhistidine tagged by subcloning into the pAcH6N1 vector.

4. Expression and purification of recombinant proteins

4.1. Expression in bacteria

The IκBα fusion proteins of GST-IκBα, GST-NIK (1-55 aa), GST-ANK (55-222 aa) and GST-CIK (272-317 aa) were isolated from *E.coli* DH5α strain (GIBCO/BRL) following a 3h induction with 1 mM IPTG (Pharmacia) at 37°C. Induced bacteria were then harvested resuspended in PBS and sonicated. To the extract, 1% Triton X-100 final volume was added and centrifugated at 10,000 g to remove cellular debris. The clear bacterial extracts in PBS/1% Triton X-100 were then incubated with glutathione sepharose beads (Pharmacia) for 20 min at room temperature. After washing three times with PBS, the fusion proteins were stored on the beads with the addition of

protease inhibitors for use in affinity chromatography or eluted with 15 mM GSH and stored at -80°C for use in EMSA.

4.2 Expression in Sf9 insect cells

Tax and c-Rel were polyhistidine tagged by subcloning into the pAcH6N1 vector. For the production of polyhistidine tagged protein, recombinant baculoviruses were prepared using the BaculoGold™ transfection kit as recommended by the manufacturer (Novagen, pET System manual). Sf9 cells were infected with recombinant baculoviruses and cultured for 4 days at 28°C. Infected cells were harvested, washed with PBS, and lysed in binding buffer (5 mM imidazole, 500 mM NaCl, 20 mM Tris-HCl, pH 7.9). Recombinant proteins were purified using rapid affinity purification with His-Bind metal chelation resin under non-denaturing conditions as recommended by the manufacturer (Novagen, pET System Manual).

5. Analysis of protein interactions

5.1. Affinity chromatography

The GST fusion proteins were expressed and immobilized on glutathione beads as described above. The GST-NF-κB proteins immobilized onto the glutathione agarose beads were washed three times with HNTG (20 mM Hepes pH 7.9, 150 mM NaCl, 10% glycerol, and 0.1% Triton). For protein interactions, 300 ng of glutathione agarose bound GST-NF-κB was incubated overnight at 4°C with 50 ng of His-Tax in a final HNTG volume of 200 µl. Following incubation, the beads were washed three times in 500 µl of HNTG and 20 µl of SDS sample buffer was added. The samples were then boiled and loaded on an SDS-PAGE for immunoblot analysis with anti-Tax antibody.

The GST-IκBα, GST-NIK, GST-ANK and GST-CIK fusion proteins were expressed and immobilized on glutathione beads as described above. GST-IκB proteins immobilized onto glutathione agarose beads were washed three times with HNTG (20 mM Hepes pH 7.9, 150 mM NaCl, 10% glycerol, and 0.1% Triton). For protein interactions, 300 ng of glutathione agarose bound GST-IκB was incubated overnight at 4°C with 50 ng of His-Tax in a final HNTG volume of 200 µl. Following incubation, the beads were washed three times in 500 µl of HNTG and 20 µl of SDS sample buffer was added. The samples were then boiled and loaded on a 10% SDS-PAGE. After electrophoresis, the proteins were transferred to Hybond transfer membrane (Amersham). The membrane was blocked by incubation in phosphate-buffered saline (PBS) containing 5% dried milk for 1h and then probed with anti-Tax antibody in 3% BSA/PBS, at a dilution of 1:1000. These incubations were done at 4°C overnight. After three 15 minute washes with PBS, membranes were reacted with peroxidase-conjugated secondary goat anti-rabbit antibody (Amersham) at a dilution of 1:1000. The reaction was then visualized with the enhanced chemiluminescence detection system (ECL) as recommended by the manufacturer (Amersham Corp).

5.2. Immunoprecipitations

Cells were lysed in TNN buffer (20 mM Tris-HCl (pH 7.5), 200 mM NaCl and 0.5% NP40). Extracts were then subjected to immunoprecipitation as follows: protein (500 µg) was diluted in TNN. The extract was first pre-cleared by incubation with normal rabbit or mouse serum at a final dilution of 1:25 for 1h at 4°C, followed by recovery of non-specific immune reactions on protein A-Sepharose (4°C, 1h). Polyclonal anti-Tax antiserum was then added to a final dilution of 1:25 and incubated for an additional 1h at 4°C. The specific immune complexes were recovered with protein A-Sepharose by a final incubation of 1h at 4°C. The beads and immune complexes were washed three times in TNN, resuspended in sample buffer, boiled and resolved on SDS-PAGE.

5.3. Protein crosslinking

Chemical crosslinking of recombinant NF-κB proteins was performed using 50-200 ng of NF-κB protein alone or in the presence of 50-200 ng of His-Tax. NF-κB proteins were allowed to incubate with or without Tax in binding buffer (20 mM HEPES, pH 7.9; 200 mM NaCl; 20 mM Tris-HCl, pH 7.5 and 1 mM DTT) for 30 min. at room temperature. Dimethyl pimelimidate-2HCl (DMP) or glutaraldehyde was added to the reaction mixture at a final concentration of 5 mM and 0.05% respectively, and incubated for an additional 15 min. at room temperature. Crosslinking was terminated by bringing the solution to 100 mM Tris-HCl pH 7.5 and the products were then analyzed by 10% SDS-PAGE and visualized by immunoblotting.

5.4. Detection of hyperphosphorylated IκBα

N-terminally hyperphosphorylated IκBα migrates at a higher molecular weight on SDS-PAGE. To resolve the hyperphosphorylated form IκBα, 20 μg to 50 μg of protein extracts were resolved by 10% or 15% SDS-PAGE. Proteins were transferred on nitrocellulose and both hyperphosphorylated and N-terminally unphosphorylated IκBα were detected using monoclonal IκBα antibody. Hyperphosphorylated IκBα migrates more slowly and appears as a distinct band sensitive to phosphatase treatment. Specific detection of the hyperphosphorylated IκBα were detected using antibody that recognized only Ser32 phosphorylated IκBα (New England biolabs). *In vitro* dephosphorylation of IκBα was achieved by incubating 20 μg of extracts with 2 units of calf intestinal alkaline phosphatase (CIP, 1 unit/ml, Promega) for 30 min. at 37°C. Final volumes were adjusted to 20 μl with 10x CIP buffer (0.5M Tris HCl, pH 9.0, 10 mM $MgCl_2$, 1 mM $ZnCl_2$, 10 mM spermidine) and water. Additional reactions also contained both CIP and phosphatase inhibitors (Na_3VO_4, 10 mM and NaF, 50 mM, final), to block *in vitro* dephosphorylation of IκBα. SDS sample buffer was added to 1X final concentration and samples were boiled and loaded on 12% SDS-PAGE gels.

To prevent IκBα hypophosphorylation, antioxidants N-acetylcysteine (NAC) (Boeringer Mannheim GmbH) and pyrrolidine dithiocarbamate (PDTC) (Sigma) were used. To prevent the degradation of IκBα and therefore accumulate hypophosphorylated IκBα, the proteasome inhibitor Calpain Inhibitor I (ICN) or MG132 were used. Cells were pretreated with an antioxidant or proteasome inhibitor for 1h.

6. Immunoblotting

Gels were transferred to nitrocellulose and incubated overnight with monoclonal IκBα or rabbit Ser32 phosphorylated specific IκBα antibody (New England Biolabs). Similarly, Peroxidase-conjugated anti-mouse antibody was used against the monoclonal antibody and the bands visualized by the enhanced chemiluminescence detection system (Amersham).

6.1. Whole cell extracts

For preparation of whole cell protein extracts, cells were collected and washed with phosphate buffer saline (PBS). The cells were then lysed in WBL buffer (10 mM Tris HCl pH 8.0, 60 mM KCl, 1 mM EDTA, 1 mM dithiothreitol (DTT), 0.5% Nonidet P-40, 0.5 mM PMSF, 0.01 μg/μl Leupeptin, 0.01 μg/μl Pepstatin, 0.01 μg/μl Aprotinin). Insoluble cellular debris was removed by centrifugation at 10,000 g for 5 min. at 4°C. The protein concentration of extracts was estimated using the Bradford protein assay from Bio-Rad. Equivalent amount of protein samples were aliquoted and boiled in a final concentration of 1x sample buffer. The samples were then resolved on a 10% to 15% sodium dodecyl sulfate (SDS)-polyacrylamide gel electrophoresis (PAGE) and transferred to nitrocellulose membrane (Amersham).

7. Measuring the half life of IκBα

The IκBα protein half life was examined from Jurkat cells and the HTLV-I infected cell lines, MT-2, MT-4 and C8166-45. Cells were incubated in the presence of 50 μg/ml of cycloheximide and time points were taken for upto 8 hours. Samples were then analyzed by western blot.

8. Pulse Chase analysis

NIH 3T3 cells transfected with 7 μg of IκBα, IκBα(2N) and 293 cells with ΔNIκBα with and without Tax (10 μg) were cultured for 1 hour in methionine-free RPMI supplemented with 2% dialyzed fetal calf serum, pulse-labeled for 1h with ^{35}S-methionine (0.5 mCi/ml, ICN, Trans-label), and chased with cold methionine for 0, 4, 8 and 16 hours. Cells were harvested and lysed in TNN buffer (20 mM Tris HCl, pH 7.5, 200 mM NaCl, 0.5% Nonidet P-40 (NP40), 0.5 mM phenylmethysulfonyl fluoride (PMSF), 5 mg/ml leupeptin, 5 mg/ml pepstatin, 5 mg/ml aprotinin, 10 mM NaF and 0.4 mM Na_3VO_4). Extracts were then subjected to a double immunoprecipitation as follows: 500 μg of protein was first pre-cleared by incubation with 5 μl of preimmune rabbit serum and 20 μl of protein A- Sepharose beads (Pharmacia) for 1 h at 4°C. The extract was incubated with 10 μl of anti-IκBα antibody specific for the N-terminus (IκBα, IκBα(2N)) or C-terminus (ΔNIκBα) and 30 μl of protein A-Sepharose beads overnight at 4°C. Specific immune complexes were recovered on protein A-Sepharose beads, washed three times with 500 μl of TNN buffer, resuspended in sample buffer, boiled and resolved on a 10% SDS-PAGE. After gels were run, they were fixed, enhanced for flurography (Amplify, Amersham), dried and autoradiographed at -80°C.

9. Freeze-thaw lysis of cells

About 10^7 cells were washed with cold PBS and resuspended in 60 µl of 0.25 M Tris-HCl, pH 7.8. Cells were lysed by three cycles of freeze (15 min on dry ice)-thaw (5 min in 37°C water bath). Debris were microfuged for 5 min, and supernatants were collected and assayed for protein concentration by the Bio-Rad protein assay.

10. CAT assays

48 hr after transfection, cells were harvested and assayed for accumulated CAT activity by standard procedure (122). The appropriate amount of freeze-thaw extract (see figure legends) was diluted in 0.25 M Tris-HCl, pH 7.8, to a total volume of 60 µl. The following was then added: 70 µl of 1 M Tris-HCl, pH 7.8, 20 µl of 3.5 mg/ml acetyl coenzyme-A (Pharmacia) and 0.5 µl of D-threo-(dichloroacetyl-1-^{14}C) chloramphenicol (Amersham, 54 mCi/mmol). This mixture was incubated in a 37°C water bath for the appropriate period of time (see figure legends) and the labeled chloramphenicol was extracted with 1 ml of ethyl acetate which was subsequently evaporated under dry air. Pellets were resuspended in 30 µl of ethyl acetate, spotted on a TLC plate (Whatman), and resolved by ascending thin layer chromatography (TLC) in 95% chloroform- 5% methanol. The plate was dried, enhanced with Amplify (Amersham) and autoradiographed at -80°C. Percent acetylation was determined by dividing the radioactivity in the acetylated forms by the sum of the acetylated and nonacetylated forms. The relative inducibility was obtained by dividing percent acetylation of treated sample by the percent acetylation of the untreated sample. A plasmid carrying the β-galactosidase gene (under the control of the RSV promoter) was co-transfected as a control for transfection efficiencies. CAT activity was normalized to the β-galactosidase activity.

11. Electrophoretic Mobility Shift Assay (EMSA)

Complementary oligonucleotides containing the NF-κB binding sites found in HIV-1-LTR or MHC I were mixed together in TNE buffer (10 mM Tris-HCl, pH 7.5, 100 mM NaCl, 1 EDTA), heated for 10 min. at 85°C and slowly cooled down to room temperature to maximize annealing. Double stranded oligonucleotides were purified on a TBE (50 mM Tris-HCl, pH 8.0, 50 mM boric acid, 1 mM EDTA) 12% polyacrylamide gel (19;1 cross link) and eluted overnight in TE (10 mM Tris HCl pH 8.0, 1 mM EDTA). The HIV-1 NF-κB probe which contains two NF-κB binding sites (5'-AGGGACTTTCCGCTGGGGA CTTTCC-3') and the MHC I probe (5'-CAGTGGGGAATCCCCATAG-3') were labeled with T4 polynucleotide kinase and γ-^{32}P-ATP. The binding reactions were carried out with recombinant protein and 0.2 ng of probe in a final concentration of 10 mM HEPES (pH 7.9), 50 mM KCl. 0.1 mM EDTA, 0.25 mM DTT, 1 μg of poly(dI-dC) and 10% glycerol and the final volume brought to 20 μl with H_2O. Recombinant proteins were incubated with the probe for up to 1h at room temperature; the mixture was loaded on a 5% polyacrylamide gel (60:1 acrylamide:N, N-methylene bisacrylamide) prepared in 1X Tris-Glycine (pH 8.3) and electrophoresed at 200V for 2-3 h. Gels were then dried and exposed on film at -80°C overnight. In competition reactions a 100-fold excess of unlabeled oligonucleotide was added to the reaction mixture for 15 min prior to the addition of radiolabeled probe.

11.1. Nuclear and cytoplasmic extracts

Cells were washed once with cold PBS, twice with buffer A (10 mM Hepes, pH 7.9, 1.5 mM $MgCl_2$, 10 mM KCl, 0.5 mM DTT, 0.5 mM PMSF, 5 μg/ml each of pepstatin, leupeptin and aprotinin), and resuspended in buffer A with 0.1% NP-40 (20 μl per 10^7 cells). After a 10 min incubation on ice, nuclei were gently mixed and microfuged 10 min at 4°C. The supernatant (cytoplasmic extract) was removed and diluted with 75 μl

of modified buffer D (20 mM Hepes, pH 7.9, 0.05 M KCl, 20% glycerol, 0.5 mM EDTA, 0.5 mM PMSF, 0.01 mg/ml each of leupeptin, pepstatin and aprotinin). The nuclear pellet was resuspended in 15 ml of buffer C (20 mM Hepes, pH 7.9, 25% glycerol, 0.42 M NaCl, 1.5 mM $MgCl_2$, 0.2 mM EDTA, 0.5 mM PMSF, 5 µg/ml each of leupeptin, pepstatin and aprotinin, 0.5 mM DTT), incubated 15 min on ice and finally microfuged 10 min at 4°C. The supernatant was collected (nuclear extract).

12. RNA detection

12.1. Preparation of RNA

Total cellular RNA was isolated from approximately 10^8 cells by a modified guanidium isothiocyanate procedure. Cells were collected by low-speed centrifugation, washed with PBS, resuspended in 5 ml of solution D (4 M guanidium isothiocyanate, 25 mM sodium citrate, pH 7.0, 0.5% sarcosyl, 0.1 M β-mercaptoethanol), and vortexed briefly to ensure lysis. 0.5 ml of 2 M sodium acetate, pH 4.0, 5 ml phenol:water, 2 ml of chloroform:isoamyl alcohol (49:1) were then sequentially added and vortexed. After 15 min on ice, phases were separated by a 20 min, 10, 000 rpm spin at 4°C (HB-4 rotor, Sorvall). The aqueous phase was collected, mixed to an equal volume of isopropanol and precipitated overnight at -20°C. The RNA was pelleted by a 20 min centrifugation (10 000 rpm, 4°C), resuspended in 0.6 ml of solution D and isopropanol-precipitated again. The RNA was finally resuspended in sterile water and the concentration was determined. For reverse transcriptase-polymerase chain reactions (RT-PCR), RNA was further treated with 1 U of RNase-free DNase (RQ1 DNase; Promega Biotec) for 15 min at 37°C in 40 mM Tris-HCl, pH 7.9, 10 mM NaCl, 6 mM $MgCl_2$. RNA was phenol extracted, ethanol precipitated, and stored at - 80°C.

12.2. Northern blot analysis

Total RNA (20 μg) was denatured, electrophoresed in a denaturing formaldehyde/1.2% agarose gel, and transferred to nylon membrane. Specific mRNA was visualized by Northern blot hybridization using DNA fragment labeled with [a-^{32}P]dCTP by nick translation using the Oligolabelling Kit (Pharmacia Biotech).

Chapter 3

Constitutive Phosphorylation and Turnover of IκBα in HTLV-I Infected and Tax-Expressing Cells

Previous studies demonstrated that Tax expressing and HTLV-I infected T cells exhibited constitutive NF-κB binding activity, composed of c-Rel, p52(NF-κB2) and p50(NF-κB1) (12,97,101,106). A Tax-dependent correlation was established between expression of NFKB2(p100 and p52), induction of c-Rel and *trans*-activation of NF-κB-mediated gene expression. Furthermore, NF-κB2 p100 physically associated with c-Rel and with Tax in HTLV-I infected cells (38,101). To understand further Tax-NF-κB/Rel interactions we have examined regulation of IκBα activity in HTLV-I infected T-cells (MT-2, MT-4), Tax expressing Jurkat T cells (19D) and Jurkat cells.

Constitutive NF-κB binding activity in HTLV-I infected cells.

In unstimulated Jurkat cells (Fig. 11A, lane 1), no NF-κB specific protein-DNA complexes were detected in nuclear extracts by mobility shift analysis (6,38,97,101,188) with a ^{32}P-labeled probe containing the human immunodeficiency virus (HIV-1) enhancer (5'-AGGGACTTTCCGCTGGGGACTTTCC-3'). After PMA treatment for 2h, NF-κB DNA binding activity was induced at least twenty fold (Fig. 11A, lane 2). Shifted shift analysis using NF-κB specific antibodies (131) demonstrated that p65, p50 and c-Rel were the main components of the protein-DNA complex (Fig. 11A, lanes 3, 6, 9); no reactivity with p52 antibody was detected (Fig. 11A, lane 12). Specificity of the shift reactions was verified by competition with an excess of peptide against which the antiserum was raised (Fig. 11A, lanes 4, 7, 10, 13). In contrast, constitutive NF-κB binding activity in MT-2 cells was composed predominantly of c-Rel, p52 and p50; with MT-2 extracts these antibodies partially inhibited formation of the NF-κB-DNA complex and also produced a shifted complex (Fig. 11B, lanes 2, 5, 8, 11). As previously demonstrated, the relative amount of p65

Figure 11. NF-κB-binding in Jurkat and MT-2 cells. Nuclear extracts were prepared from untreated or PMA-treated cells (final concentration, 25 ng/ml) as previously described {178}. Nuclear extracts (5 μg) were incubated with a 32P-radiolabeled HIV-1 enhancer probe and analyzed by electrophoretic mobility shift assay. In shifted-shift reactions, antibody specific for each NF-κB subunit (indicated above the lanes) was incubated with extract prior to probe addition. For peptide competition (indicated as + above the lanes), both antibody and peptide (1 μg) were incubated with extracts before probe addition.. Arrows indicate the antibody-protein-DNA complex. **(A) Jurkat cells.** Extracts form untreated (lane 1) or 2h PMA-induced (lanes 2 to 13), Jurkat cells were used. Lanes 1 to 4 represent a 16h exposure; lanes 5 to 13 represent a 60h exposure. **(B) MT-2 cells.** Extracts from uninduced MT-2 cells were used.

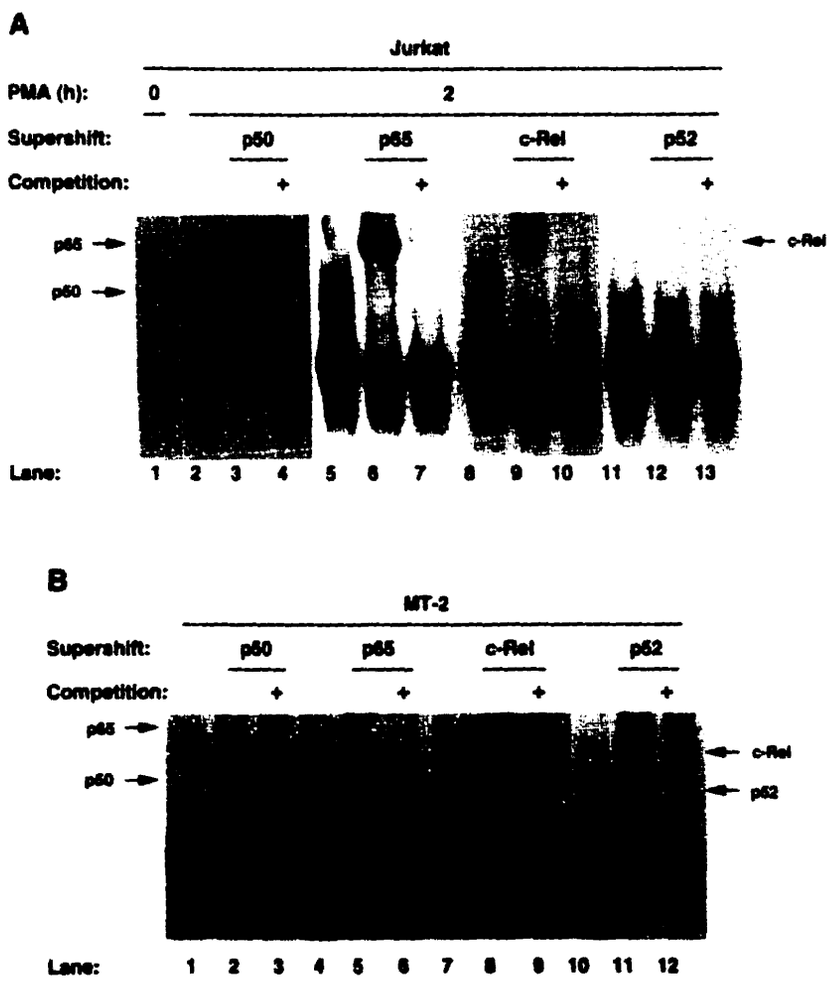
A
Jurkat
PMA (h):
0
2
Supershift:
p50
p65
c-Rel
p52
Competition:
+
+
+
+
p65
p50
c-Rel
Lane:
1 2 3 4 5 6 7 8 9 10 11 12 13
B
MT-2
Supershift:
p50
p65
c-Rel
p52
Competition:
+
+
+
+
p65
p50
c-Rel
p52
Lane:
1 2 3 4 5 6 7 8 9 10 11 12

binding activity was decreased in MT-2 cells compared to Jurkat cells (compare Fig. 11A, lane 6 and Fig. 11B, lane 5), suggesting that either p65 binding activity or protein expression was altered in HTLV-I-infected T cells.

Constitutive IκBα phosphorylation.

Phosphorylation of IκBα have been implicated as critical steps leading to NF-κB activation following induction (20,27,154,169), we examined the possibility that the constitutive NF-κB binding activity observed in HTLV-I infected and Tax-expressing cells correlated with the modification of IκBα phosphorylation state and increased IκBα turnover. Extracts from untreated or PMA-treated Jurkat and MT-2 cells were examined for the presence of phosphorylated forms of IκBα by SDS-polyacrylamide gel electrophoresis and immunoblotting using an IκBα specific antisera, essentially as described previously (139). Phosphorylated IκBα was not detected in Jurkat cells following PMA treatment for times ranging from 0 to 60 min (Fig. 12A, lanes 1 to 7, a dark exposure is shown). On the other hand, a band migrating just above IκBα was detected immediately after PMA addition to MT-2 cells (Fig. 12A, lane 10). Most importantly, darker exposure of the immunoblot revealed the slower migrating band in untreated MT-2 cells, indicating a constitutive level of IκBα phosphorylation in MT-2 cells (Fig. 12A, lane 8). PMA treatment of MT-2 cells increased IkBa levels and also increased the amount of the putative phosphorylated form (Fig. 12A, lanes 10-15). To ensure that the slower migrating form represented phosphorylated IκBα, MT-2 extracts (0 and 30 min) were treated with calf alkaline intestinal phosphatase (CIP) or CIP plus phosphatase inhibitors to dephosphorylate IκBα *in vitro* (Fig. 12B). Dephosphorylation was achieved by incubating extracts (100 μg) with 5 units of CIP for 1 hour at 37°C. Another reaction contained both CIP and phosphatase inhibitors (10 mM Na_3VO_4 and 50 mM NaF), to block *in vitro* dephosphorylation of IκBα, as previously described (20). The disappearance of the upper band with CIP treatment

Figure 12. Phosphorylated IκBα in HTLV-I infected and Tax-expressing T cells. (A) Detection of phosphorylated forms of IκBα. Whole-cell extracts were prepared from untreated Jurkat (lane 1) and MT-2 (lanes 8 and 9) cells and from cells treated with PMA for 0 min. (lanes 2 and 10), 1 min. (lanes 3 and 11), 2.5 min. (lanes 4 and 12), 5 min. (lanes 5 and 13), 15 min. (lanes 6 and 14), and 60 min. (lanes 7 and 15). The phosphorylated form of IκBα is indicated as P-IκBα by western blot analysis. Lane 8 represents a darker exposure of lane 9. **(B) In vitro dephosphorylation of phosphorylated IκBα.** Extracts from MT-2 cells treated for 0 min. (lanes 1-3) and 30 min. (lanes 4-6) with PMA were incubated at 37°C for 1h in the absence (lanes 1-4) or presence (lanes 2, 3, 5 and 6) of 5 U of CIP. Inhibitors of phosphatases (10 mM Na_3VO_4 and 50 mM NaF) were also included in reactions loaded on lanes 3 and 6. IκBα signals were detected as described above. **(C) Phosphorylated IκBα in Tax-expressing 19D cells.** Whole cell extracts were prepared from untreated 19D cells (lane 1) and from cells treated with PMA for 0, 5, 15, 30 and 60 min. (lanes 2-6, respectively). Samples were examined for phosphorylated IκBα as described above. Lane 7 is a positive control loaded with MT-2 cell extracts. **(D) Analysis of phosphorylated IκBα in untreated and TNFα treated Jurkat cells and in untreated C8166-45, MT-2 and MT-4 cells.** Whole cell extracts from untreated Jurkat cells (lane 1), Jurkat cells treated with TNF (10 ng/ml) (lane 2), C8166-45 (lane 3), MT-2 (lane 4) and MT-4 (lane 5) cells were analyzed for IκBα phosphorylation by western blot, as described above.

A

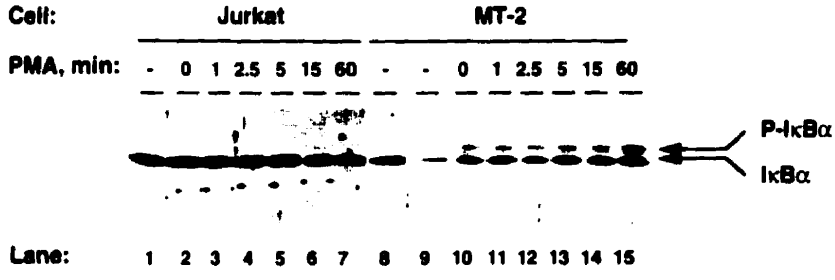
Cell:
Jurkat
MT-2
PMA, min:
- 0 1 2.5 5 15 60 - - 0 1 2.5 5 15 60
P-IκBα
IκBα
Lane:
1 2 3 4 5 6 7 8 9 10 11 12 13 14 15

B

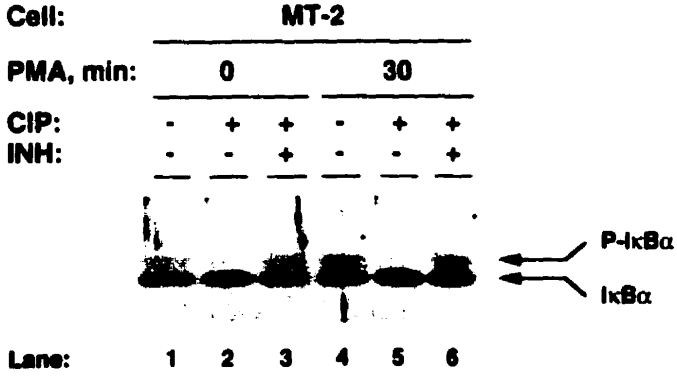
Cell:
MT-2
PMA, min:
0
30
CIP:
- + + - + +
INH:
- - + - - +
P-IκBα
IκBα
Lane:
1 2 3 4 5 6

(Fig. 12B, lanes 2 and 5) and its reappearance in the presence of CIP plus inhibitors (Fig. 12B, lanes 3 and 6), demonstrated that the slower migrating band is phosphorylated IκBα. Tax-expressing Jurkat T cells (19D) were subjected to the same analysis and also contained phosphorylated IκBα (JL, data not shown). Appropriately exposed autoradiograms were scanned by laser densitometry to determine the ratio of phosphorylated to unphosphorylated IκBα. The ratio of IκBα:P-IκBα varied from about 5:1 in unstimulated MT-2 cells (Fig. 12A, lanes 10, 11) to 2:1 in MT-2 cells treated with PMA for 60 min (Fig. 12A, lane 15). In 19D cells, the IκBα:P-IκBα ratio was 10:1 after induction with PMA. These results demonstrate that phosphorylated IκBα is present constitutively in HTLV-I-infected and Tax-expressing cells.

To extend the observation that Tax expression correlated with the presence of constitutively phosphorylated IκBα, similar analyses were performed with Tax-expressing 19D Jurkat cells (Figure 12C) and HTLV-I-infected cell lines C8166 and MT-4 (Figure 12D). Unphosphorylated IκBα was detectable in 19D cells, and immediately after addition of PMA, induced expression of phosphorylated IκBα was also detectable (Fig. 12C, lanes 1 and 2); this result was in contrast to Jurkat cells in which phosphorylated IκBα was not detected (Fig. 12A). PMA treatment further increased expression of phosphorylated IκBα in 19D cells without affecting the levels of the unphosphorylated form (Fig. 12C, lanes 3 to 6). Laser densitometry established that the IκBα-to-phosphorlylated IκBα ratio was 10:1 after induction with PMA (Fig. 12C).

C8166 and MT-2 cells express Tax, whereas MT-4 cells do not (data not shown). Phosphorylated IκBα was easily detected in C8166 cells by immunoblot analysis (Fig. 12D, lane 3), as well as in MT-2 cells (Fig. 12D, lane 4). Control reactions with CIP and phosphatase inhibitors demonstrated the phosphorylated nature of the upper band

C

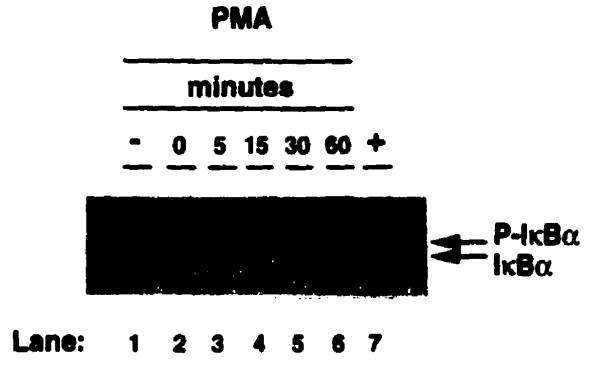
PMA
minutes
- 0 5 15 30 60 +
P-IκBα
IκBα
Lane: 1 2 3 4 5 6 7

D

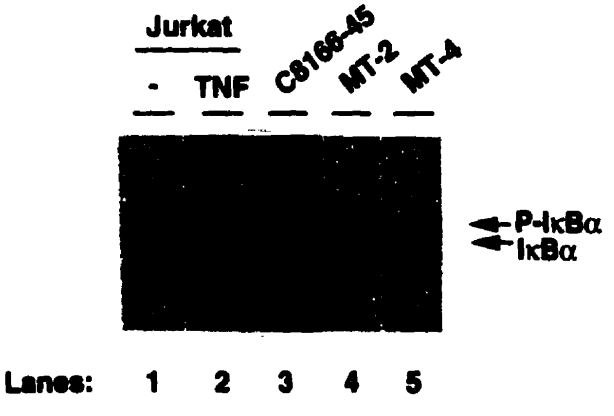
Jurkat
- TNF C8166-45 MT-2 MT-4
P-IκBα
IκBα
Lanes: 1 2 3 4 5

(data not shown). Interestingly, MT-4 cells did not express any detectable phosphorylated IκBα (Fig. 12D, lane 5). Taken together, these results demonstrate that expression of Tax proteins in T cells is correlated with the presence of phosphorylated IκBα.

Figure 12D also illustrates that treatment of Jurkat cells with TNFα (140 U/ml) for 5 min resulted in the appearance of a slower migrating phosphorylated IκBα species (Fig. 12D, lane 2). This phosphorylated IκBα form appeared to be quite unstable, since it was not detected after 15 min of TNFα treatment as described previously (20), or after PMA treatment of Jurkat cells (Fig. 12A).

Increased IκBα Turnover

Next examined was whether increased phosphorylation in MT-2 and C8166 cells was accompanied by increased turnover of IκBα. IκBα protein expression and turnover were analyzed by immunoblotting in Jurkat and MT-2 cells treated with the protein synthesis inhibitor cycloheximide for times ranging from 0 to 8 hours (Figure 13). Jurkat cell extracts contained about 7 fold more IκBα protein than MT-2 cells (Figure 13, lanes 1 and 6). Furthermore, the turnover of IκBα was more rapid in MT-2 cells (Fig. 14, lanes 7 to 10) than in Jurkat cells (Fig. 13, lanes 2 to 5). The graph shown in Figure 13 represents a quantitative analysis of the decay of IκBα in Jurkat and MT-2 cells derived from three independent experiments. The half life of IκBα in Jurkat, MT-2 and C8166 cells was calculated as 2.6±0.1, 0.85±0.04 h and 0.72± 0.27h, respectively (p<0.01) (Table 1). The treatment of Jurkat cells reduced the half life of IκBα 3-4 fold to 1.0±0.2h (Table 1). These results demonstrate that IκBα turnover is increased three fold in HTLV-I infected cells and support the model that phosphorylation of IκBα by cellular kinases may target IκBα for rapid degradation (20,27,154,169).

Figure 13. IκBα turnover in Jurkat and MT-2 cells. Jurkat cells (lanes 1-5) and MT-2 cells (lanes 6-10) were treated with cycloheximide (50 μg/ml) for times ranging from 0-8 hours, as indicated above the lanes. Whole cell extracts (20 μg) were analyzed for IκBα by immunoblotting with an IκBα-specific antibody (AR20) and visualized by chemiluminescence (Amersham). Bands corresponding to the IκBα signal were quantified by laser densitometry and the IκBα half-life was determined; the graph represents the average of three separate experiments. The level of IκBα in Jurkat (empty squares) and MT-2 (filled squares) cells at a given time, divided by the IκBα level at time zero, is plotted.

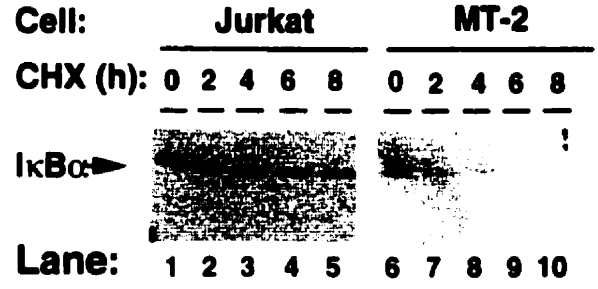
Cell:
Jurkat
MT-2
CHX (h):
0 2 4 6 8
0 2 4 6 8
IκBα
Lane:
1 2 3 4 5
6 7 8 9 10

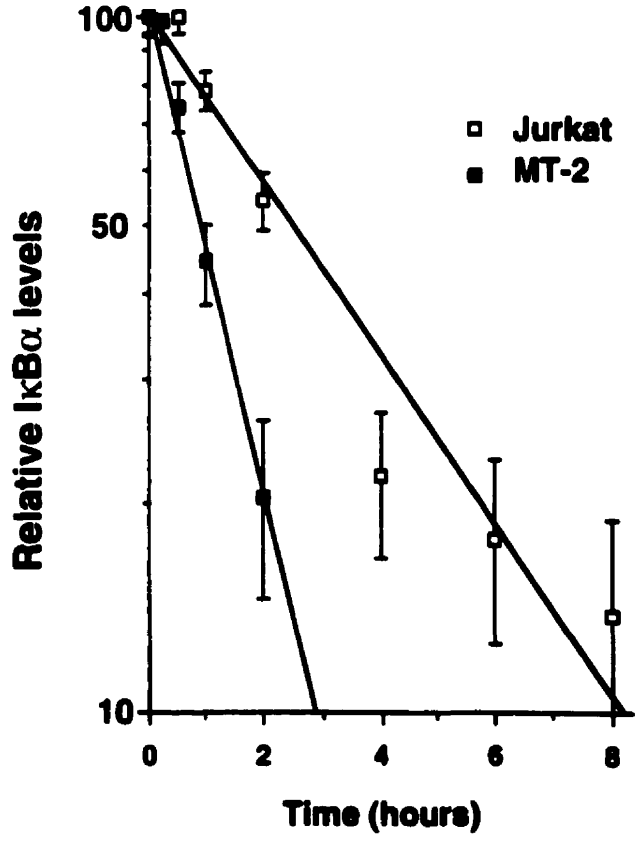
100
50
10
Relative IκBα levels
Jurkat
MT-2
0
2
4
6
8
Time (hours)

Table 1. IκBα Turnover in Normal, HTLV-I and Tax Expressing T Cells

Cells	IκBα Turnover (hr)[1]
Jurkat	2.6+/-0.1
Jurkat-PMA[2]	1.0+/-0.2
MT-2	0.85+/-0.04
C8166-45	0.72+/-0.27

[1] The indicated cells were treated with cycloheximide (50 μg/ml) for 0 to 8 hours. Whole cell extracts were prepared and analyzed for IκBα by immunoblotting as described in materials and methods. IκBα signals were quantified by laser densitometry and plotted against time of treatment. Turnover rates were averaged from 2 to 3 separate experiments.

[2] Cells were co-treated with PMA (25 ng/ml).

Overexpression of IκBα mRNA in HTLV-I infected and Tax-expressing cells.

One consequence of constitutive NF-κB binding activity is increased expression of NF-κB regulated genes, including transcriptional induction of the MAD-3(IκBα) gene itself (6,47,106,188). Therefore, to examine whether rapid turnover of IκBα and increased NF-κB binding activity correlated with increased transcription, MAD-3(IκBα) expression was analyzed by Northern blotting using poly A+ mRNA (5 μg) from Jurkat, Tax-expressing 19D, and HTLV-I-infected (MT-2 and MT-4) T cells (Figure 14). An Rsa-1 fragment of IκBα (74) labeled by random priming with [α-^{32}P]dCTP, served as IκBα specific probe. RNA signals were scanned by laser densitometry, normalized to β-actin expression and plotted as relative mRNA levels. MAD-3(IκBα) gene activity was strikingly higher in Tax-expressing and HTLV-I infected cells compared to Jurkat cells. IκBα mRNA levels were 7 to 20 fold higher in 19D, MT-2 and MT-4 cells (Fig. 14, lanes 2-4) than in normal Jurkat cells (Figure 14, lane 1). In similar experiments, the mRNA levels of NF-κB1, RelA, and c-Rel genes were also transcriptionally stimulated about two to four fold in MT-2 and MT-4 cells compared to Jurkat cells (data not shown). Thus, decreased IκBα protein level detected in MT-2 cells is not due to impaired MAD-3 gene activity; rather IκBα mRNA expression is upregulated by constitutive NF-κB activity observed in Tax-expressing cells.

The present study demonstrates that constitutive phosphorylation and increased turnover of IκBα protein occurs in HTLV-I-infected and Tax-expressing T cells. IκBα mRNA transcript levels are also increased 7 to 20 fold in Tax expressing cells, probably as a consequence of constitutive NF-κB binding activity. These results support a model in which HTLV-I Tax indirectly induced phosphorylation of IκBα targeting IκBα for degradation (74). Disruption of the NF-κB/IκB autoregulatory

Figure 14. Northern blot analysis of MAD-3 (IκBα) gene expression. Poly (A)+ RNA (5 μg) was prepared from Jurkat (lane 1), 19D (lane 2), MT-2 (lane 3), and MT-4 (lane 4) cells as described previously {54}. mRNA run on a formaldehyde agarose gel, was transferred and immobilized onto a nylon membrane. The filter was hybridized with a 32P-labeled RsaI fragment of MAD-3(IκBα) and with a β-actin probe as an internal control. The signals were quantified by laser densitometry; IκBα levels were expressed relative to β-actin mRNA.

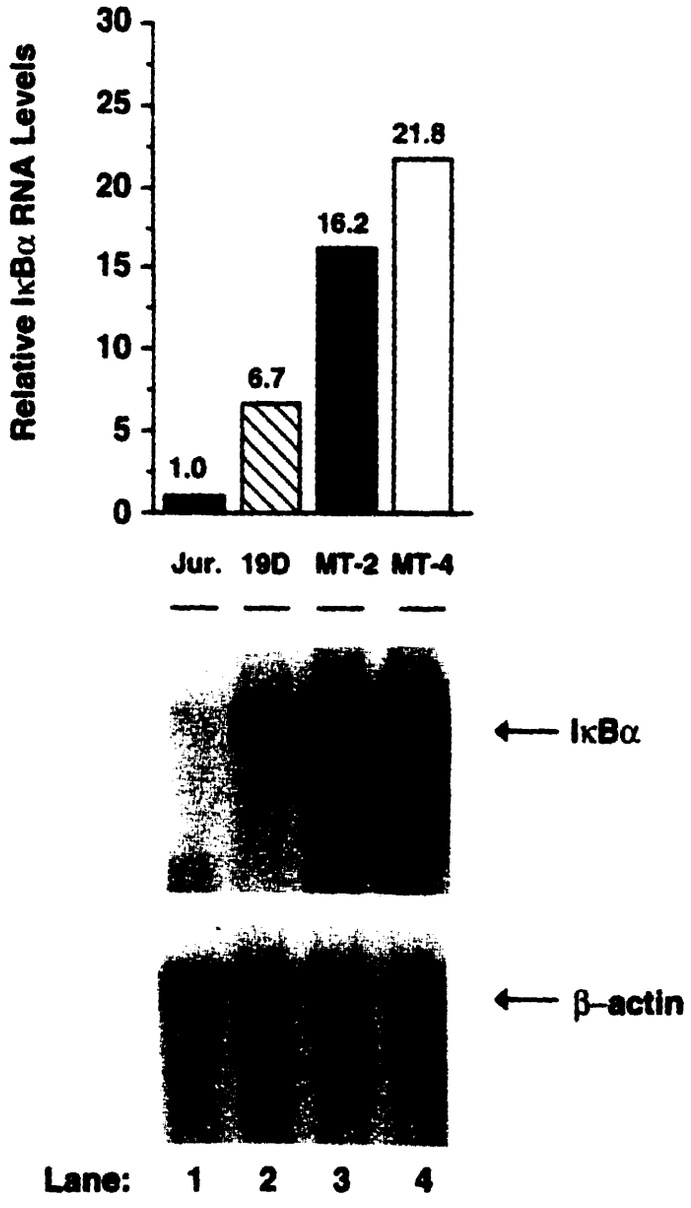
Relative IκBα RNA Levels
30
25
20
15
10
5
0
1.0
6.7
16.2
21.8
Jur.
19D
MT-2
MT-4
IκBα
β-actin
Lane: 1 2 3 4

pathway results in constitutive NF-κB DNA binding activity that may promote aberrant NF-κB dependent gene expression in T cells (6,38,97,101,188).

Despite increased IκBα mRNA expression in HTLV-I infected MT-2 and MT-4 cells, IκBα protein levels were on average about 7 fold lower than in Jurkat cells; this apparent discrepancy was partially resolved by the rapid turnover of IκBα in these cells. In unstimulated Jurkat cells, IκBα half life was 2.6h (156 min) while in MT-2 cells, IκBα half life was reduced to 0.85 hours (51 min). However, the activity of the protease(s) involved in IκBα degradation must also be increased at least ten-fold in HTLV-I infected cells to account for the rapid and continuous turnover of IκBα. A similar conclusion was also reached in a recent study of NF-κB activity and IκBα turnover during B-cell differentiation (120).

In HTLV-I infected and Tax expressing cells, alterations in NF-κB subunits involved in DNA binding have been reported. In Jurkat cells, p50 and p65 subunits represented the main DNA binding components early after induction (Fig. 11); at later times, c-Rel and p50 were the abundant DNA binding subunits, in part due to the transcriptional induction of c-Rel (101,106). In Tax-expressing and HTLV-I infected cells, c-Rel, p52(NF-κB2) and p50(NF-κB1) were the major DNA binding components (101). Although p65 protein levels were similar or elevated in HTLV-I infected cells compared to Jurkat cells (NP, data not shown), p65 binding was reduced, indicating that p65 activity was sequestered in HTLV-I infected cells. Several possibilities may account for decreased p65 binding activity: 1) p65 may be targeted for rapid degradation because of its association with phosphorylated IκBα; 2) despite its rapid turnover, IκBα may be able to sequester p65 in the cytoplasm; 3) competition for target sites by other NF-κB proteins such as c-Rel and NF-κB2 may limit p65 activity.

Chapter 4

HTLV-I Tax Protein Increases NF-κB Dimer Formation and Antagonizes the Inhibitory Activity of the IκBα Regulatory Protein

In this study, we addressed the specificity and function of Tax interaction with members of the NF-κB/IκBα family. Using a variety of techniques, we demonstrate that: 1) Tax binds to all NF–κB DNA binding subunits *in vitro* and to IκBα; 2) Tax enhances NF-κB binding to DNA by increasing the formation of NF-κB dimers which can be detected in the absence of DNA; 3) Tax interacts with IκBα *in vivo* and 4) Tax and IκBα have antagonistic effects on NF-κB binding and gene activity.

Expression and purification of NF-κB, IRF-1 and Tax proteins.

To obtain relatively large amounts of protein for *in vitro* studies, the E. *coli* glutathione S-transferase gene fusion and baculovirus expression systems were used to express NF-κB subunits (Figure 15A). The cDNAs encoding the NF-κB subunits p50, p52, pN'65 were expressed as glutathione S-transferase fusion proteins and purified from bacterial lysates by affinity chromatography using glutathione-Sepharose 4B. The c-Rel, IRF-1 and Tax proteins were separately expressed in baculovirus as polyhistidine-tagged proteins, isolated from insect cell lysates under native elution conditions by a rapid affinity purification using His-Bind metal chelation resin. Purified proteins were analyzed by SDS-polyacrylamide gel electrophoresis; the purity estimated from Coomassie stained gels was 60, 90, 80, 90, 70, 80 and 90% for c-Rel, Tax, N'p65, IRF-1, IκBα, p52 and p50 respectively (Fig. 15B; lanes 1-7, respectively).

Figure 15. Expression of recombinant proteins. (A) Schematic representation of recombinant NF-κB proteins expressed as glutathione S-transferase (GST) fusion proteins or as polyhistidine-tagged proteins. The histidine-tagged proteins contain 12-21 histidine residues at their N-termini  The boxes represent different protein domains:  Rel homology domain;  transactivation domain; ankyrin repeat; PEST domain; Glutathione S-Transferase; IRF-1 DNA-binding domain; nuclear localization sequences.; CREB binding site in Tax; sequence required for NF-κB activation in Tax. **(B)** Coomassie-stained SDS-polyacrylamide gel of purified recombinant proteins (100 ng each); the dots indicate the full length protein.

A

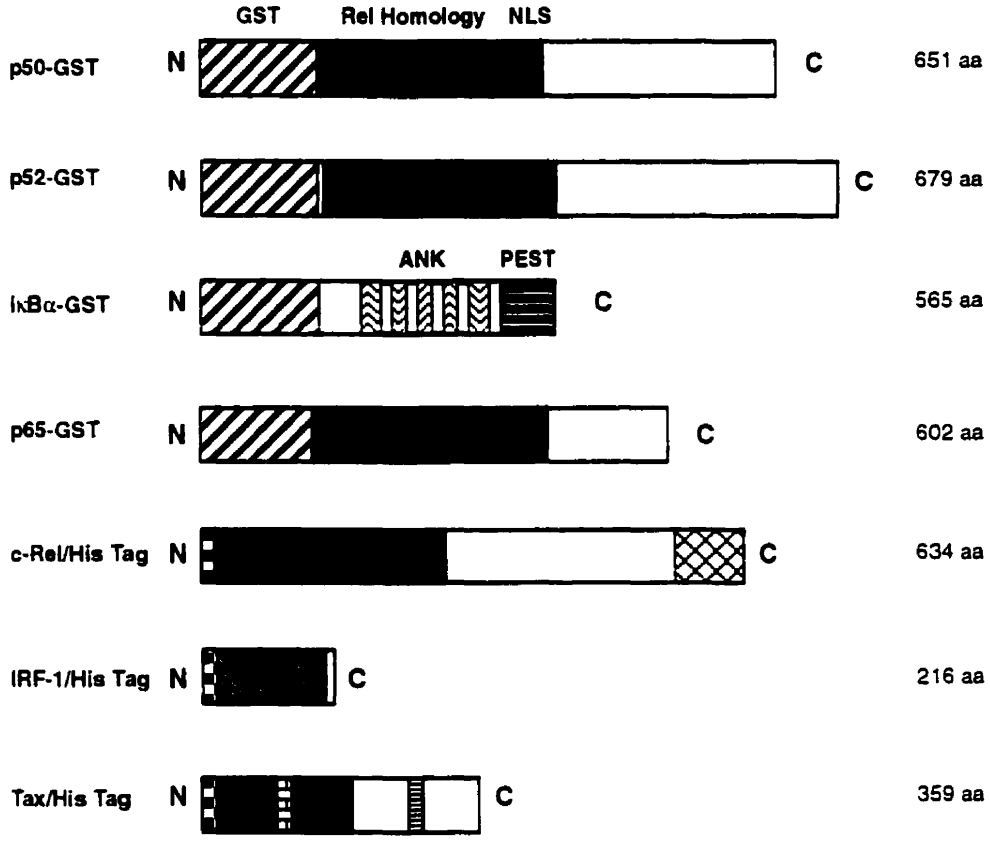
GST
Rel Homology
NLS
p50-GST
N
C
651 aa
p52-GST
679 aa
ANK
PEST
IκBα-GST
565 aa
p65-GST
602 aa
c-Rel/His Tag
634 aa
IRF-1/His Tag
216 aa
Tax/His Tag
359 aa

B

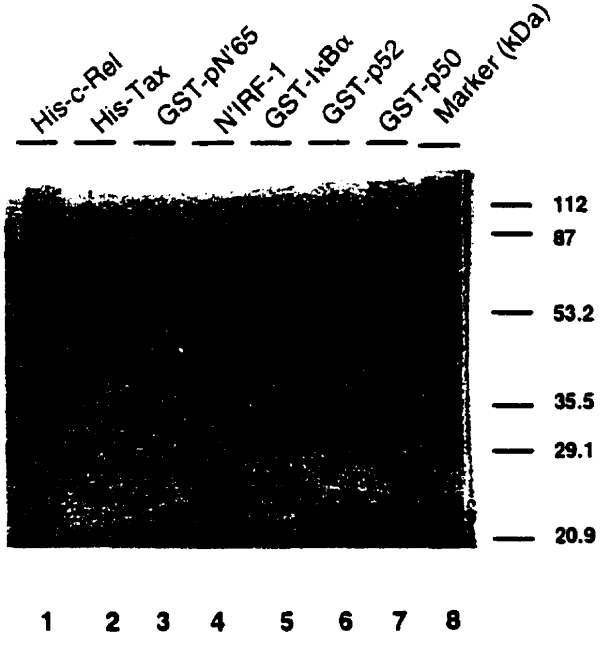
His-c-Rel
His-Tax
GST-pN'65
N'IRF-1
GST-IκBα
GST-p52
GST-p50
Marker (kDa)
112
87
53.2
35.5
29.1
20.9
1 2 3 4 5 6 7 8

Tax stimulates NF-κB binding to the NF-κB DNA binding sequence.

Tax enhances binding and dimerization of the CREB/ATF family of bZIP proteins (65,188). To determine whether Tax similarly enhanced binding of NF-κB to DNA, recombinant NF-κB proteins were tested for their ability to bind to DNA in the presence or absence of Tax in EMSA (Figure 16), using the HIV-1 NF-κB or MHC-I probes and the PRD1 probe for IRF-1 binding. NF-κB proteins were incubated without Tax (Fig. 16, lanes 1, 4, 7, 10) , with Tax (Fig. 16; lanes 2, 5, 8, 11) or with baculovirus Sf9 extract (Fig. 16; lanes 3, 6, 9, 12) for 60 min. Tax differentially stimulated binding of all NF-κB subunits to DNA by 15, 25, 30 and 30 fold for p52, p50, c-Rel and p65, respectively (Fig. 16; lanes 2, 5, 8, 11) The electrophoretic mobility of the NF-κB/DNA complexes was not altered by the presence of Tax, indicating that Tax affected NF-κB DNA binding without forming a ternary complex with NF-κB and DNA. Tax had no intrinsic DNA binding activity (Fig. 16, lane 13) and the effect of Tax was specific since enhanced binding was not observed using Sf9 cell extract alone (Fig. 16; lanes 3, 6, 9, 12); similarly Sf9 extract alone displayed no intrinsic NF-κB like binding activity (Fig. 16; lane 14).

Association of NF-κB/Rel with DNA is increased by Tax.

To investigate the association of NF-κB with DNA, binding of NF-κB to DNA at different times after Tax addition was measured (Figure 17). In the absence of Tax, only weak binding of c-Rel (0.2 ng), p65 (1.0 ng) and p52 (0.5 ng) was observed even after 60 min of incubation with radiolabeled probe (Fig. 17A, lane 7; Fig. 17B, lane 8; and Fig. 17C lane 1, respectively). In the presence of Tax, the level of NF-κB increased dramatically, reaching a maximum at 20 to 30 min for c-Rel (Fig.17A; lanes 2-4), p65 (Fig. 17B; lanes 2-5) and p52 (Fig. 17C; lanes 7-8). The total NF-κB protein-DNA binding in the presence of Tax increased approximately 30, 35 and 20 fold for p65, c-Rel and p52, respectively. In contrast, recombinant IRF-1 protein was not

Figure 16: Enhanced NF-κB-DNA binding mediated by Tax. Recombinant proteins of p52 (0.5 ng), p50 (0.2 ng), c-Rel (0.2 ng) and p65 (1.0 ng) were assayed for binding to 0.2 ng of MHCI probe (for p52; lanes 1-3) or to 0.2 ng of HIV-1 enhancer probe (lanes 4-12), in the absence of Tax (lanes 1, 4, 7, 10), presence of Tax (25 ng) (lanes 2, 5, 8, 11) or in the presence of Sf9 extract (25 ng) (lanes 3, 6, 9). Lanes 13 and 14 contain His-Tax and Sf9 extract (25 ng each), respectively.

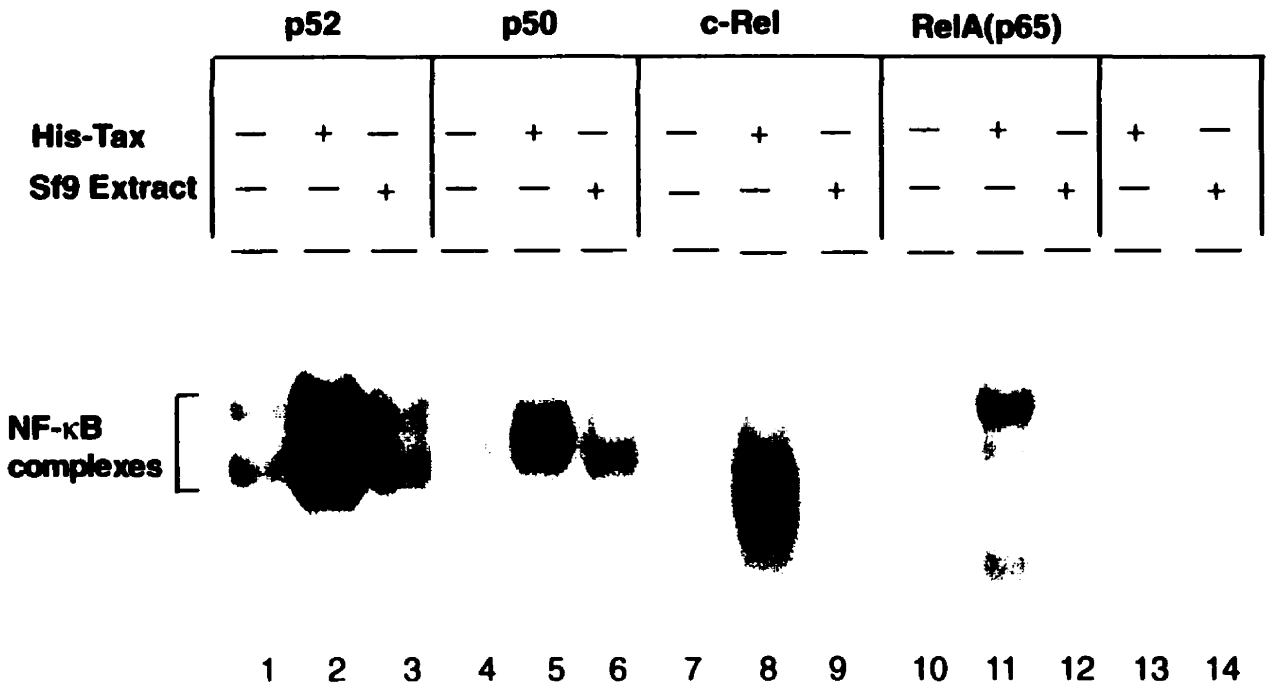
p52
p50
c-Rel
RelA(p65)
His-Tax
Sf9 Extract
NF-κB
complexes
1 2 3 4 5 6 7 8 9 10 11 12 13 14

Figure 17: Association of NF-κB/Rel with DNA is mediated by Tax. (A). Recombinant c-Rel (0.2 ng) was incubated with 0.2 ng of HIV-1 enhancer probe and Tax (25 ng) for 0-60 minutes (lanes 1-6). c-Rel was incubated with probe for 60 minutes alone (lane 7) or with Sf9 extract (lane 8). IRF-1 (0.2 ng) was incubated alone (lane 9) with Tax (25 ng) (lane 10) or with Sf9 extract (25 ng) (lane 11) for 60 min. **(B)** p65 (1.0 ng) was incubated with Tax (25 ng) for 0-60 min. (lanes 1-6) or without Tax for 60 min. (lanes 7-8). **(C)** NF-κB2(p52) (0.5 ng) was incubated without Tax for 60 min. (lanes 1-2) or with Tax (25 ng) for 0-60 min (lanes 3-8).

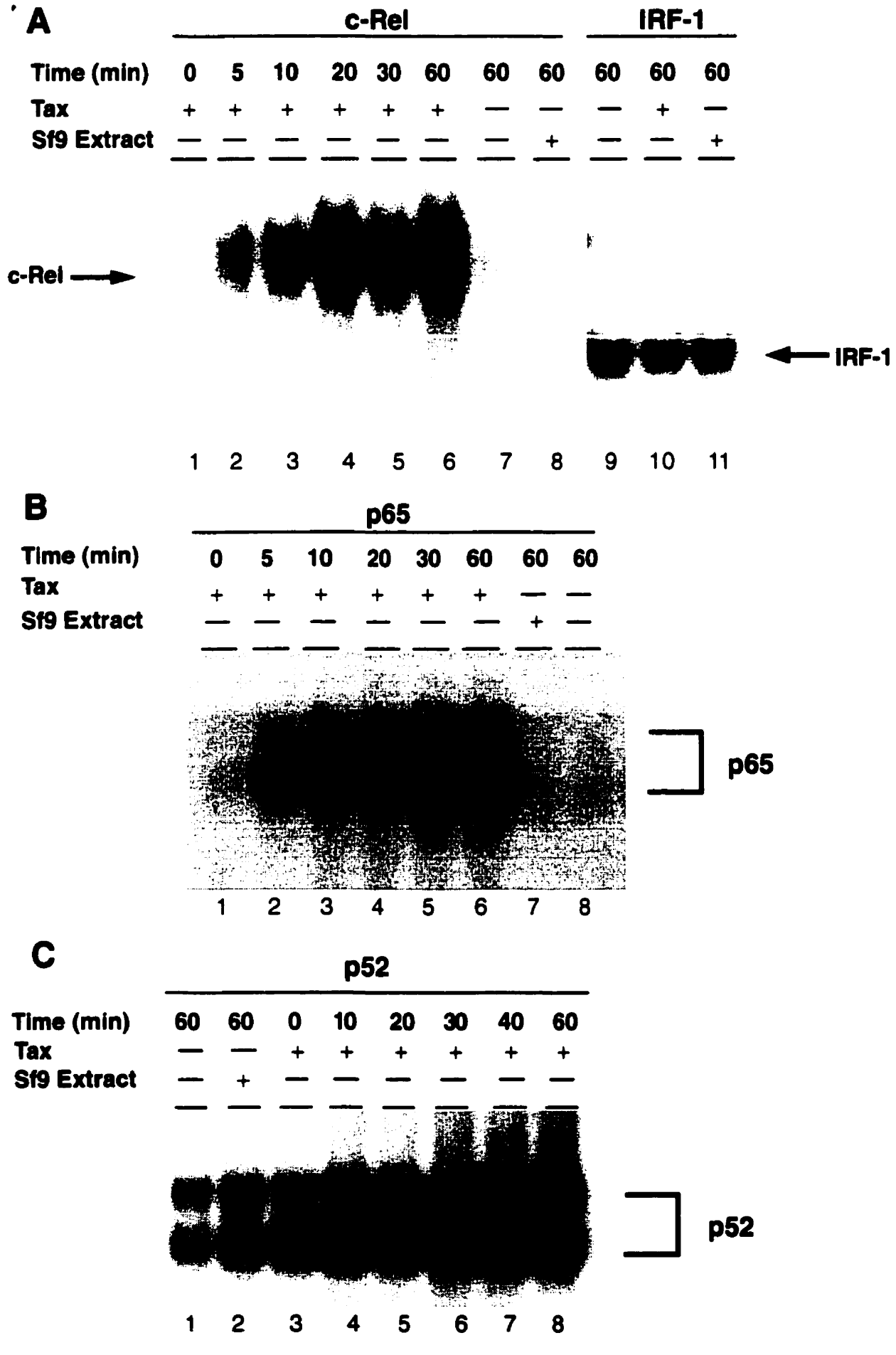
A
c-Rel
IRF-1
Time (min) 0 5 10 20 30 60 60 60 60 60 60
Tax + + + + + + — — — + —
Sf9 Extract — — — — — — — + — — +
c-Rel
IRF-1
1 2 3 4 5 6 7 8 9 10 11
B
p65
Time (min) 0 5 10 20 30 60 60 60
Tax + + + + + + — —
Sf9 Extract — — — — — — + —
p65
1 2 3 4 5 6 7 8
C
p52
Time (min) 60 60 0 10 20 30 40 60
Tax — — + + + + + +
Sf9 Extract — + — — — — — —
p52
1 2 3 4 5 6 7 8

affected by incubation with Tax(Fig. 17A; lanes 9-11) (188). This result indicates that Tax can increase the on-rate of NF-κB-DNA binding activity. To determine the effect of Tax on the dissociation of NF-κB-DNA complexes, a reaction mixture of p65-DNA was incubated in the absence or presence of Tax for 40 min, followed by the addition of a 100 fold excess of specific competitor DNA (Figure 18). Note that in order to obtain approximately equivalent amounts of p65-DNA complex, a 30-fold excess of p65 was added to the reaction mixture without Tax (Fig.18; lanes 5-7). The amount of NF-κB-DNA complex remaining after addition of DNA, measured as a function of time, was analyzed by EMSA. As shown in Figure 18, p65 dissociated from the DNA probe at a comparable rate in the presence (Figure 18; lanes 2-4) or absence of Tax (Figure 18; lanes 5-7); similar results were also observed for other NF-κB subunits (data not shown). Thus, Tax affects the association of NF-κB with the DNA probe but does not alter the dissociation of NF-κB-DNA complexes.

Tax increases the formation of NF-κB/Rel dimers in the absence of DNA.

NF-κB/Rel proteins contact DNA as dimers and dimerization is a prerequisite for DNA binding (70,149). Tax may therefore increase protein dimerization or the subsequent interaction between the NF-κB/Rel dimer and DNA. To determine if Tax was involved in the enhancement of dimerization, a protein-protein chemical crosslinking analysis was performed. GST-p52 was incubated in the presence or absence of Tax and after addition of the chemical crosslinker DMP, the products were fractionated on an SDS-PAGE gel and analyzed by immunoblotting (Figure 19A). GST-p52 at a concentration of 50 ng migrated predominantly as a monomer of 82 kDa (Fig. 19A; lane 6); increasing the concentration of GST-p52 to 100 ng resulted in a small amount of dimerization, with some crosslinked protein at 164 kDa (Fig. 19A; lane 7). The addition of increasing concentrations of Tax (50-200 ng) increased the formation of homodimers by 40 to 110 fold (Fig. 19A; lanes 3-5); non-specific formation

Figure 18: Dissociation of pN'65-DNA complexes is not affected by Tax. Dissociation of pN'65 from probe DNA was analyzed in the presence of pN'65 (1.0 ng) and Tax (25 ng) (lanes 2-4) or with pN'65 (30 ng) and in the absence of Tax (lanes 5-7). The complex was allowed to form for 40 min, followed by addition of a 100 fold excess of unlabeled HIV-1 probe for 10, 20, or 40 min .(lanes 2-7). In lane 1, the amount of pN'65 (1.0 ng) binding at 40 min. in the absence of Tax is shown.

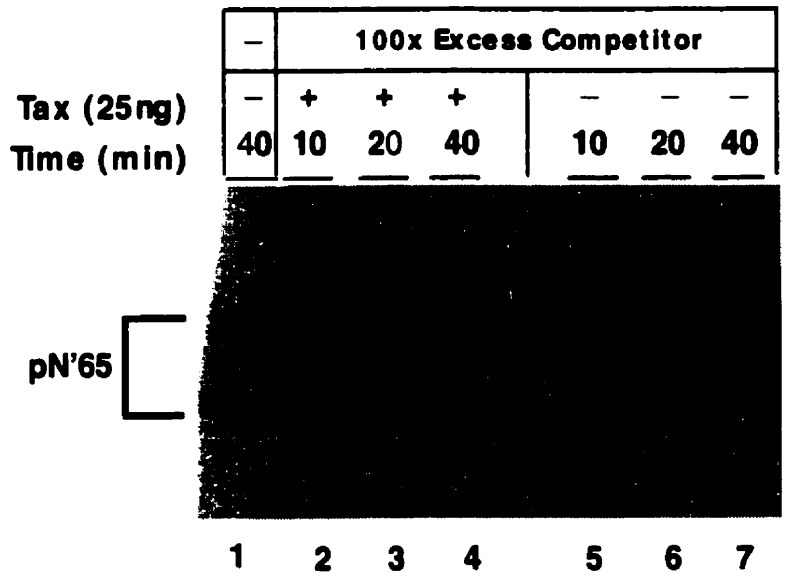

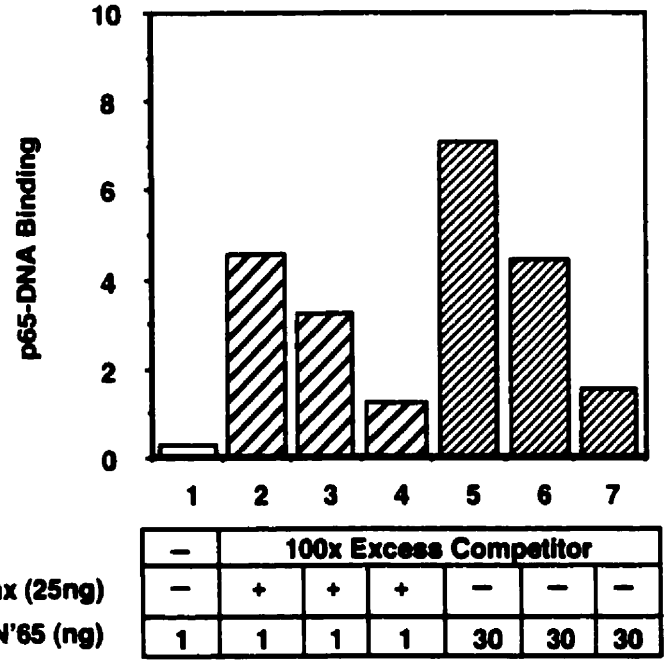

–	100x Excess Competitor						
Tax (25ng)	–	+	+	+	–	–	–
pN'65 (ng)	1	1	1	1	30	30	30

Figure 19: Tax mediated enhancement of dimerization of NF-κB2(p52) and pN'65. **(A)** Recombinant GST-p52 was incubated in the presence (lanes 2-5) or absence of Tax (lanes 1, 6 and 7). Reaction mixtures were treated with 5 mM DMP crosslinker (lanes 3-7) in the presence of GST-p52 and Tax 50-200 ng (lanes 3-5) or GST-p52 alone at concentrations of 50 and 100 ng, respectively (lanes 6 and 7). **(B)** GST-pN'65 was crosslinked using 0.05% glutaraldehyde (lanes 1-3). pN'65 at 50 ng was incubated alone in the presence of crosslinker (lane 1). Reaction mixtures were incubated with pN'65 (50 ng) and with 100 ng or 50 ng of Tax (lanes 2 and 3). Lanes 4 and 5 contain reactions of pN'65 with Tax and pN'65 in the absence of crosslinker, respectively The products were fractionated by 10% SDS-PAGE and detected by immunoblotting.

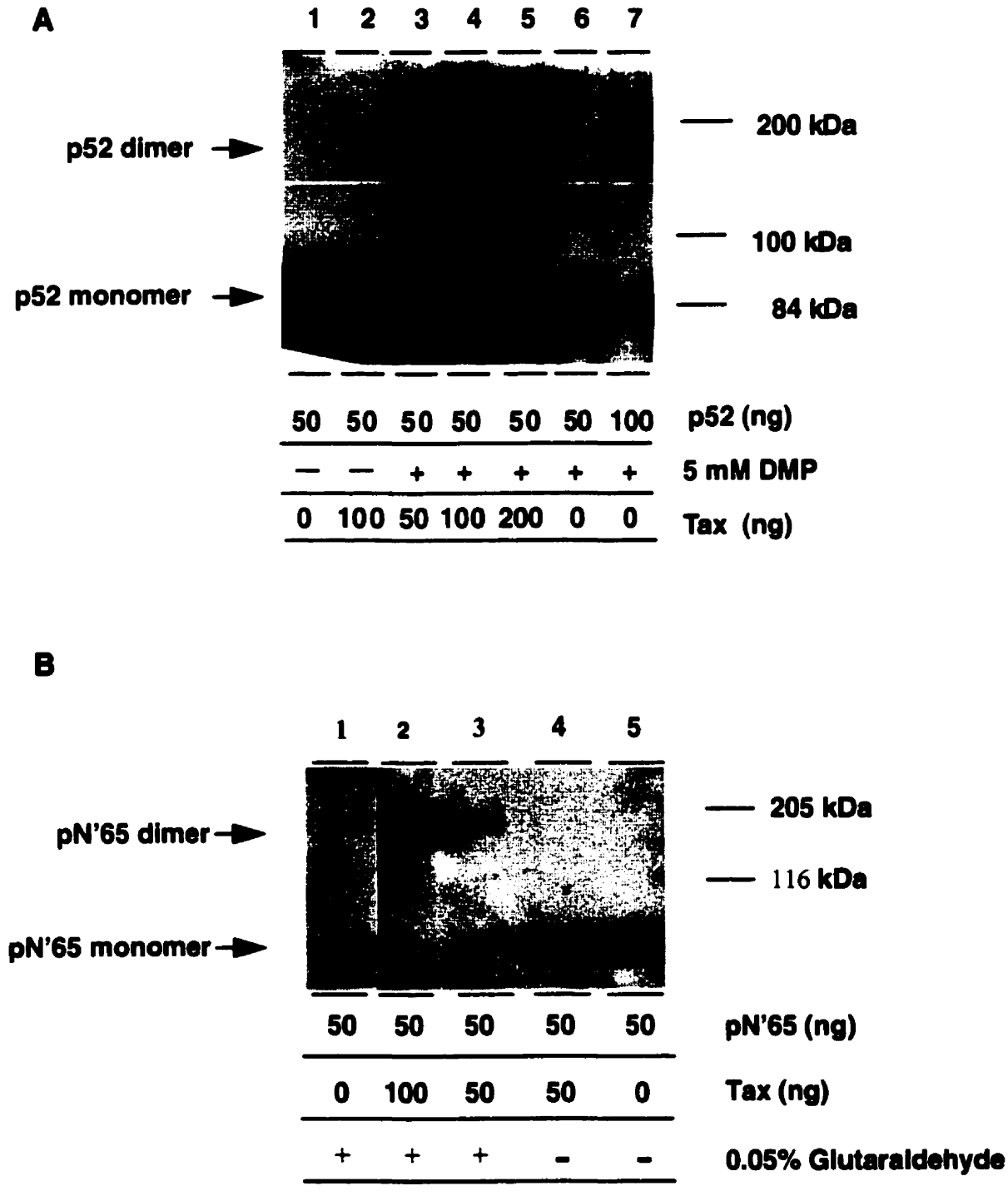
A
1 2 3 4 5 6 7
p52 dimer
p52 monomer
200 kDa
100 kDa
84 kDa
50 50 50 50 50 50 100
p52 (ng)
— — + + + + +
5 mM DMP
0 100 50 100 200 0 0
Tax (ng)
B
1 2 3 4 5
pN'65 dimer
pN'65 monomer
205 kDa
116 kDa
50 50 50 50 50
pN'65 (ng)
0 100 50 50 0
Tax (ng)
+ + + - -
0.05% Glutaraldehyde

of a 164 kDa complex did not occur in the absence of DMP (Fig. 19A; lanes 1 and 2). This protein-protein cross-linking experiment illustrates that Tax alone in the absence of DNA increases the formation of NF-κB2 p52 dimers. Immunoblots were stripped and probed with anti-Tax antibody; no Tax was present in the 82 kDa or 164 kDa bands, indicating that Tax was not a component of the observed complex (data not shown). Similarly, Tax also enhanced the dimerization of p65 (Fig. 19B, lanes 2 and 3); dimerization of p65 did not occur to an appreciable extent in the absence of Tax (Fig. 19B, lanes 1 and 5).

Effect of Tax on NF-κB binding activity in the presence of IκBα.

NF-κB-DNA complex formation can be inhibited *in vitro* by incubation with IκBα; also IκBα is able to dissociate preformed protein-DNA complexes (186). This property of IκBα may be relevant to the inhibition of NF-κB mediated activation of gene expression since recent studies have demonstrated that newly synthesized IκBα can be localized to the nucleus (4). To examine the effect of IκBα on Tax-stimulated NF-κB binding activity, the binding of p65 to NF-κB DNA in the presence of Tax and/or IκBα was examined. As shown in Figure 20, p65 binding to the NF-κB element was stimulated in the presence of Tax (Fig. 20, lane 2) but was inhibited by the addition of IκBα (Fig. 20, lane 4). Addition of increasing amounts of IκBα (1, 5 and 10 ng) with p65, followed by the addition of a constant amount of Tax (Fig 20, lanes 5-7) resulted in complete inhibition of p65-DNA complex formation at the higher IκBα concentrations. However, in the reverse reaction with increasing concentrations of Tax and a constant amount of IκBα, p65 DNA binding was stimulated (Fig. 20, lanes 8-12), illustrating that Tax was able to overcome the inhibitory effect of IκBα. In previous experiments, we also observed that Tax could overcome the inhibitory effects of IκBα on gene expression (98), thus supporting the idea that Tax and IκBα have antagonistic effects on NF-κB binding.

Figure 20: Competition for NF-κB binding activity by Tax and IκBα. Recombinant p65 (1.0 ng) was incubated with Tax (10 ng) and increasing concentrations of IκBα (1-10 ng) (lanes 5-7), with IκBα added to the reaction mixture before Tax. IκBα (1.0 ng) was incubated with increasing concentrations of Tax (0.5-10 ng) (lanes 8-12). Tax was added to the reaction mixture with IκBα (lanes 5-12); p65 protein was incubated with HIV-1 enhancer probe alone (lane 1) with Tax (lane 2) with Sf9 extract (lane 3) and with IκBα (lane 4).

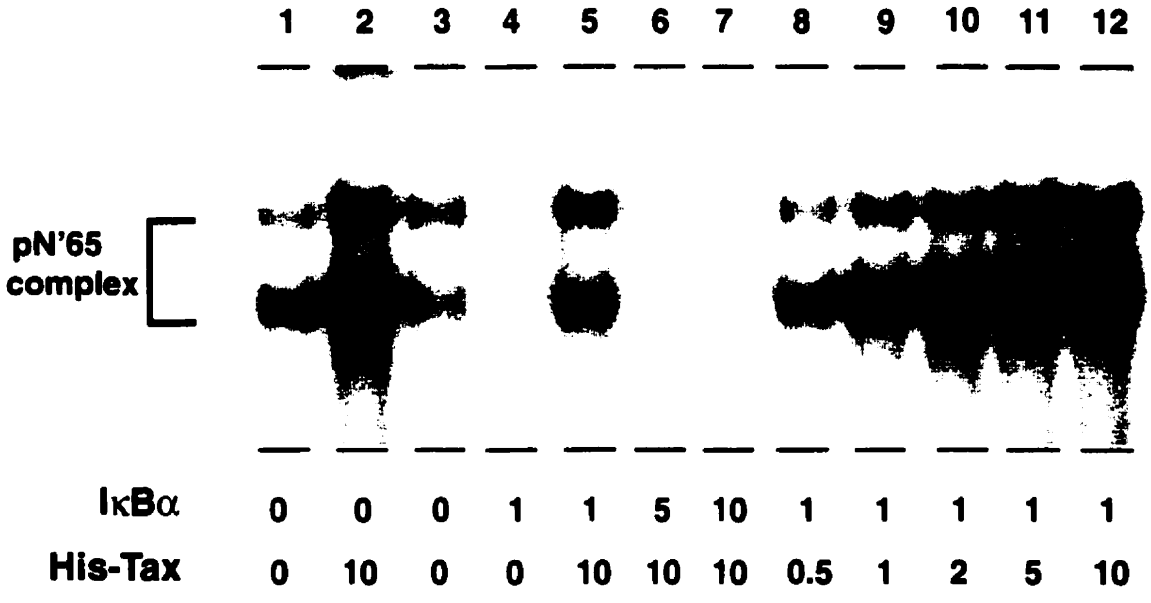
1 2 3 4 5 6 7 8 9 10 11 12
pN'65 complex
IκBα 0 0 0 1 1 5 10 1 1 1 1 1
His-Tax 0 10 0 0 10 10 10 0.5 1 2 5 10

Tax directly associates with the inhibitor IκBα.

Next, *In vitro* GST-affinity chromatography was used to determine whether Tax can associate with IκBα directly, as well as with other recombinant NF-κB proteins (Figure 21). Equivalent amounts of GST-NF-κB subunits and GST-IκBα were immobilized on GST-Sepharose beads followed by the addition of His-Tax. As expected, Tax interacted with each of the NF-κB subunits p50, p52, p65 and c-Rel (Fig. 21, lanes 1, 3, 5, 6) but not with GST alone; a strong Tax-IκBα interaction was also observed (Fig. 21, lane 4).

To determine if the Tax-IκBα interaction observed *in vitro* was also observed *in vivo*, N-Tera 2 cells were co-transfected with plasmids expressing Tax and the truncated form of IκBα, IκBΔ4 (a C-terminal deletion of aa296-317) (18,107). As illustrated in Figure 22, immunoprecipitation with anti-Tax antibody from transfected cells also immunoprecipitated endogenous IκBα and increasing amounts of IκBαΔ4 (Fig. 22B, lanes 1-4). Similarly, the Tax mutants M22 (NF-κB$^-$/CREB$^+$) and M47 (NF-κB$^-$/CREB$^+$) (163) also immunoprecipitated endogenous IκBα and increasing amounts of transfected IκBαΔ4 (Fig.22B; lanes 5-9). The reverse co-immunoprecipitation was also performed and anti-IκBα antibody immunoprecipitated endogenous IκBα, increasing amounts of transfected IκBαΔ4 and wild type Tax (Fig.22A; lanes 1-4), mutant Tax M22 (Fig.22A; lanes 5-8), and Tax M47 (Fig. 22A; lane 9).

Co-immunoprecipitation studies were also performed using the HTLV-I transformed T cell line C8166 which expresses relatively high levels of Tax, displays constitutive NF-κB binding activity and has a higher rate of IκBα turnover when compared to non-transformed T cell lines (88,99,167). Surprisingly, with the immunoprecipitation conditions used in the previous experiment, Tax was unable to co-immunoprecipitate IκBα (Fig 22C; lane 4), possibly due to the high rate of IκBα turnover (173). To

Figure 21: *In vitro* binding of Tax protein to different NF-κB proteins. GST- NF-κB-p50, p65, p52 (lanes 1, 2 and 4), His-tagged c-Rel (lane 6), GST alone (lane 2) and IκBα (lane 3) proteins (300 ng) were immobilized onto glutathione Sepharose beads or His-Bind metal chelation resin; affinity chromatography using His-Tax (50 ng) was performed as described in Materials and Methods. Lanes 7 contained 25 ng of Tax alone. Recombinant Tax protein retained by the fusion proteins was eluted and visualized by immunoblot analysis with anti-Tax antibody.

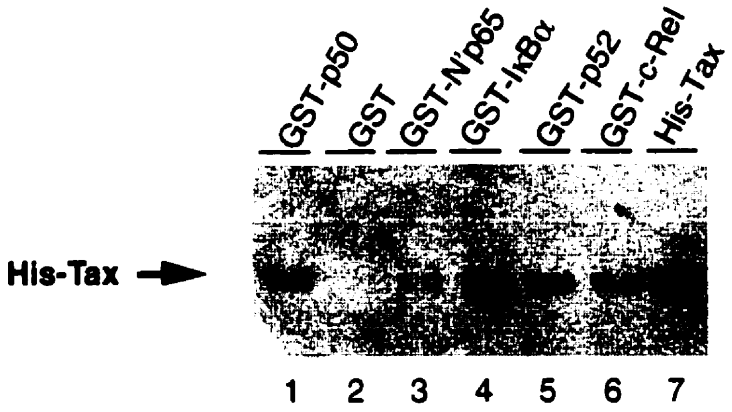
GST-p50
GST
GST-N'p65
GST-IκBα
GST-p52
GST-c-Rel
His-Tax
His-Tax
1 2 3 4 5 6 7

Figure 22: Co-immunoprecipitation of Tax and IκBα. **(A)** N-Tera 2 cells were transfected with expression plasmids encoding IκBαΔ4 (0-10 μg) and wild type Tax (10 μg) (lanes 1-4), mutant Tax M22 (lanes 5-8), or mutant M47 (lane 9). Immunoprecipitation was performed with anti-IκB α antibody and co-immunoprecipitated Tax was detected by immunoblot with anti-Tax antibody. **(B)** The reverse immunoprecipitation was performed with anti-Tax antibody and blotted with anti-IκBα antibody. **(C)** Co-immunoprecipitation of Tax and IκBα from C8166 cells. C8166 cells were treated with PDTC (100 μM) (lane 5) or calpain inhibitor I (100 μM) (lane 6) for 1hr or left untreated (lane 4). Immunoprecipitations were performed using anti-Tax antibody and co-precipitated IκBα was detected by immunoblot with anti-IκBα antibody. Non-Tax expressing Jurkat cells served as control (lane 3). Lanes 1 and 2 indicate the endogenous levels of IκBα from Jurkat cells and C8166 cells, respectively.

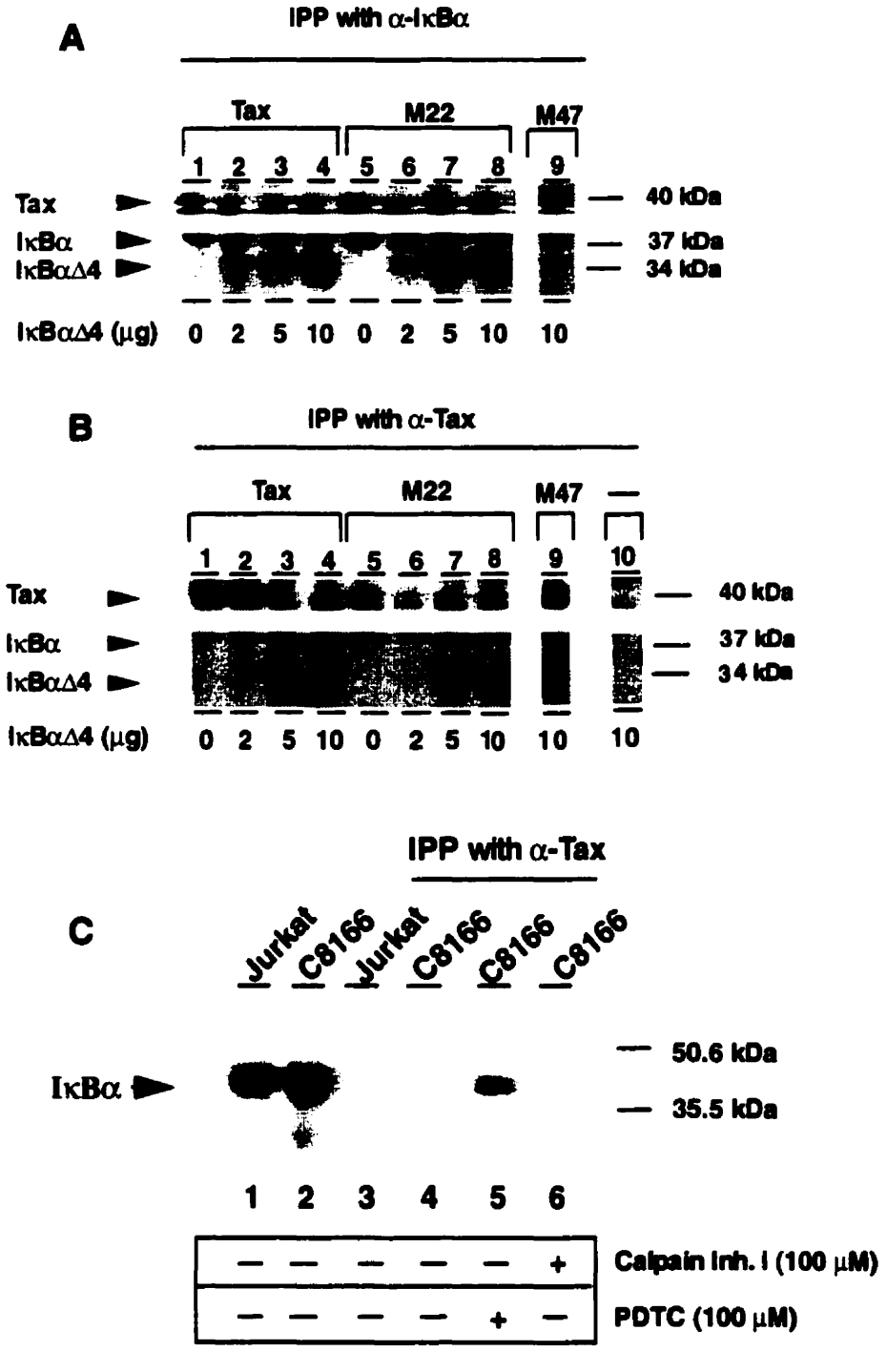
A
IPP with α-IκBα
Tax
M22
M47
1 2 3 4 5 6 7 8 9
Tax
IκBα
IκBαΔ4
40 kDa
37 kDa
34 kDa
IκBαΔ4 (μg) 0 2 5 10 0 2 5 10 10
B
IPP with α-Tax
Tax
M22
M47
1 2 3 4 5 6 7 8 9 10
Tax
IκBα
IκBαΔ4
40 kDa
37 kDa
34 kDa
IκBαΔ4 (μg) 0 2 5 10 0 2 5 10 10 10
IPP with α-Tax
C
Jurkat
C8166
Jurkat
C8166
C8166
C8166
IκBα
50.6 kDa
35.5 kDa
1 2 3 4 5 6
Calpain Inh. I (100 μM)
PDTC (100 μM)

circumvent this possibility, Calpain inhibitor I and the antioxidant pyrrolidine dithiocarbamate (PDTC) were used to block IκBα degradation (15). PDTC is both a metal chelator and an antioxidant and absorbs metal ions required for the Haber Weiss reaction (158) while Calpain inhibitor I inhibits proteasome mediated catalytic activity (41). Both PDTC and Calpain inhibitor I block NF-κB activation by interfering with IκBα degradation (17,38,76,169,182); PDTC stabilizes IκBα by blocking its phosphorylation whereas Calpain inhibitor permits the accumulation of the phosphorylated and ubiquitinated form of IκBα (17) but blocks at the level of proteasome mediated degradation. Interestingly, in C8166 cells treated with Calpain inhibitor I, IκBα was not immunoprecipitable with an anti-Tax antibody (Figure 23C, lanes 4 and 6). However, from PDTC treated cells, Tax and IκBα were co-immunoprecipitated (Figure 23; lane 5), suggesting that Tax may preferentially interact with an unmodified form of IκBα.

To further characterize the antagonistic effects of Tax and IκBα on regulation of NF-κB dependent gene expression, a series of co-transfection experiments was performed in N-Tera-2 cells using the HIV-1 LTR-CAT reporter gene (Δ23/CAT) and different amounts of Tax, IκBα and p65 expression plasmids. Co-transfection of p65, Tax or Tax and p65 expression plasmids increased the activity of the HIV-1 LTR at 48h after transfection between 5 and 20 fold (Fig. 23, lanes 2-4), while the addition of IκBα together with p65 eliminated gene activity (Fig. 23, lane 5). The addition of increasing amounts of Tax plasmid was able to reverse the inhibitory effects of IκBα on gene activity Fig. 23, lanes 6-9), indicating that the Tax and IκBα antagonistic effects observed in DNA binding analysis is also reflected in changes in NF-κB dependent gene activity.

Figure 23: Analysis of the effect of Tax-IκBα antagonism on gene activity. Human N-Tera-2 cells were transfected by the calcium phosphate method with Δ23/CAT (3 μg) (Δ23/CAT contains the -167 to +80 region of the HIV-1 LTR linked to CAT and includes the two NF-κB binding sites in the -100 region) and with the indicated amounts of the CMV-based p65 and Tax cDNA expression vectors and SVK3-based IκBα expression vector. At 40 h after transfection, the cells were either treated with Calpain Inhibitor I (125 μM) for 6h (lane 8) or not treated (lane 9), harvested and protein extracts (300 μg) were subjected to CAT analysis. The percent acetylation was determined by quantifying the acetylated and substrate chloramphenicol and presented as a bar graph. The results are representative of three independent experiments.

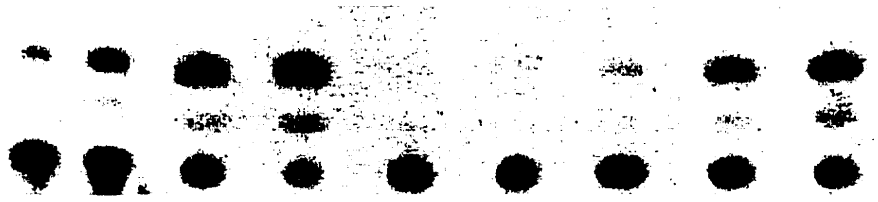

3	3	3	3	3	3	3	3	3	Δ23/CAT
—	3	—	3	3	3	3	3	3	p65
—	—	10	10	—	1	5	10	10	Tax
—	—	—	—	1	1	1	1	1	IκBα

Calpain Inh. I
125 μM
6Hrs

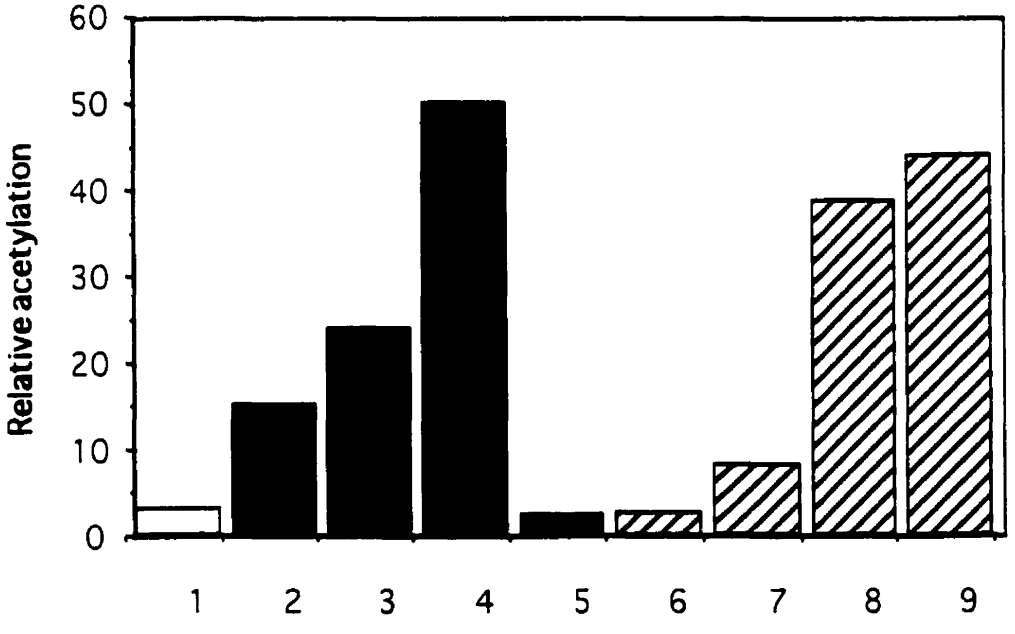

Chapter 5

Tax-IκBα Association is Dependent on the Phosphorylation State

Upon T cell activation, IκBα is rapidly phosphorylated, ubiquitinated and degraded by the 26S proteasome, releasing NF-κB from cytoplasmic sequestration. However, it remains unclear as to how Tax induces a persistent NF-κB activity. We demonstrated that Tax induces turnover of IκBα and that Tax can directly interact with IκBα. Therefore, we sought to examine the physiological function of a Tax-IκBα. Here we demonstrate that Tax preferentially interacts with N-terminally hypophosphorylated/newly synthesized IκBα and targets IκBα to proteasome, HsN3. This mechanism suggests that Tax can target IκBα for degradation before it binds to NF-κB and enhance IκBα constitutive turnover.

Tax interacts with the ankyrin repeats of IκBα

Previous studies demonstrated that Tax interacted with IκBα *in vivo* and *in vitro* (142,173) and is complementary to the observation that Tax interacts with the NF-κB p105 precursor through C-terminal ankyrin repeat of p105 (9,80). Therefore, to identify the IκBα domain necessary for interaction with Tax, GST-IκBα deletions were generated, containing the N-terminal, signal response domain (GST-NIK, aa 1-55), the ankyrin repeats (GST-ANK, aa 55-222) and the C-terminus (GST-CIK, aa 272-317) (Fig. 24A). Using GST affinity chromatography, recombinant Tax specifically interacted with full length IκBα and specifically through the ankyrin repeat domain (Fig. 24B, lanes 6 and 3 respectively).

Tax interacts with N-terminally unphosphorylated IκBα

The interaction between Tax and IκBα in C8166 cells was stabilized by agents such as NAC or pyrrolidinedithiocarbamate (PDTC) but not in untreated cells or in cells treated with the proteasome inhibitor MG132 (103). PDTC and NAC prevent the inducible phosphorylation of IκBα (103). Treatment of C8166 cells with the

Figure 24: Tax interacts with the ankyrin repeats of IκBα. **(A)** Truncated IκBα fusion proteins, GST-ANK (lane 2), GST-NIK (lane 3) and GST-CIK (lane 4) and full length GST-IκBα (lane 6) were expressed (as described in Materials & Methods) and fusion proteins checked by coomassie stain of the SDS-PAGE. **(B)** His-Tax (lane 1), GST-NIK, -ANK, -CIK (lanes 2, 3 and 4), GST alone (lane 5) and full length GST-IκBα (lane 6) proteins (300 ng) were immobilized onto glutathione sepharose beads; affinity chromatoghraphy using His-Tax (50 ng) was performed as described under Materials and Methods. Recombinant Tax protein retained by the fusion proteins was eluted and visualized by immunoblot analysis with anti-Tax antibody.

A

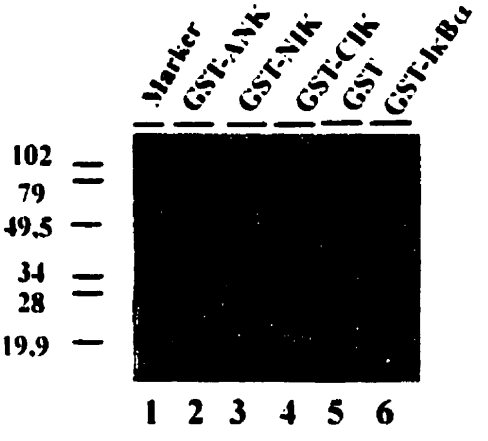
Marker
GST-ANK
GST-NIK
GST-CIK
GST
GST-IκBα
102
79
49.5
34
28
19.9
1 2 3 4 5 6

B

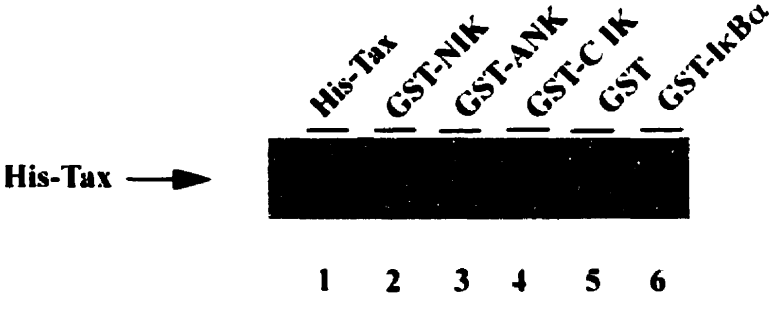
His-Tax
GST-NIK
GST-ANK
GST-C IK
GST
GST-IκBα
His-Tax
1 2 3 4 5 6

Figure 25: Tax interacts with hypophosphorylated IκBα. C8166 cells were pretreated for 30 minutes with the proteasome inhibitor MG132 (30 μM) (lanes 2 and 6) or with the anti-oxidant NAC (50 μM) (lanes 3, 5 and 7), followed by treatment with TNFα (10 ng/ml) (lanes 2, 3, 4-7) for 1 hour. Cell extracts (50 μg) (lanes 1-3) were analyzed for Ser32 phosphorylated IκBα **(A)** or IκBα **(B)**. Immunoprecipitations with 500 μg of cell extract with anti-Tax were performed (lanes 4-7) and immunoblotted for Ser32 phosphorylated IκBα **(A)** or IκBα **(B)**. MT-4 cells (non-Tax expressors) were used as a control for testing Tax antibody specificity (lane 7). **(C)** The levels of Tax from untreated (lane 1), MG132 (lane 2) or NAC treated (lane 3) C8166 cells (50 μg) were examined by western blot analysis.

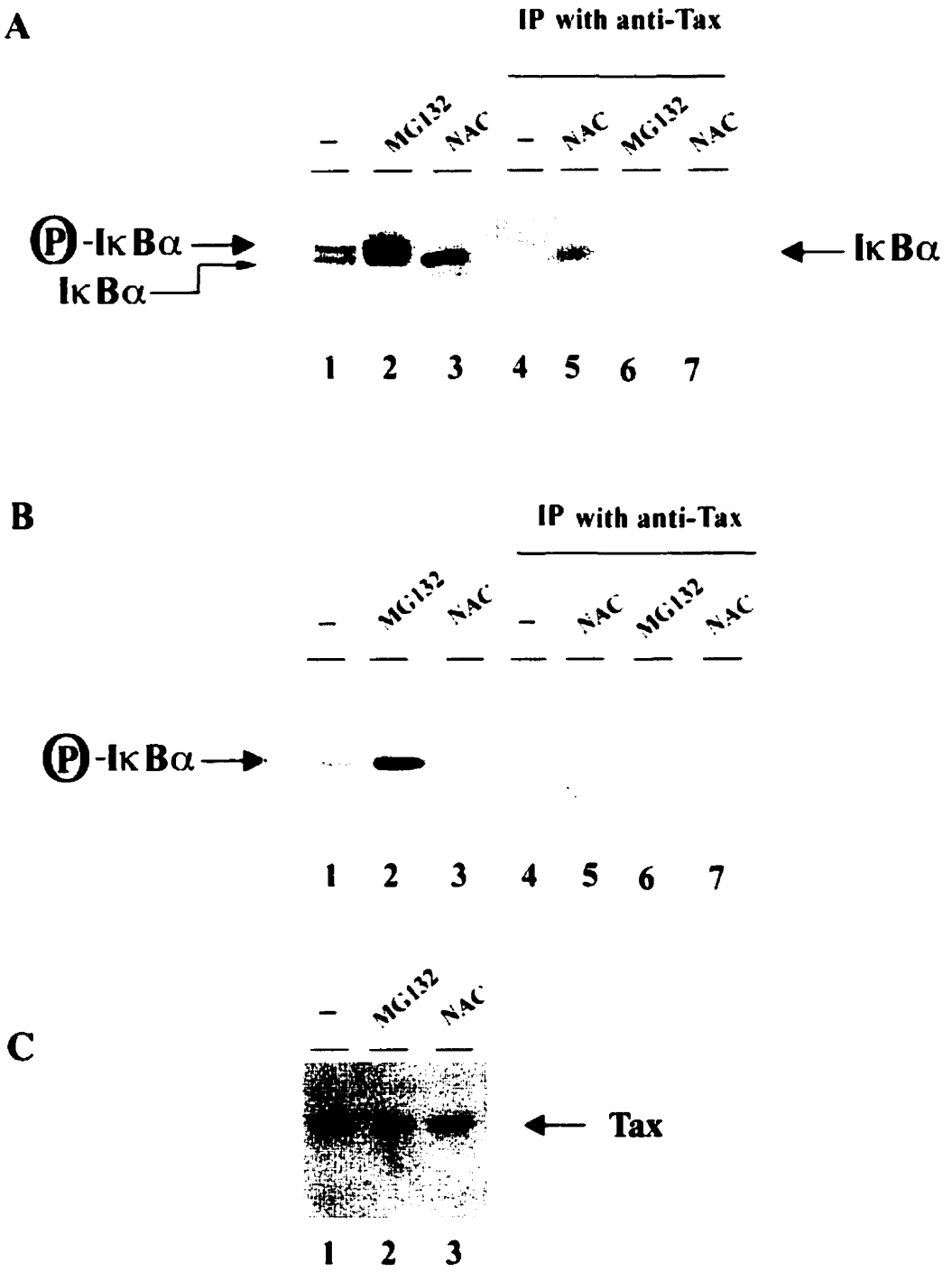
A
IP with anti-Tax
–
MG132
NAC
–
NAC
MG132
NAC
Ⓟ-IκBα
IκBα
IκBα
1 2 3 4 5 6 7
B
IP with anti-Tax
–
MG132
NAC
–
NAC
MG132
NAC
Ⓟ-IκBα
1 2 3 4 5 6 7
C
–
MG132
NAC
Tax
1 2 3

antioxidants created a stable intracellular pool of IκBα that was almost exclusively N-terminally unphosphorylated (compare Fig. 25A, lane 3 and Fig. 25B, lane 3). Conversely, MG132 and Calpain inhibitor I inhibit proteasome activity and MG132 treatment prevented IκBα degradation but did not alter inducible phosphorylation of IκBα. By inhibiting IκBα degradation, an intracellular population of IκBα accumulated that consisted of IκBα Ser32/Ser36 phosphorylated IκBα (compare Fig. 25A, lane 2 and Fig. 25B, lane 2). To examine if Tax preferentially interacted with distinct forms of IκBα, differing in their phosphorylation state, extracts from untreated C8166 cells, or cells treated with MG132 or NAC (Fig. 25A and B, lanes 1-3) were immunoprecipitated using anti-Tax antibody and were selectively immunoblotted for total IκBα (Fig. 25A) or Ser32 phosphorylated IκBα (Fig. 25B). Tax coimmunoprecipitated IκBα from cell extracts treated with NAC but not with MG132 (Fig. 25A, lanes 5 and 6). The immunoprecipitated IκBα in association with Tax was not phosphorylated on Ser32 (Fig. 25B, lane 5) as detected by the phosphoserine 32 specific IκBα antibody (Fig. 25A, lane 5). Treatment of cells with NAC or MG132 did not affect Tax expression, in C8166 cells (Fig. 25C, compare lanes 1-3).

To confirm the association between Tax and hypophosphorylated IκBα, other experimental conditions were examined: Jurkat cells were transiently transfected with C-terminally truncated IκBαΔ4 (Fig. 26) or with T7 tagged K21/22R (Fig. 27) together with Tax. The Δ4 truncation removes 22 C-terminal amino acids and can be distinguished from endogenous IκBα. Since T7-K21/22R contains lysine to arginine point mutations at amino acids 21 and 22, this mutant can be phosphorylated but will not be ubiquitinated on Lys21/22; thus phosphorylated IκB will accumulate in the cells and provide a measure of the interaction between hypo- and hyperphosphorylated IκBα and Tax. Transfected cells were treated with TNFα from 0-60 min and cellular extracts were immunoprecipitated for Tax. TNFα induced phosphorylation of

Figure 26: Tax immunoprecipitates hypophosphorylated IκBα and IκBαΔ4. The IκBαΔ4 wild type protein contains a 22aa deletion (aa295-317) at the C-terminus of IκBα. 293 cells were transfected with the IκBαΔ4 and Tax expression vectors. Following a 48h incubation, cells were treated with TNFα (10 ng/ml) for 0-60 minutes. Cell extracts (20 μg) (lanes 1-4) were analyzed for IκBα **(A)** or Ser32 phosphorylated IκBα **(B)**. Immunoprecipitations using 500 μg of cell extract with anti-Tax were performed (lanes 5-9) and immunoblotted for IκBα **(A)** or Ser32 phosphorylated IκBα **(B)**.

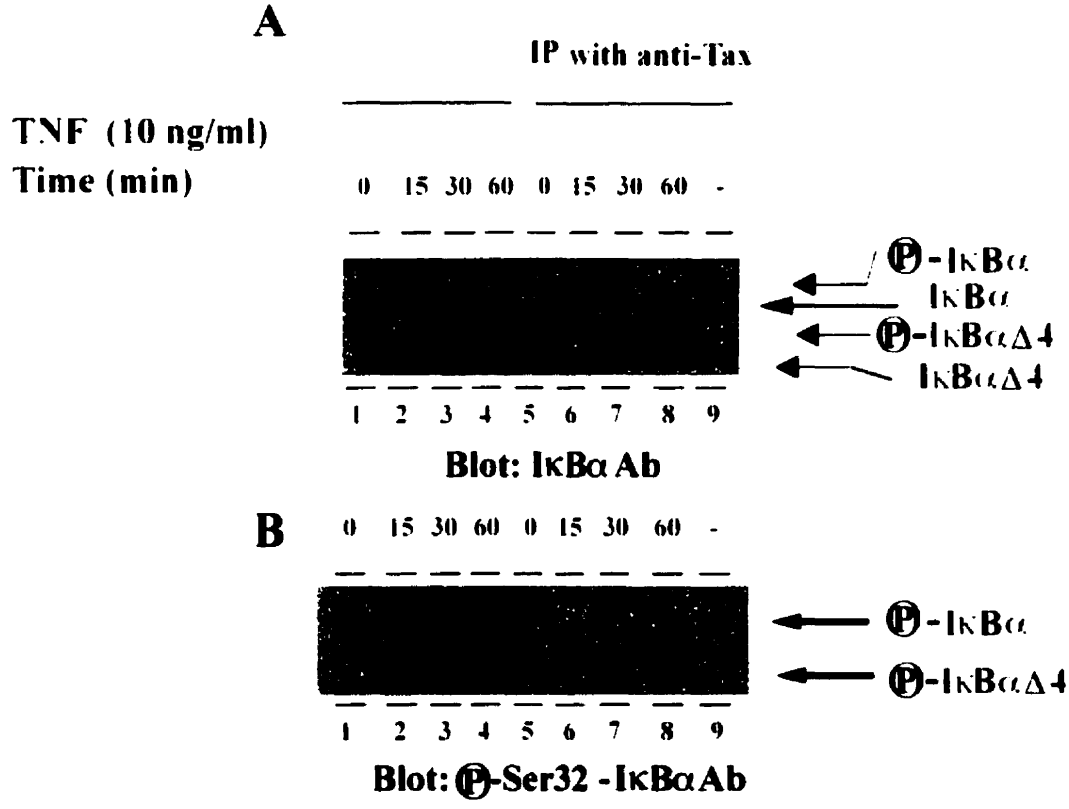
A
IP with anti-Tax
TNF (10 ng/ml)
Time (min)
0 15 30 60 0 15 30 60 -
Ⓟ-IκBα
IκBα
Ⓟ-IκBαΔ4
IκBαΔ4
1 2 3 4 5 6 7 8 9
Blot: IκBα Ab
B
0 15 30 60 0 15 30 60 -
Ⓟ-IκBα
Ⓟ-IκBαΔ4
1 2 3 4 5 6 7 8 9
Blot: Ⓟ-Ser32 -IκBα Ab

Figure 27: Tax immunoprecipitates hypophosphorylated IκBα (T7-K21/22R). The T7 tagged IκBα transdominant mutants contains K to R substitutions at aa 21 and 22. 293 cells were transfected with T7-K21/22R and Tax expression vectors. Following 48h post-transfection, cells were treated with TNFα (10 ng/ml) for 0-60 minutes. Cell extracts (20 μg) (lanes 1-4) were analyzed for IκBα **(A)** or Ser32 phosphorylated IκBα **(B)**. Immunoprecipitations using 500 μg of cell extract with anti-Tax antibody were performed (lanes 5-19) and immunoblotted for IκBα **(A)** or Ser32 phosphorylated IκBα **(B)**.

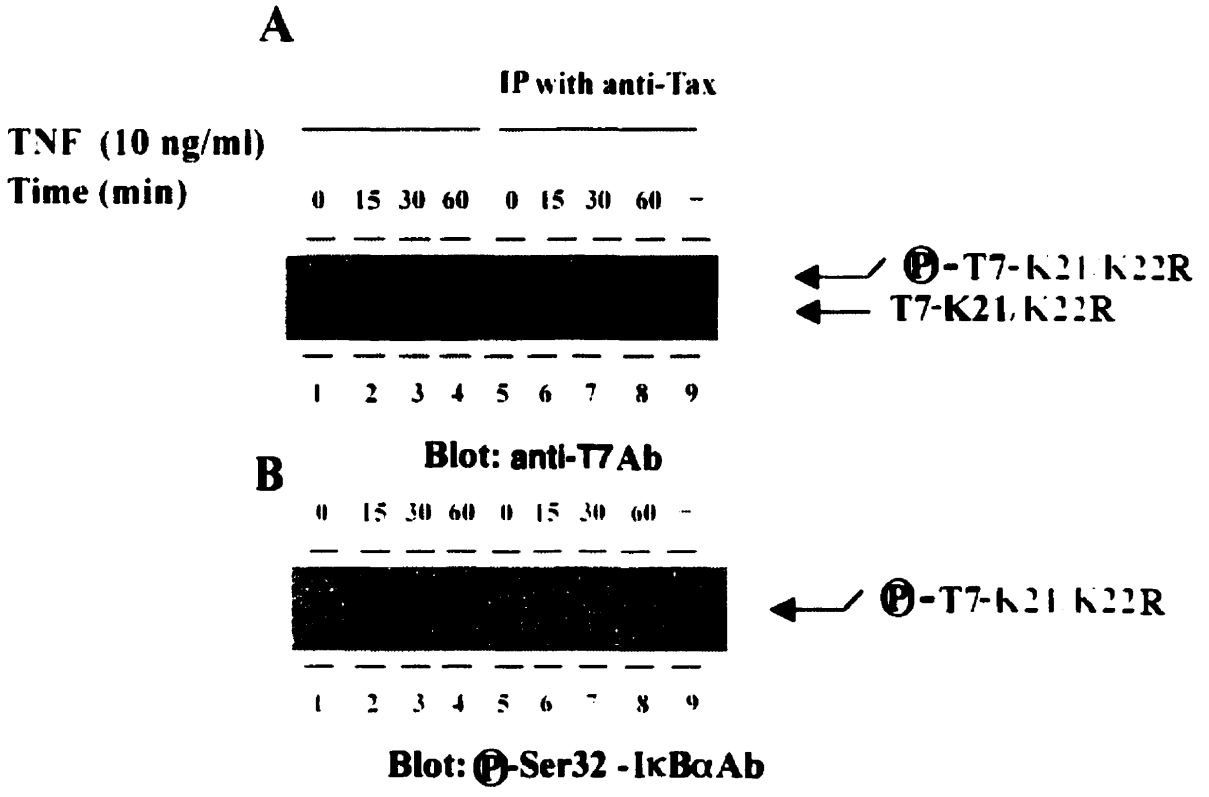
A
IP with anti-Tax
TNF (10 ng/ml)
Time (min)
0 15 30 60 0 15 30 60 –
1 2 3 4 5 6 7 8 9
Blot: anti-T7 Ab
B
0 15 30 60 0 15 30 60 –
1 2 3 4 5 6 7 8 9
Blot: P-Ser32 - IκBα Ab

endogenous IκBα and IκBαΔ4 (compare Fig. 26A, lanes 1-4 and Fig. 26B, lanes 1-4). However, only N-terminally hypophosphorylated IκBα was detected following Tax immunoprecipitation (compare Fig. 26A, lanes 5-8 and Fig. 26B, lanes 5-8). The T7-K21/22R mutant was inducibly phosphorylated upon TNFα treatment (Fig. 27B, lanes 1-4). As the levels of phosphorylated T7-K21/22R increased (Fig. 27B, lanes 1-4), the levels of T7K21/22R coimmunoprecipitated by Tax decreased (Fig. 27A, lanes 5-8), indicating the preferential association of Tax with the hypophosphorylated form of IκBα.

Tax interacts with newly synthesized IκBα in C8166 cells.

In C8166 cells, inducible turnover of IκBα is rapid (99,134) and since the pool of N-terminally unmodified IκBα is small, ^{35}S-methionine labeling was used to monitor IκBα turnover. NAC inhibited Ser32 and Ser36 phosphorylation of IκBα, permitting intracellular accumulation of unphosphorylated, ^{35}S labeled IκBα. Inhibition of proteasome activity with MG132 resulted in the intracellular accumulation of Ser32/Ser36 radiolabeled IκBα. Cells were labeled in the absence of any stimulus (Fig. 28 lane 1) or in presence of TNFα (Fig. 28, lanes 2-6) pretreated with MG132 (Fig. 28, lane 3) and NAC (Fig. 28, lanes 4-6). Cell extracts immunoprecipitated with Tax also coimmunoprecipitated newly synthesized IκBα at low levels (Fig. 28, lanes 1-3). However, from extracts of C8166 cells pretreated with MG132, Tax did not immunoprecipitate IκBα (Fig. 28, lane 3). When NAC was used, newly synthesized IκBα was not inducibly phosphorylated and a 10 fold increase in Tax association with IκBα was observed (Fig. 28, lane 4). MT-4 cells which do not express Tax were used as a control for monitoring the specificity of the Tax antibody (Fig. 28, lane 5).

Figure 28: Tax immunoprecipitated endogenous newly synthesized IκBα from C8166 cells. C8166 and MT-4 cells were ^{35}S methionine labeled in the presence of NAC (50 μM) (lanes 4-6) or MG132 (30 μM) (lane 3) for 1 hour followed by treatment with TNF. (10 ng/ml) for an additional hour in lanes 2-6. Double immunoprecipitations using 500 μg of cells extract with anti-IκBα antibody were performed (as described in Materials & Methods). The samples were run on a 12% SDS-polyacrylamide gel and exposed onto x-ray film for 3 days.

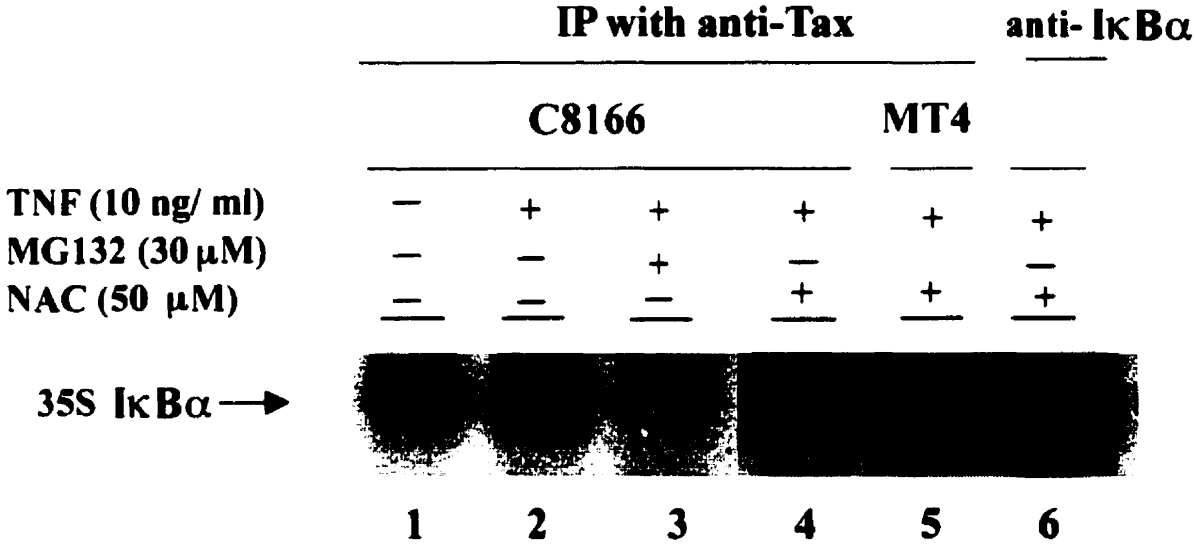
IP with anti-Tax
anti- IκBα
C8166
MT4
TNF (10 ng/ ml)
MG132 (30 μM)
NAC (50 μM)
35S IκBα
1
2
3
4
5
6

Tax enhances binding of IκBα to the proteasome.

Tax was shown to bind with equal affinities to two proteasome subunits, HC9 and HsN3 (150). Moreover, p105 bound preferably to the HC9 subunit; as a consequence, proteasome interaction as well as p105 processing was enhanced in the presence of Tax (150). Since Tax interacts with IκBα through the ankyrin repeats, we next sought to determine if Tax played a similar role in IκBα turnover. Jurkat cells were transfected with the T7-K21/22R mutant and either HC9 or HsN3. The level of T7-K21/22R binding to the proteasome subunits was analyzed by immunoprecipitation of the proteasome subunits, in the presence or absence of Tax (Fig. 29A-C). Although IκBα bound to the HC9 subunit, no significant enhancement of binding was observed in the presence of Tax, when immunoprecipitation was performed using anti-HC9 (Fig. 29A, compare lanes 2 and 3). Similarly, when the reverse immunoprecipitation was performed using anti-T7 tag antibody, equal levels of HC9 interacted with IκBα (Fig. 29A, compare lanes 4 and 5). Interestingly however, a Tax dependent binding of IκBα to the HsN3 proteasome subunit was detected by co-immunoprecipitation (compare Fig. 29B, lanes 2 and lane 3, as well as lanes 4 and 5). Tax is capable of interacting with T7-K21/22R in the absence of the proteasome subunits (Fig. 29C; lane 1). In addition, Tax alone demonstrated an interaction with both HsN3 (Fig. 29C, lane 2) and HC9 (Fig. 29C, lane 3). No T7-K21/22R was immunoprecipitated in the absence of Tax (Fig. 29C, lane 4).

Constitutive turnover of IκBα in the presence of Tax.

Constitutive IκBα degradation occurs independently of phosphorylation and ubiquitination (93). Since the IκBα 2N and ΔNIκBα mutants are resistant to signal mediated degradation, but maintain constitutive turnover, these IκB forms were used to investigate whether Tax promotes signal independent turnover of IκBα. To do so, wild type IκBα, 2N, or ΔNIκBα expressing plasmids, were transfected into murine

Figure 29: A Tax enhances the binding of IκBα to the proteasome. 293 cells were co-transfected with T7-K21/22R (5 μg), Tax (5 μg) and with pSGF-HC9 (5 μg) or pSGF-HsN3 (5 μg). Cells were harvested after 48h and 500 μg of cells extract was used per immunoprecipitation reaction. **(A) Analysis of the association of IκBα with the HC9 proteasome subunit and Tax.** Cell extract from cells transfected with T7-K21/K22R, HC9 and Tax expression vectors (lanes 3 and 5) or without Tax (lanes 2 and 4) were immunoprecipitated with anti-Flag antibody for HC9 (lanes 2-3) or anti-T7 tag antibody (lanes 4-5) and immunoblotted for T7-K21/22R or HC9, respectively. Specificity for anti-flag and anti-T7 were tested in lanes 1 and 6, respectively. **(B) Analysis of the association of IκBα with the HsN3 proteasome subunit and Tax.** Cell extract from cells transfected with T7-K21/22R and pSGF-HsN3 and Tax expressing vectors (lanes 3 and 5) or without Tax (lanes 2 and 4), were immunoprecipitated with anti-flag for HsN3 (lanes 2-3) or anti-T7-tag antibody for IκBα (lanes 4-5) and immunoblotted for T7-K21/22R or HsN3, respectively. Specificity of binding was analyzed by incubation of extract in the absence of anti-flag antibody (lane 1) and anti-T7 antibody (lane 6). **(C) Analysis of the affinity of T7-K21/22R for Tax and for HC9 and HsN3 in the presence of Tax.** The binding of T7-K21/22R to Tax (lane 1), or Tax in the presence of HsN3 (lane 2) or HC9 (lane 3). The specificity of binding of Tax to T7-K21/22R was tested by incubating extract without anti-Tax (lane 4).

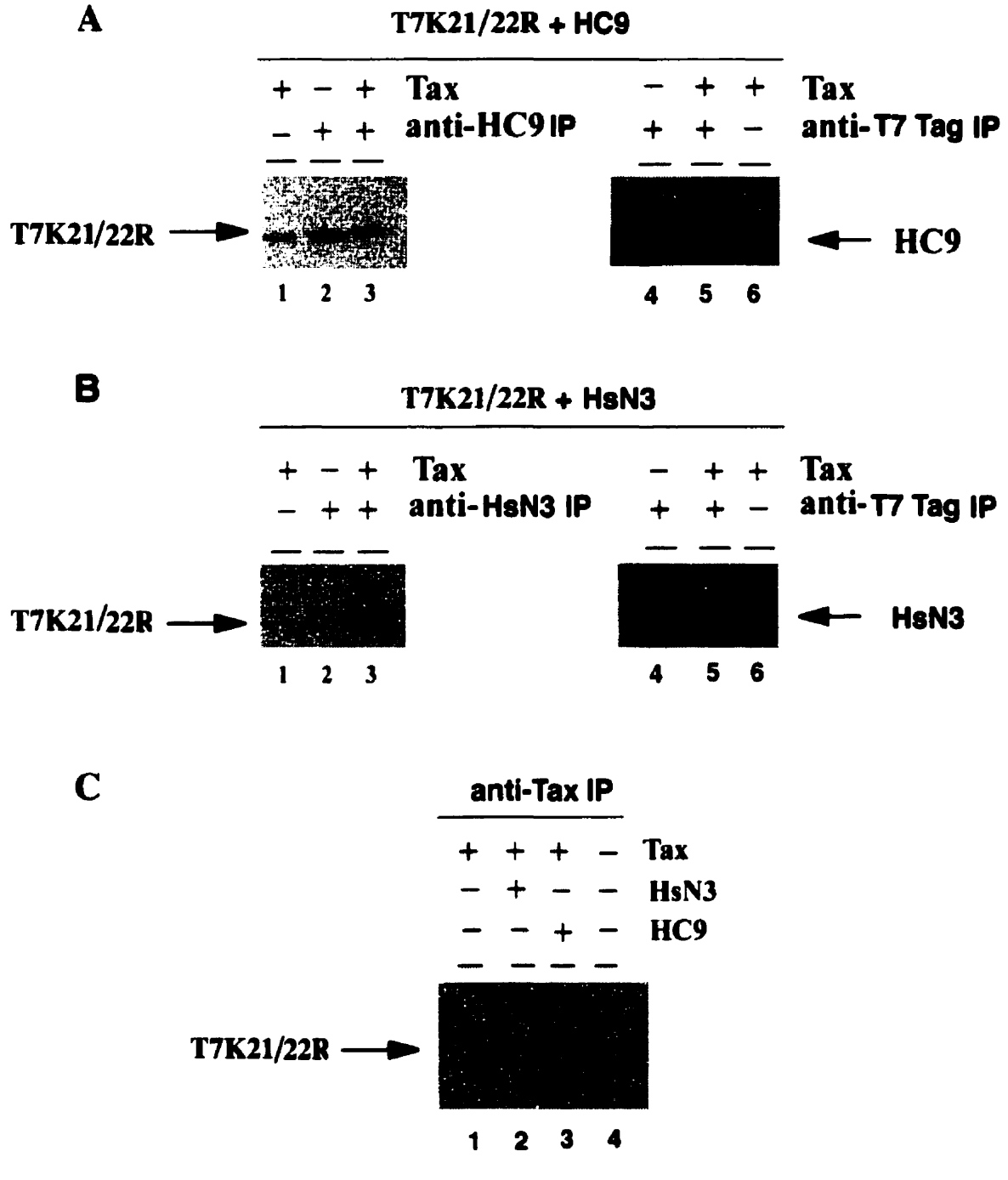
A
T7K21/22R + HC9
+ − + Tax
− + + anti-HC9 IP
− + + Tax
+ + − anti-T7 Tag IP
T7K21/22R
HC9
1 2 3
4 5 6
B
T7K21/22R + HsN3
+ − + Tax
− + + anti-HsN3 IP
− + + Tax
+ + − anti-T7 Tag IP
T7K21/22R
HsN3
1 2 3
4 5 6
C
anti-Tax IP
+ + + − Tax
− + − − HsN3
− − + − HC9
T7K21/22R
1 2 3 4

Figure 30: Tax enhances the constitutive turnover of IκBα. Murine NIH 3T3 cells were transfected with 7 μg of IκBα **(A)**, IκBα(2N) **(B)** or ΔNIκBα **(C)** alone (lanes 1-4), or with 10 μg of Tax expression vector (A-C, lanes 5-8). Following a 48h incubation, cells were pulse-labeled with ^{35}S methionine for 1 hour and chased with cold methionine of 0, 4, 8, and 16 hours. Cells were lysed in TNN buffer and with 500 μg of extract, a double immunoprecipitation was performed. Antibody used for immunoprecipitations was specific for the N-terminal region of IκBα, in the case of IκBα and 2N, or C-terminus for ΔNIκBα. Samples were then resolved on 10% SDS-polyacrylamide gel and exposed on film for 3 days. **(A)** The turnover of IκBα (lanes 1-4, upper band indicated) in the absence of Tax, was compared with IκBα turnover in the presence of Tax (lanes 5-8). The bands were quantified by densitometry and represented, graphically adjacent to the gel. Similarly, for 2N **(B)** and ΔNIκBα **(C)**.

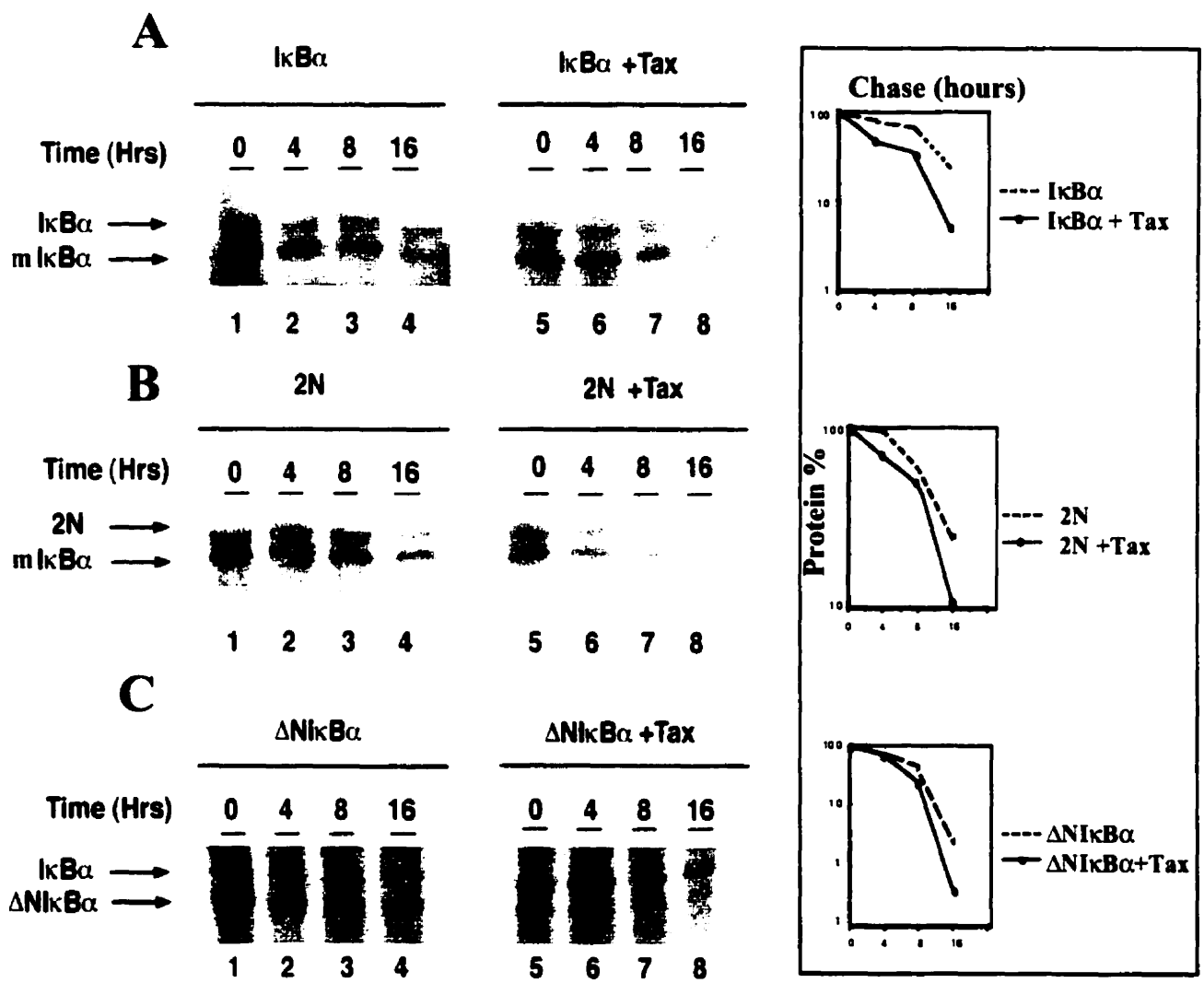
A
IκBα
IκBα +Tax
Time (Hrs)
0 4 8 16
0 4 8 16
IκBα
m IκBα
1 2 3 4
5 6 7 8
B
2N
2N +Tax
Time (Hrs)
0 4 8 16
0 4 8 16
2N
m IκBα
1 2 3 4
5 6 7 8
C
ΔNIκBα
ΔNIκBα +Tax
Time (Hrs)
0 4 8 16
0 4 8 16
IκBα
ΔNIκBα
1 2 3 4
5 6 7 8
Chase (hours)
Protein %
IκBα
IκBα + Tax
2N
2N +Tax
ΔNIκBα
ΔNIκBα+Tax

NIH 3T3 and 293 cells in the presence or absence of Tax expressing plasmid. Following a 48h incubation, cells were labeled with ^{35}S methionine for 1h, chased with cold methionine for 0-16h, followed by preparation of cell extracts and immunoprecipitation. The turnover of the IκB proteins was analyzed by SDS-PAGE and densitometry. As shown in Fig. 30A-C, the turnover wild type IκBα alone (Fig. 30A, lanes 1-4) was slower in the (absence compared to the presence Tax (Fig. 30A, lanes 5-8). In the case of IκBα(2N), Fig. 30B, lanes 1-4) about 75% of the protein was degraded by 16h but in the presence of Tax, 90% turnover was observed (graphic representation of adjacent gels). Similarly, ΔNIκBα (without the signal response domain), demonstrated increased turnover in the presence of Tax (Fig. 30C, lanes 1-4). Therefore, Tax enhanced constitutive IκBα turnover in the absence of phosphorylation and ubiquitination .

Chapter 6

General Discussion

Despite intense work performed by our group and many others, the precise mechanism by which HTLV-I transforms $CD4^+$ T cells still remains elusive. What has become evident is that a number of pathways can be envisioned by which HTLV-I can manipulate to maintain T cells in a permanent state of proliferation. Irrespective of pathways, what is clear is that the NF-κB/Rel transcription factors play a significant role in the road to cellular activation and transformation. Essential for HTLV-I gene expression and cellular transformation is the viral protein Tax.

Tax induces constitutive phosphorylation and turnover of IκBα

In all cases studied, Tax-expressing and HTLV-I infected T cells exhibited constitutive NF-κB binding activity (202). Interestingly, a comparison of the NF-κB complex composition between HTLV-I infected and Tax expressing cells was different from that of Jurkat cells immediately following NF-κB stimulation (88,101). HTLV-I infected or Tax expressing cell lines contained complexes composed of p50/c-rel and p52/c-rel heterodimers, whereas normal Jurkat cells following a two hour stimulation with PMA were composed exclusively of p50/RelA heterodimers (88,101). Prolonged PMA stimulation of Jurkat cells resulted in NF-κB complexes containing c-Rel and/or NF-κB2/ p52, in agreement with the high level expression of c-Rel and p52 observed in HTLV-I infected cells (88,101,167). Induction of NF-κB activity also stimulated c-Rel and NF-κB2 transcription, thus accounting for the sustained levels of c-Rel and p52 (43,47,106). Therefore, the Tax-induced constitutive NF-κB activity was a consequence of upregulated c-Rel and NF-κB expression.

To elucidate the mechanism by which Tax expressing and HTLV-I infected cells maintain constitutive NF-κB-DNA binding activity, the NF-κB regulatory protein, IκBα was investigated. These investigations demonstrated that constitutive phosphorylation and increased turnover of IκBα protein occur in HTLV-I and Tax

expressing T cells. An inverse correlation between Tax protein expression and steady state levels of IκBα was observed; higher levels of Tax in HTLV-I infected cells (MT-2 and C8166) resulted in greater levels of phosphorylated IκBα and increased rates of IκBα turnover. As a consequence of constitutive NF-κB activity in Tax expressing cells, a 7-10 fold increase of levels of (MAD-3)IκBα mRNA was observed.

Similar results were reported by other groups (88,167). Kanno *et al.* analyzed mad-3 gene expression using a Tax inducible cell line (88). Upon induction of Tax expression, mad-3 gene expression was increased dramatically (88). Although IκBα protein levels remained unaffected by Tax expression, turnover was significantly increased when compared to IκBα turnover in cells expressing a mutant Tax protein which does not induce NF-κB binding (88). The kinetics of Tax-mediated induction of NF-κB DNA binding activity were analyzed using an inducible Tax expression system, regulated in Jurkat T cells (JPX-9 cells) by the heavy metal responsive metallothionein promoter. The initial NF-κB binding activity observed after Tax induction by zinc was composed predominantly of p50/p65 heterodimers, activated by a posttranslational mechanism involving a Tax-induced proteolytic degradation of IκBα (88). At later times after Tax activation, NF-κB complexes containing c-Rel and NF-κB2 p52 accumulated, in part due to a transcriptional upregulation of c-Rel and NF-κB2 expression (88). Upon induction of Tax expression, *mad*-3 gene expression was also increased. Although the steady state levels of IκBα were unaffected by Tax expression in JPX-9 cells, IκBα turnover was increased significantly in cells expressing a wild type Tax but not a mutant Tax protein (163). The positive autoregulation of c-Rel and NF-κB2 (101,106,167) together with Tax-induced degradation of IκBα alters the intracellular accumulation of NF-κB heterodimers and may continuously weaken IκBα inhibition of DNA binding activity.

Constitutive phosphorylation and increased degradation of IκBα were also detected in other HTLV-I infected and Tax expressing T cell models (99,167). In general, an inverse correlation between Tax protein expression and steady state levels of IκBα was observed in these studies; i.e. higher levels of Tax in HTLV-I infected cells (MT-2 and C8166-45) resulted lower levels of IκBα, higher levels of phosphorylated IκBα, and faster IκBα turnover. Disruption of the NF-κB/IκB autoregulatory pathway results in constitutive NF-κB DNA binding activity that may promote aberrant NF-κB-dependent gene expression in T cells.

Accordingly, Sun *et al*, concluded that Tax expression induced constitutive phosphorylation and rapid turnover of IκBα (167). However, the half life of IκBα in C8166 cells (< 5 min.) (167) differed significantly from the one shown in Table 1 (43 min). This discrepancy may be explained by the fact that Sun *et al.* measured turnover of the phosphorylated form of IκBα, while the turnover of the whole IκBα pool (both unphosphorylated and phosphorylated) was measured in the experimental results presented in Table 1 Several recent studies have examined the role of Tax in inducer-mediated degradation of IκBα (90,167); furthermore mutation of Ser-32 and/or Ser-36 prevents Tax mediated degradation of IκBα (35,89). Together, these results support a model in which HTLV-I Tax induces a signal transduction pathway involved in the phosphorylation and degradation of IκBα .

Interestingly, pre-B to B cell differentiation involves changes in NF-κB activity that are very analogous to those described in T cells versus HTLV-I infected T cells. NF-κB activity is highly inducible in pre-B cells and in normal T cells, but constitutive in both mature B cells and Tax-expressing T cells. In these latter two cell types, MAD-3 and *c-rel* mRNAs are overexpressed and c-Rel is a major component of the constitutive DNA binding activity. Importantly, IκBα turns over rapidly with a half life

between 40 and 50 minutes in mature B cells and Tax-expressing T cells, whereas in pre-B and normal T cells, IκBα half life is between 150 and 160 minutes. Moreover, in mature B cells, increased IκBα turnover is due to increased activity of a serine protease, since TPCK, an inhibitor of serine proteases, stabilizes IκBα and inhibits NF-κB binding activity (120). At this time, we and others proposed that HTLV-I Tax may physically associate with and activate a host kinase that phosphorylates IκBα; phosphorylation in turn may target IκBα for degradation. Finally, after years of searching and speculation, Yin, M-J. *et al.*, 1998, provided the missing link to the mechanism of constitutive phosphorylation of IκBα in HTLV-I cells . The Tax protein binds to the amino terminus of MEKK1 to stimulate IκB kinase activity and NF-κB activation (201). The Tax-MEKK1 interaction leads to the activation of the IκBα kinase (IKK) heterocomplex involved in the phosphorylation of IκBα (201). However, the mechanism by which Tax activates MEKK1 remains unclear (201). Other activities associated with Tax such as transcription factor dimerization (7,183) and/or transcriptional activation (53,54,177) would then promote Tax mediated gene activity.

HTLV-I Tax protein increases NF-κB dimer formation and antagonizes the inhibitory activity of IκBα.

From an evolutionary standpoint, the viral Tax protein is a unique and efficiently designed molecule. To date, no cellular homologue of Tax has been identified. Molecular analysis of Tax through mutagenesis revealed no one identifiable domain responsible for specific interactions with host factors. Rather, amino acids that were important for function were interspersed throughout the molecule. Yet, Tax is capable of interacting with many proteins whose structure and function is highly variable between the protein species.

Physical associations of Tax with the CREB/ATF family was shown to increase protein dimerization (14,67,96,171). *In vitro*, Tax was found to interact with a basic leucine zipper motif (bZIP) found within CREB/ATF proteins (65). More recently, *in vivo* studies found that Tax was able to colocalize with CREB in the nucleus (60). Although CREB dimerization is essential for DNA binding, it is not sufficient for gene transactivation (179). The Tax mutant M47, which fails to activate the HTLV-I LTR, continues to enhance DNA binding of several bZIP proteins (179). This suggests that Tax plays an additional role in mediating CREB transactivation. Giebler *et al* proposed that Tax directly interacts with the cellular coactivator CREB binding protein (CBP), recruiting it directly to CREB and the viral promoter and bypassing the requirement for protein kinase A phosphorylation of CREB. Once tethered to the promoter by Tax, CBP appears to facilitate transcriptional activation by recruitment of the general transcription machinery (60). In addition, Tax directly interacts with both the bZIP domain of CREB and CBP (60). This Tax-CREB-CBP containing complex binds to DNA with high affinity, anchoring the coactivator to the HTLV-I promoter (60).

HTLV-I Tax expressing cells demonstrate constitutive NF-κB binding activity in addition to CREB activity. Previous studies have demonstrated that Tax interacted directly with NF-κB proteins; predominantly with NF-κB2(p100/p52), as well as with NF-κB1(p105/p50), p65 and c-Rel (27,79,126,174). However, in the case of the NF-κB transcription factors, the NF-κB dimer complex alone has been shown to be sufficient for gene transactivation (108). Therefore, it was of interest to see if NF-κB binding was directly enhanced by Tax, similarly to CREB dimerization.

Recombinant NF-κB, IκBα and Tax proteins were used to evaluate the effect of Tax-NF-κB interactions on DNA binding activity and gene activity. First, to determine if a

Tax-NF-κB interaction would result in enhanced DNA binding by stimulation of NF-κB dimer formation. Tax specifically stimulated the DNA binding of NF-κB subunits by 20 to 40 fold and the effect was maximal at low concentrations of NF-κB protein. In contrast, Tax mediated enhancement of DNA binding was not observed with the unrelated IRF-1 factor, indicating a specificity of Tax for NF-κB/Rel proteins, as well as bZIP proteins (188). Second, Tax enhanced the amount and the rate of association of NF-κB binding to DNA but had no effect on the rate of dissociation of protein-DNA complexes. Once dimerization has occurred, Tax may no longer be required in the NF-κB/DNA complex. This model, as originally proposed for Tax-bZIP interactions, could explain why Tax is not observed as a component of the NF-κB/DNA complex (188,192). Other studies using transient transfection in NF-κB mediated gene expression assays demonstrated that increasing amounts of Tax resulted in the stimulation of NF-κB mediated gene activity despite the presence of IκBα (98,115), although the dose dependent effect of Tax was greatly diminished when cells were pretreated with inhibitors of IκBα degradation (115).

Immunocytochemisty and electron microscopy were used to study the localization of Tax and NF-κB subunits (28). Bex *et al* demonstrated that Tax is present in distinct nuclear structures in HTLV-I transformed T lymphocytes (28). In cells transfected with Tax expression vectors, Tax also distributed in nuclear structures which include the NF-κB subunits p50 and RelA(p65). In addition, the Tax containing nuclear structures also contain splicing factors Sm and SC-35 and the large subunit of RNA polymerase II (28). Within these nuclear structures where Tax colocalized with NF-κB, mRNA of genes specifically activated by Tax were present (28). Taken together, these studies support a model where Tax can activate NF-κB mediated transactivation by directly enhancing dimerization of the NF-κB subunits in the absence of DNA.

Using affinity chromatography, transient transfection and immunoprecipitations we were also able to demonstrate Tax-IκBα interactions. Tax interactions with the IκB family members, p105 and IκBγ have been demonstrated previously (79,80,189). Tax interactions with p105 and IκBγ occurred specifically through the ankyrin repeats (79,80,189). Interactions with Tax and IκBγ or p105 dissociated the IκB molecule from NF-κB complexes, resulting in nuclear translocation of NF-κB proteins (79,80,189). We provide additional evidence that Tax can either compete for or physically remove IκBα from the NF-κB-DNA complex, since Tax can overcome IκBα mediated inhibition of NF-κB binding in EMSA. The recent observation that IκBα can shuttle into the nucleus (4) also lends support to the idea that IκBα may directly inhibit gene expression by dissociating NF-κB-DNA complexes *in vivo*. In support of Tax-IκBα interactions, binding of Tax to the NF-κB1 and NF-κB2 molecules via the ankyrin repeats was shown previously to increase nuclear translocation of Rel/NF-κB proteins (27,90,101,167). Interestingly, wild type Tax as well as mutant Tax M22 ($NF\text{-}\kappa B^{-}/CREB^{+}$) and M47 ($NF\text{-}\kappa B^{+}/CREB^{-}$) were able to bind to IκBα *in vivo*. The fact that the Tax M22 mutant was still able to bind to IκBα, despite a block in NF-κB mediated transactivation (32), suggested that the inability of Tax M22 to activate NF-κB function was not be due to a block in Tax-NF-κB/IκB interaction but rather to an inability of Tax M22 to target IκBα for degradation.

In this regard, Tax was found recently to associate with two subunits of the 20S proteasome, HsN3 and HC9 (150). Tax-NF-κB1(p105) association led to increased proteasome mediated processing of the p105 precursor to the DNA binding form p50 (150). These experiments provide a vital link between the proteasome and NF-κB on the one hand and Tax activity on the other. However, the increased proteolysis of NF-κB1 in the presence of Tax is limited (150) and also does not account for the dramatic increases in NF-κB2 and c-Rel levels observed in HTLV-I transformed and Tax-

expressing cell lines (27,43,88,101,173). Nevertheless, Tax may likewise target IκBα for degradation via the same mechanism. The inability of Tax M22 to mediate NF-κB induction may be due to the inability of Tax M22 to bind to the proteasome and form a ternary complex. Interestingly, preliminary evidence indicates that Tax may bind preferentially to hypophosphorylated IκBα, since it was not possible to immunoprecipitate a Tax-IκBα complex from C8166 cells after treatment with Calpain inhibitor I, which blocks the activity of the proteasome but not IκBα phosphorylation or ubiquitination. Compounds such as Calpain inhibitor I and MG132 would thus be expected to abolish Tax mediated NF-κB transactivation (115). On the other hand, the use of PDTC which effectively blocks IκBα phosphorylation permitted the immunoprecipitation of Tax-IκBα complexes. The ability of Tax to stimulate NF-κB binding activity thus occurs at multiple levels (81) including Tax enhanced dimerization of NF-κB subunits in the absence of DNA, stimulation of NF-κB binding, physical interaction of Tax with IκBα and interference with the regulatory function of IκBα.

Tax-IκBα association is dependent on the phosphorylation state of IκBα.

In this present study, we demonstrate that (1) HTLV-I Tax interacts with the ankyrin repeats of IκBα, which are essential for interaction with the Rel domain of the NF-κB/Rel proteins; (2) Tax preferentially interacts with N-terminally hypophosphorylated IκBα; (3) in addition, Tax enhanced constitutive degradation of wild-type and mutated forms of IκBα in the absence of phosphorylation and ubiquitination; and finally (4) Tax also enhanced binding of IκBα to the proteasome subunit HsN3. The interaction of Tax with hypophosphorylated IκBα may serve the dual purpose of preventing IκBα from binding to and sequestering NF-κB and also acting as a viral chaperone to target IκBα to the proteasome for degradation via a phosphorylation-independent pathway.

In support of this idea, Tax was found to activate NF-κB in cell lines in which IκBα cannot be inducibly degraded. Induction of NF-κB in these cell lines involved degradation of IκBα by the proteasome without phosphorylation (42). Furthermore, Tax is able to directly associate with the proteasome subunits HC9 and HsN3 and enhance the constitutive processing of p105, forming a ternary complex between p105, Tax, and HC9 (26,150). The model emerging for IκBα degradation involves two pathways: phosphorylation/ubiquitination-dependent and-independent pathways. The phosphorylation/ubiquitination-dependent pathway requires phosphorylation within the signal response domain (SRD) of IκBα at Ser32 and Ser36 in response to a broad spectrum of stimuli including cytokines, LPS, PMA and viruses (18,156,181). Ser32/Ser36 phosphorylation by the IκB kinase (IKK), is a prerequisite to ubiquitination at Lys 21 and Lys 22 that then targets IκBα to the 26S proteasome for degradation (119,156,198). The C-terminal PEST domain of IκBα is also required for signal-induced degradation (18,36,94). The PEST sequence is a highly acidic domain (rich in proline, glutamic acid, serine and threonine), involved in proteolysis of several cellular proteins (reviewed by (146). Several reports indicate that IκBα requires NF-κB in order to be a target for signal-induced breakdown, a process mediated both by the SRD and the PEST sequence (36,93,94). Although the PEST sequence is required for signal-induced degradation, it is not clear in what way the sequence contributes to targeting the protein for the degradation machinery (94,148,191).

The phosphorylation/ubiquitination-independent pathway is not well understood but appears to be involved in the constitutive turnover of IκBα (93). By this mechanism, IκBα need not be phosphorylated nor ubiquitinated to be degraded by the proteasome (93). Substrate ubiquitination is not an absolute requirement for degradation by the proteasome, as has been demonstrated for the c-Jun protein (85,93). Constitutive turnover of IκBα requires the C-terminal PEST region, a domain upstream of the PEST

domain, and the ankyrin repeats (93,94). Although signal-independent destruction of IκBα is accomplished by the proteasome (since proteasome inhibitors such as MG132 inhibit both inducible and constitutive turnover), there exists the possibility of an as yet unknown molecular chaperone controlling or antagonizes IκBα breakdown that is itself degraded by the proteasome.

IκBα protein domains involved in induced breakdown are not required for basal turnover (93). Deletion of the N-terminal SRD or the C-terminal PEST has been shown to affect neither the high turnover of free IκBα nor the reduced turnover of NF-κB bound IκBα. Since both N- and C-terminally deleted IκBα could still bind to NF-κB, proteolysis of the two mutants due to improper folding is unlikely (18,93). Furthermore, these deletion mutants displayed similar turnover kinetics, suggesting that the same mechanism was involved (93). In addition, high IκBα turnover was not influenced by replacing all lysine residues with arginine (41); in cells carrying a temperature sensitive, E1 ubiquitination mutant the turnover of IκBα was not affected when the E1 enzyme was inactivated after shifting to the restrictive temperature (93). The possibility of low level activation of IκBα via phoshorylation has also been excluded (93). Thus, substrate ubiquitination does not appear to be required for IκBα constitutive turnover *in vivo*, suggesting the existence of different mechanisms controlling signal-dependent and constitutive degradation.

Three recent studies have demonstrated that Tax enhances the phosphorylation-dependent mechanism of IκBα degradation by stimulating the IκB kinase activity (IKK), responsible for phosphorylation of Ser32 and Ser36 (8,119,193,203). In one study, Tax was found to bind to the N-terminal domain of MEKK1, a component of the IκB kinase complex and stimulate MEKK1 activity. Tax expression increased the activity of IKKβ to enhance phosphorylation of IκBα. Furthermore, dominant negative

mutants of both IKKβ and MEKK1 prevented Tax activation of the NF-κB pathway, while recombinant MEKK1 stimulated IKKβ phosphorylation of IκBα (199). Another study demonstrated that Tax associated with the IKK in Tax transfectants of HTLV-I-infected T lymphocytes. Point mutations in Tax that disrupted the IKK-binding function of Tax also blocked Tax-mediated activation of IKK and NF-κB (40). Similarly, constitutive IKK activation was demonstrated in Tax-expressing and HTLV-I-infected cells with the additional involvement of the NF-κB inducing kinase (NIK). Inactive forms of either IKKs or NIK attenuated Tax-mediated NF-kB activation (185). In accord with the above studies, Nicot *et al.* recently demonstrated that cytoplasmic forms of Tax caused a reduction in the amount of IκBα and constitutive activation of NF-κB DNA binding in the nucleus, consistent with the alteration of the NF-κB signaling pathway by cytoplasmic Tax (133). This latter study also reinforces the potential importance of cytoplasmic relocalization of Tax in T-cell transformation and viral latency (27,101,139). These observations are particularly appealing since they provide a molecular mechanism for signal-induced degradation of IκB in HTLV-I-infected cells and the constitutive presence of NF-κB DNA binding activity as a consequence of the coupling of the viral Tax oncoprotein to the IKK-MEKK1 signaling pathways (40,185,199).

Normally, NF-κB is transiently active. Many genes involved in the immune response and cellular growth are controlled by NF-κB. Therefore, the induced IκBα degradation and subsequent increase in NF-κB activity would be balanced by an increase in IκBα synthesis, once again binding to and sequestering NF-κB. However, Tax plays a dual role in maintaining NF-κB activity. First, Tax targets IκBα for degradation by activating MEKK1, leading to IKK activation and IκBα phosphorylation, targeting IκBα for degradation. Second, Tax guards against inhibition of NF-κB by binding to and sequestering newly synthesized IκBα. Introduction of IκBα transdominant

mutants abolishes induced IκBα degradation (35,89). Yet, constitutive turnover being independent of the MEKK1 pathway, the ability Tax to enhance constitutive turnover of IκBα remains unaffected. The population of IκBα that would be affected by Tax would most likely be free IκBα considering that NF-κB bound IκBα no longer has the ankyrin repeats accessible for binding.

Multiple levels of Tax mediated NF-κB Transactivation

The molecular mechanism by which Tax maintains a persistent NF-κB activity is slowly being unraveled. Based on the results presented here and other published reports, NF-κB transactivation is mediated at multiple levels.

The model proposed for constitutive NF-κB activity induced by Tax involves: 1) an activation of the signal transduction pathway involving signal induced degradation of IκBα, freeing NF-κB dimers to translocate to the nucleus. 2) Direct Tax-NF-κB interactions enhance NF-κB dimer formation and in turn enhanced NF-κB-DNA binding. 3) Tax-IκBα interactions can result in Tax preventing IκBα from interacting with NF-κB dimers. 4) Tax enhances the constitutive turnover of IκBα by interacting with hypophosphorylated IκBα, targeting it to the proteasome for degradation. The resulting constitutive NF-κB activity and aberrant expression of genes involved in T cell activation can initiate events involved in the proliferation of $CD4^+$ T lymphocytes and trigger events leading to leukemogenesis.

Contributions to Original Knowledge

The present studies on the molecular mechanism of Tax mediated transactivation have contributed to a better understanding of the mechanisms by which Tax interacts with the NF-κB/Rel transcription factors and the inhibitory IκBα protein to initiate and maintain constitutive NF-κB activity leading to aberrant gene expression. The results presented in this thesis contributed to original knowledge in the following manner:

1. In HTLV-I infected and Tax expressing T cells, Tax expression promoted constitutive phosphorylation of the inhibitor IκBα. Although the mad-3 gene was overexpressed, protein levels were 7 to 10 fold lower than in normal T cells, suggesting an increased IκBα turnover. Indeed, IκBα turnover rates were 3 fold more rapid in cells that constitutively expressed the Tax protein. Therefore, Tax activates the signal response pathway involved in signal induced degradation of IκBα.

2. NF-κB-Tax interactions result in a Tax mediated enhancement of NF-κB dimer formation and a 20 to 40 fold increase in DNA binding. Tax enhanced the association of NF-κB binding to DNA but had no effect on dissociation.

3. Tax was also able to interact with IκBα. In vitro, Tax was able to interfere with IκBα binding to NF-κB. Tax may either compete for or physically remove IκBα from the NF-κB-DNA complex since Tax can overcome IκBα mediated inhibition of NF-κB binding in EMSA.

4. Analysis of the Tax-IκBα interaction revealed that Tax preferentially interacted with the N-terminally hypophosphorylated IκBα. In addition, IκBα formed a Tax

dependent association with proteasome subunit HsN3. In the presence of Tax, IκBα turnover was increased in the absence of inducer.

This study indicates that Tax acts at multiple levels to activate and maintain NF-κB mediated transcription in HTLV-I infected cells.

Chapter 7

References

1. **Adachi, Y., T.D. Copeland, M. Hatanaka and S. Oroszlan.** 1993. Nucleolar targeting signal of Rex protein of human T-cell leukemia virus type I specifically binds to nucleolar shuttle protein B-23. J.Biol.Chem. **268**:13930-13934.

2. **Adachi, Y., T.D. Copeland, C. Takahashi, T. Nosaka, A. Ahmed, S. Oroszlan and M. Hatanaka.** 1992. Phosphorylation of the Rex protein of human T-cell leukemia virus type I. J.Biol.Chem. **267**:21977-21981.

3. **Alkalay, I., A. Yaron, A. Hatzubai, S. Jung, A. Avraham, O. Gerlitz, I. Pashut-Lavon and Y. Ben-Neriah.** 1995. *In vivo* stimulation of IκB phosphorylation is not sufficient to activate NF-κB. Mol.Cell.Biol. **15**:1294-1301.

4. **Arenzana-Seisdedos, F., J. Thompson, M.S. Rodriguez, F. Bachelerie, D. Thomas and R.T. Hay.** 1995. Inducible nuclear expression of newly synthesized IκBα negatively regulates DNA-binding and the transcriptional activities of NF-κB. Mol.Cell.Biol. **15**:2689-2696.

5. **Arenzana-Seisdedos, F., P. Turpin, M. Rodriguez, D. Thomas, R.T. Hay, J-L. Virelizier and C. Dargemont.** 1997. Nuclear localization of IκBα promotes active transport of NF-κB from the nucleus to the cytoplasm. J.Cell Sci. **110**:369-378.

6. **Arima, N., J.A. Molitor, M.R. Smith, J.H. Kim, Y. Daitoku and W.C. Greene.** 1991. Human T-cell leukemia virus type I Tax induces expression of the *rel*-related family of κB enhancer-binding proteins: evidence for a pretranslational component of regulation. J.Virol. **65**:6892-6899.

7. **Armstrong, A.P., A.A. Franklin, M.N. Uittenbogaard, H.A. Giebler and J.K. Nyborg.** 1993. Pleiotropic effect of the human T-cell leukemia virus Tax protein on the DNA binding activity of eukaryotic transcription factors. Proc.Natl.Acad.Sci. **90**:7303-7307.

8. **Baeuerle, P.A. and D. Baltimore.** 1988. IκB: a specific inhibitor of the NF-κB transcription factor. Science **242**:540-546.

9. **Baeuerle, P.A. and T. Henkel.** 1994. Function and activation of NF-κB in the immune system. Annu.Rev.Immunol. **12**:141-179.

10. **Baldi, L., K. Brown, G. Franzoso and U. Siebenlist.** 1996. Critical role for lysines 21 and 22 in signal-induced, ubiquitin-mediated proteolysis of IκBα. J.Biol.Chem. **271**:376-379.

11. **Ballard, D.W., E. Bohnlein, J.W. Lowenthal, Y. Wano, B.R. Franza and W.C. Greene.** 1988. HTLV-I tax induces cellular proteins that activate the kappa B element in the IL-2 receptor alpha gene. Science **241**:1652-1655.

12. **Ballard, D.W., W.H. Walker, S. Doerre, S. Sista, J.A. Molitor, E.P. Dixon, N.J. Peffer, M. Hanninck and W.C. Greene.** 1990. The v-rel oncogene encodes a κB enhancer binding protein that inhibits NF-κB function. Cell **63**:803-814.

13. **Bantignies, F., R. Rousset, C. Desbois and P. Jalinot.** 1996. Genetic characterization of transactivation of the human T-cell leukemia virus type 1 promoter: Binding of Tax to Tax-responsive element 1 is mediated by the cyclic AMP-responsive members of the CREB/ATF family of transcription factors. Mol.Cell Biol. **16**:2174-2182.

14. **Beauparlant, P. and J. Hiscott.** 1996. Biological and biochemical inhibitors of the NF-κB/Rel proteins and cytokine synthesis. Cyt.Growth Fact.Rev. **7**:175-190.

15. **Beauparlant, P., I. Kwan, R. Bitar, P. Chou, A.E. Koromilas, N. Sonenberg and J. Hiscott.** 1994. Disruption of IκBα regulation by antisense RNA expression leads to malignant transformation. Oncogene **9**:3189-3197.

16. **Beauparlant, P., H. Kwon, M. Clarke, R. Lin, N. Sonenberg, M. Wainberg and J. Hiscott.** 1996. Transdominant mutants of IκBα block Tat-TNF synergistic activation of HIV-1 expression and virus multiplication. J.Virol. **70**:5777-5785.

17. **Beauparlant, P., R. Lin and J. Hiscott.** 1996. The role of the C-terminal domain of IκBα in protein degradation and stability. J.Biol.Chem. **271**:10690-10696.

18. **Beg, A.A. and S. Baldwin,Jr..** 1993. The IκB proteins: multifunctional regulators of Rel/NF-κB transcription factors. Genes Dev **7**:2064-2070.

19. **Beg, A.A., T.S. Finco, P.V. Nantermet and A.S. Baldwin,Jr..** 1993. Tumor necrosis factor and interleukin-1 lead to phosphorylation and loss of IκBα: a mechanism for NF-κB activation. Mol.Cell Biol. **13**:3301-3310.

20. **Beg, A.A., S.M. Ruben, R.I. Scheinman, S. Haskill, C.A. Rosen and A.S. Baldwin,Jr..** 1992. IκB interacts with the nuclear localization sequence of the subunits of NF-κB: a mechanism for cytoplasmic retention. Genes Dev **6**:1899-1913.

21. **Beg, A.A., W.C. Sha, R.T. Bronson, S. Ghosh and D. Baltimore.** 1995. Embryonic lethality and liver degeneration in mice lacking the RelA component of NF-κB. Nature **376**:167-170.

22. **Beimling, P. and K. Moelling.** 1992. Direct interaction of CREB protein with 21bp Tax-response elements of HTLV-I LTR. Oncogene **7**:257-262.

23. **Belvin, M.P., Y. Jin and K.V. Anderson.** 1995. Cactus protein degradation mediates *Drosophila* dorsal-ventral signaling. Genes Dev **9**:783-793.

24. **Benkirane, M., C. Neuveut, R.F. Chun, S.M. Smith, C.E. Samuel, A. Gatignol and K.T. Jeang.** 1997. Oncogenic potential of TAR RNA binding protein TRBP and its regulatory interaction with RNA-dependent protein kinase PKR. EMBO J. **16**:611-624.

25. **Beraud, C., S-C. Sun, P. Ganchi, D.W. Ballard and W.C. Greene.** 1994. Human T-cell leukemia virus type I Tax associates with and is negatively regulated by the NF-κB2 p100 gene product: Implications for viral latency. Mol.Cell Biol. **14**:1374-1382.

26. **Bex, F., A. McDowall, A. Burny and R. Gaynor.** 1997. The human T-cell leukemia virus type 1 transactivator protein Tax colocalizes in unique nuclear structures with NF-κB proteins. J.Virol. **71**:3484-3497.

27. **Blank, V., P. Kourilsky and A. Israël.** 1991. Cytoplasmic retention, DNA binding and processing of the NF-κB p50 precursor are controlled by a small region in its C-terminus. EMBO J. **10**:4159-4167.

28. **Bose, H.R.,Jr** 1992. The Rel family: models for transcriptional regulation and oncogenic transformation. Biochim.Biophys.Acta. **1114**:1-17.

29. **Brabin, L., B.J. Brabin, R.R. Doherty, I.D. Gust, M.P. Alpers, R. Fujino, J. Imai and Y. Hinuma.** 1989. Patterns of migration indicate sexual transmission of HTLV-I infection in non-pregnant women in Papua New Guinea. Int.J.Cancer **44**:59-62.

30. **Brasier, A.R., D. Ron, J.E. Tate and J.F. Habener.** 1990. A family of constitutive C/EBP-like DNA binding proteins attenuate the IL-1α induced, NF κB mediated *trans*-activation of the angiotensinogen gene acute-phase response element. EMBO J. **9**:3933-3944.

31. **Brass, A., E. Kehrli, C. Eisenbeis, U. Storb and H. Singh.** 1996. Pip, a lymphoid restricted IRF, contains a regulatory domain that is important for autoinhibition and ternary complex formation with the Ets factor PU.1. Genes Dev **10**:2335-2347.

32. **Bressler, P., K. Brown, W. Timmer, V. Bours, U. Siebenlist and A.S. Fauci.** 1993. Mutational analysis of the p50 subunit of NF-κB and inhibition of NF-κB activity by trans-dominant p50 mutants. J.Virol. **67**:288-293.

33. **Brockman, J.A., D.C. Scherer, T.A. McKinsey, S.M. Hall, X. Qi, W.Y. Lee and D.W. Ballard.** 1995. Coupling of a signal response domain in IκBα to multiple pathways for NF-κB activation. Mol.Cell.Biol. **15**:2809-2818.

34. **Brown, K., G. Franzoso, L. Baldi, L. Carlson, L. Mills, Y.-C. Lin, S. Gerstberger and U. Siebenlist.** 1997. The signal response of IκBα is regulated by transferable N- and C- terminal domains. Mol.Cell.Biol. **17**:3021-3027.

35. **Brown, K., S. Gerstberger, L. Carlson, G. Franzoso and U. Siebenlist.** 1995. Control of IκB-α proteolysis by site-specific, signal-induced phosphorylation. Science **267**:1485-1488.

36. **Brown, K., S. Park, T. Kanno, G. Franzoso and U. Siebenlist.** 1993. Mutual regulation of the transcriptional activator NF-κB and its inhibitor, IκBα. Proc.Natl.Acad.Sci.USA **90**:2532-2536.

37. **Chinnadurai, G.** 1991. Modulation of HIV-enhancer activity by heterologous agents: a minireview. Gene **101**:165-170.

38. **Ciechanover, A.** 1994. The ubiquitin-proteasome proteolytic pathway. Cell **79**:13-21.

39. **Courtois, G., S.T. Whiteside, C.H. Sibley and A. Israel.** 1997. Characterization of a mutant cell line that does not activate NF-κB in response to multiple stimuli. Mol.Cell.Biol. **17**:1441-1449.

40. **Crenon, I., C. Béraud, P. Simard, J. Montagne, P. Veschambre and P. Jalinot.** 1993. The transcriptionally active factors mediating the effect of the HTLV-I tax transactivator on the IL-2Rα κB enhancer include the product of the c-*rel* proto-oncogene. Oncogene **8**:867-875.

41. **D'Agostino, D.M., V. Ciminale, L. Zotti, A. Rosato and L. Chieo-Bianchi.** 1997. The human T cell lymphotropic virus type 1 Tof protein contains a bipartite nuclear localization signal that is able to functionally replace the amino- terminal domain of Rex. J.Virol. **71**:75-83.

42. **Daenkes, S., S. Nightingale, J.K. Cruickshank and C.R. Bangham.** 1990. Sequence variants of HTLV-I from patients with tropical spastic paraparesis and adult T cell leukemia do not distinguish neurological from leukemic isolates. J.Virol. **64**:1278-1282.

43. **DiDonato, J.A., F. Mercurio and M. Karin.** 1995. Phosphorylation of IκBα precedes but is not sufficient for its dissociation from NF-κB. Mol.Cell Biol. **15**:1302-1311.

44. **Duckett, C.S., N.D. Perkins, T.F. Kowalik, R.M. Schmid, E.-S. Huang, A.S. Baldwin, Jr. and G.J. Nabel.** 1993. Dimerization of NF-κB2 with RelA(p65) regulates DNA binding, transcriptional activation, and inhibition by an IκB-α (MAD3). Mol.Cell Biol. **13**:1315-1322.

45. **Escalante, C.R., J. Yie, D. Thanos and A.K. Aggarwal.** 1998. Structure of IRF-1 with bound DNA reveals determinants of interferon regulation. Nature **391**:103-106.

46. **Finco, T.S., A.A. Beg and A.S. Baldwin,Jr.** 1994. Inducible phosphorylation of IκBα is not sufficient for its dissociation from NF-κB and is inhibited by protease inhibitors. Proc.Natl.Acad.Sci.USA **91**:11884-11888.

47. **Fracchiolla, N.S., L. Lombardi, M. Salina, A. Migliazza, L. Baldini, E. Berti, L. Cro, E. Polli, A.T. Maiolo and A. Neri.** 1993. Structural alterations of the NF-κB transcription factor lyt-10 in lymphoid malignancies. Oncogene **8**:2839-2845.

48. **Franchini, G., I.J. Mulloy, A. Koralnik, N. Nonico, J.J. Sparkowski, T. Andresson, D.J. Goldstein and R. Schlegel.** 1993. The human T-cell leukemia/lymphotropic virus type I p12^{I} protein cooperates with E5 oncoprotein of bovine papillomavirus in cell transformation and binds the 16 kilodalton subunit of the vacuolar H^+ ATPase. J.Virol. **67**:7701-7704.

49. **Franklin, A.A., M.F. Kubik, M.N. Uittenbogaard, A. Brauweiler, P. Utaisincharoen, M-A.H. Mattews, W.S. Dynan, J.P. Hoeffler and J.K. Nyborg.** 1993. Transactivation by the human T-cell leukemia virus Tax protein is mediated through enhanced binding of activating transcription factor-2 (ATF-2) ATF-2 response and cAMP element-binding protein (CREB). J.Biol.Chem. **268**:21225-21231.

50. **Fujii, M., H. Tsuchiya, T. Chuhjo, T. Akizawa and M. Seiki.** 1992. Interaction of HTLV-1 Tax1 with $p67^{SRF}$ causes the aberrant induction of cellular immediate early genes through CArG boxes. Genes and Devel. **6**:2066-2076.

51. **Fujisawa, J-I., M. Toita, T. Yoshimura and M. Yoshida.** 1991. The indirect association of human T-cell leukemia virus *tax* protein with DNA results in transcriptional activation. J.Virol. **65**:4525-4528.

52. **Garcia-Bustos, J., J. Heitmann and M.N. Hall.** 1991. Nuclear protein localization. Biochim.Biophys.Acta. **1071**:83-101.

53. **Geisler, R., A. Bergmann, Y. Hiromi and C. Nüsslein-Volhard.** 1992. *cactus*, a gene involved in dorsoventral pattern formation of Drosophila, is related to the IκB gene family of vertebrates. Cell **71**:613-621.

54. **Gessain, A., F. Barin, J.C. Vernant, O. Gout, L. Maurs, A. Calender and G. de The.** 1985. Antibodies to human t-lymphotropic virus type-I in patients with tropical spastic paraparesis. Lancet **2**:407-410.

55. **Gessain, A., O. Gout, F. Saal, M.T. Daniel, B. Rio, G. Flandrin, F. Sigaux, O. Lyon-Caen, J. Peries and G. de-The.** 1990. Epidemiology and immunovirology of human T-cell leukemia/lymphoma virus type I-associated adult T-cell leukemia and chronic myelopathies as seen in France. Cancer Res **50 (Supp. 17)**:5692-5696.

56. **Giam, C-Z. and Y-L. Xu.** 1989. HTLV-I *Tax* gene product activates transcription via pre-existing cellular factors and cAMP responsive element. J.Biol.Chem. **264**:15236-15241.

57. **Giebler, H.A., J.E. Loring, K. VanOrden, M.A. Colgin, J. Garrus, K. Escudero, A. Brauweiler and J.K. Nyborg.** 1997. Anchoring of CREB binding protein to the HTLV-1 promoter: a molecular mechanism of Tax transactivation. Mol.Cell.Biol. **17**:5156-5164.

58. **Gill, P., W. Harrington, M. Kaplan and et al..** 1995. Treatment of adult T-cell leukemin-lymphoma with a combination of interferon alpha and zidovudine. N.Eng.J.Med. **332**:1744-1748.

59. **Gilmore, T. and P. Morin.** 1993. The IκB proteins: members of a multifunctional family. Trends Genet. **9**:427-433.

60. **Gilmore, T.D. and H.M. Temin.** 1986. Different localization of the product of the v-*rel* oncogene in chicken fibroblasts and speen cells correlates with transformation by REV-T. Cell **44**:791-800.

61. **Gilmore, T.D. and H.M. Temin.** 1988. V-rel oncoproteins in the nucleus and in the cytoplasm transform chicken spleen cells. J.Virol. **62**:703-714.

62. **Giovanni, P., S. Wagner and M.R. Green.** 1995. Recognition of bZIP proteins by the human T-cell leukemia virus transactivator Tax. Nature **376**:602-605.

63. **Gitlin, S.D., P.F. Lindholm, S.J. Marriott and J.N. Brady.** 1991. Transdominant human T-cell lymphotropic virus type I *Tax*$_1$ mutant that fails to localize to the nucleus. J.Virol. **65**:2612-2621.

64. **Goren, I., O.J. Semmes, K-H Jeang and K. Moelling.** 1995. The amino terminus of Tax is required for Interaction with the cyclic AMP response element binding protein. J.Virol. **69**:5806-5811.

65. **Green, P.L., M.T. Yip, Y. Xie and I.S. Chen.** 1992. Phosphorylation regulation RNA binding by the human T cell leukemia virus Rex protein. J.Virol. **66**:4325-4350.

66. **Grilli, M., J.J.-S. Chiu and M.J. Lenardo.** 1993. NF-κB and Rel: participants in a multiform transcriptional regulatory system. Int.Rev.Cytol. **143**:1-62.

67. **Grimm, S. and P. Baeuerle.** 1993. The inducible transcription factor NF-κB: structure-function relationship of its protein subunits. Biochem.J. **290**:297-308.

68. **Grossman, W.J., J.T. Kimata, F-H. Wong, M. Zutter and T.J. Ley.** 1995. Development of leukemia in mice transgenic for the tax gene of human T-cell leukemia virus type I. Proc.Natl.Acad.Sci.USA **92**:1057-1061.

69. **Hanchard, B.** 1987. Aspects of human T-cell lymphotrophic virus type 1-associated diseases in Jamaica [editorial]. W.Ind.Med.J. **36**:129-130.

70. **Hannink, M. and H.M. Temin.** 1990. Structure and autoregulation of the *c-rel* promoter. Oncogene **5**:1843-1850.

71. **Haskill, S., A.A. Beg, S.M. Tompkins, J.S. Morris, A.D. Yurochko, A. Sampson-Johannes, K. Mondal, P. Ralph and A.S. Baldwin,Jr..** 1991. Characterization of an immediate-early gene induced in adherent monocytes that encodes IκB-like activity. Cell **65**:1281-1289.

72. **Hatada, E.N., M. Naumann and C. Scheidereit.** 1993. Common structural constituents confer IκB activity to NF-κB p105 and IκB/MAD-3. EMBO J. **12**:2781-2788.

73. **Henkel, T., T. Machleidt, I. Alkalay, M. Kronke, Y. Ben-Neriah and P.A. Baeuerle.** 1993. Rapid proteolysis of IκB-α is neccessary for activation of transcription factor NF-κB. Nature **365**:182-185.

74. **Hermine, O., D. Bouscary, A. Gessain, P. Turlure, V. Leblond, N. Franck, A. Buzyn-Veil, B. Rio, E. Macintyre, F. Dreyfus and et al..** 1995. Treatment of HTLV-I

associated adult T-cell leukemia-lymphoma with a combinationof zidovudine and alpha-interpheron. N.Eng.J.Med. **332**:1749-1751.

75. **Hin, S.** 1990. Maternal-Infant transmission of HTLV-I: implication for disease in: Blattner W.A. ed. Human retrovirology HTLV. Raven Press 363-375.

76. **Hirai, H., J-I. Fujisawa, K. Suzuki, K. Ueda, M. Muramutsu, A. Tsuboi, N. Arai and M. Yoshida.** 1992. Transcriptional activator Tax of HTLV-1 binds to the NF-κB precursor p105. Oncogene **7**:1737-1742.

77. **Hirai, H., T. Suzuki, J.-I. Fujisawa, J.-I. Inoue and M. Yoshida.** 1994. Tax protein of human T-cell leukemia virus type I binds to the ankyrin motifs of inhibitory factor κB and induces nuclear translocation of transcription factor NF-κB proteins for transcriptional activtion. Proc.Natl.Acad.Sci.USA **91**:3584-3588.

78. **Hiscott, J., L. Petropoulos and J. Lacoste.** 1995. Molecular interections between HTLV-1 Tax protein and the NF-κB/IκB transcription complex. Virol. **214**:3-11.

79. **Hollsberg, P., K.W. Wucherpfenning, L.J. Ausubel, V. Calvo, B.E. Bierer and D.A. Hafler.** 1992. Characterization of HTLV-I in vivo infected T cell clones. IL-2-independent growth of nontransformed T cells. J.Immunol. **148**:3256-3263.

80. **Inose, M., I. Higuchi, K. Yoshimine, M. Suehara, S. Izumo, K. Arimura and M. Osame.** 1998. Pathological changes in skeletal muscle in HTLV-I associated myelopathy. J.Neurol.Sc. **110**:73-78.

81. **Inoue, J.I., L.D. Kerr, A. Kakizuka and I. Verma.** 1992. IκBγ, a 70 kd protein identical to the C-terminal half of p110 NF-κB: a new member of the IκB family. Cell **68**:1109-1120.

82. **Jariel-Encontre, I., M. Pariat, F. Martin, S. Carillo, C. Salvat and M. Peichaczyk.** 1995. Ubiquitinylation is not an absolute requirement for degradation of c-Jun by the 26S proteasome. J.Biol.Chem. **270**:11623-11627.

83. **Kamada, N., M. Sakurai, K. Miyamoto, I. Sanada, N. Sadomori, S. Fukuhara, S. Abe, Y. Shiraishi, T. Abe, Y. Kaneko and et al..** 1992. Chromosome abnormalities in adult T-cell leukemia/lymnphoma: a karyotype review committee report. Cancer Res **52**:1481-1493.

84. **Kanamori, H., N. Suzuki, H. Siomi, T. Nosaka, A. Sato, H. Sabe, M. Hatanaka and T. Honjo.** 1990. HTLV-1 $p27^{rex}$ stabilizes human interleukin-2 receptor α chain mRNA. EMBO J. **9**:4161-4166.

85. **Kanno, T., K. Brown, G. Franzoso and U. Siebenlist.** 1994. Kinetic analysis of human T-cell leukemia virus type I tax-mediated activation of NF-κB. Mol.Cell.Biol. **14**:6443-6451.

86. **Kanno, T., K. Brown and U. Siebenlist.** 1995. Evidence in support of a role for human T-cell leukemia virus type I Tax in activating NF-κB via stimulation of signaling pathways. J.Biol.Chem. **270**:11745-11748.

87. **Kanno, T., G. Franzoso and U. Siebenlist.** 1994. Human T-cell leukemia virus type I Tax-protein-mediated activation of NF-κB from p100 (NF-κB2)-inhibited cytoplasmic reservoirs. Proc.Natl.Acad.Sci.USA **91**:12634-12638.

88. **Kitajima, I., T. Shinohara, J. Bilakovics, D.A. Brown, X. Xu and M. Nerenberg.** 1992. Ablation of transplanted HTLV-I Tax-transformed tumors in mice by antisense inhibition of NF-κB. Science **258**:1792-1795.

89. **Kobayashi, N., H. Konishi, H. Sabe, K. Shegesada, T. Noma, T. Honjo and M. Hatanaka.** 1984. Genomic structure of HTLV (human T-cell leukemia virus): detection of defective genome and its amplification in MT-2 cells. EMBO J. **3**:1339-1343.

90. **Krappmann, D., F.G. Wulczyn and C. Scheidereit.** 1996. Different mechanisms control signal-induced degradation and basal turnover of the NF-κB inhibitor IκBα *in vivo*. EMBO J. **15**:6716-6726.

91. **Kroll, M., M. Conconi, M.J.P. Desterro, A. Marin, D. Thomas, B. Friguet, R.T. Hay, J-L. Virelizier, F. Arenzana-Seisdedos and M.S. Rodriguez.** 1997. The carboxy-terminus of IκBα determines susceptibility to degradation by the catalytic core of the proteasome. Oncogene **15**:1841-1850.

92. **Kumar, S. and C. Gélinas.** 1993. IκBα-mediated inhibition of v-rel DNA binding requires direct interaction with the RXXRXRXXC Rel/κB DNA-binding motif. Proc.Natl.Acad.Sci.USA **90**:8962-8966.

93. **Kwok, R.P.S., M.E. Laurance, R.J. Lundblad, P.S. Goldman, H-M. Shih, L.M. Connor, S.J. Marriott and R.H. Goodman.** 1996. Control of cAMP-regulated enhancers by the viral transactivator Tax through CREB and the co-activator CBP. Nature **380**:642-646.

94. **Lacoste, J., L. Cohen and J. Hiscott.** 1991. NF-κB activity in T cells stably expressing the Tax protein of HTLV-1. Virol. **184**:553-562.

95. **Lacoste, J., J. Lanoix, N. Pépin and J. Hiscott.** 1994. Interactions between HTLV-I Tax and NF-κB/Rel proteins in T cells. Leukemia **8**:S71-S76.

96. **Lacoste, J., L. Petropoulos, N. Pepin and J. Hiscott.** 1995. Constitutive phosphorylation and turnover of IκBα in human T-cell leukemia virus type I-infected and Tax-expressing T cells. J.Virol. **69**:564-569.

97. **Lan, N.C., M. Karin, T. Nguyen, A. Weisz, M.J. Birnbaum, N.L. Eberhardt and J.D. Baxter.** 1984. Mechanisms of glucocorticoid hormone action. J.Steroid.Biochem. **20**:77-88.

98. **Lanoix, J., J. Lacoste, N. Pepin, N.R. Rice and J. Hiscott.** 1994. Overproduction of NFKB2 (*lyt-10*) and c-Rel: a mechanism for HTLV-1 Tax-mediated *trans*-activation via the NF-κB signalling pathway. Oncogene **9**:841-852.

99. **Le Bail, O., R. Schmidt-Ullrich and A. Israël.** 1993. Promoter analysis of the gene encoding the IκB-α/MAD 3 inhibitor of NF-κB: positive regulation by members of the rel/NF-κB family. EMBO J. **12**:5043-5049.

100. **Lee, R., P. Beauparlant, H. Elford, P. Ponka and J. Hiscott.** 1997. Selective inhibition of IκBα phosphorylation and HIV LTR directed gene expression by novel antioxidant compounds. Virol. **234**:277-290.

101. **Lemasson, I., V. Robert-Hebmann, S. Hamaia, M. Duc Dodon, L.. Gazzolo and C. Devaux.** 1997. Transrepression of lck gene expression by human T cell leukemia virus type 1 encoded $p40^{tax}$. J.Virol. **71**:1975-1983.

102. **Leon-Monzon, M., I. IIIa and M.C. Dalakas.** 1994. Polymyositis in patients infected with human T-cell leukemia virus type I: the role of the virus in the cause of the disease. Annals of Neurology **36**:643-649.

103. **Li, C.-C.H., F.W. Ruscetti, N.R. Rice, E. Chen, N.-S. Yang, J. Mikovits and D.L. Longo.** 1993. Differential expression of rel family members in Human T-cell leukemia virus type I-infected cells: transcriptional activation of *c-rel* by Tax protein. J.Virol. **67**:4205-4213.

104. **Lin, L., G.N. DeMartino and W.C. Greene.** 1998. Cotranslational biogenesis of NF-kappaB p50 by the 26S proteasome. Cell **92**:819-828.

105. **Lin, R., P. Beauparlant, C. Makris, S. Meloche and J. Hiscott.** 1996. Phosphorylation of IκBα in the C-terminal PEST domain by casein kinase II affects intrinsic protein stability. Mol.Cell.Biol. **16**:1401-1409.

106. **Lin, R., D. Gewert and J. Hiscott.** 1995. Differential transcriptional activation *in vitro* by NF-κB/Rel proteins. J.Biol.Chem. **270**:3123-3131.

107. **Lin, R., A. Mustafa, H. Nguyen and J. Hiscott.** 1994. Mutational analysis of interferon (IFN) regulatory factors 1 and 2: Effects on the induction of IFN-β gene expression. J.Biol.Chem. **269**:17542-17549.

108. **Lin, Y.-C., K. Brown and U. Siebenlist.** 1995. Activation of NF-κB requires proteolysis of the inhibitor IκB-α: signal-induced phosphorylation of IκB-α alone does not release active NF-κB. Proc.Natl.Acad.Sci.USA **92**:552-556.

109. **Lindholm, P.F., S.J. Marriott, S.D. Gitlin, C.A. Bohan and J.N. Brady.** 1990. Induction of nuclear NF-κB DNA binding activity after exposure of lymphoid cells to soluble tax_1 protein. New Biol. **2**:1034-1043.

110. **Low, K.G., L.F. Dorner, D.B. Fernando, J. Grossman, K.-T. Jeang and M.J. Comb.** 1997. Human T-cell leukemia virus type 1 Tax releases cell cycle arrest induced by $p16^{INK4a}$. J.Virol. **71**:1956-1962.

111. **Lu, D., J.D. Thompson, G.K. Gorski, N.R. Rice, M.G. Mayer and J.J. Yunis.** 1991. Alterations at the *rel* locus in human lymphoma. Oncogene **6**:1235-1241.

112. **Lux, S.E., K.M. John and V. Bennett.** 1990. Analysis of cDNA for human erythrocyte ankyrin indicates a repeated structure with homology to tissue-differentiation and cell-cycle control proteins. Nature **344**:36-42.

113. **Maggirwar, S.B., E. Harhaj and S.C. Sun.** 1995. Activation of NF-κB/Rel by Tax involves degradation of IκBα and is blocked by a proteasome inhibitor. Oncogene **11**:993-998.

114. **Marriot, S.J., D. Trinh and J.N. Brady.** 1992. Activation of interleukin-2 receptor alpha expression by extracellular HTLV-I Tax1 protein: a potential role in HTLV-I pahogenesis. Oncogene **7**:1749-1755.

115. **Marriott, S.J., D. Trinh and J.N Brady.** 1992. Activation of interleukin-2 receptor alpha expression by extracellular HTLV-I Tax$_1$ protein: a potential role in HTLV-I pathogenesis. Oncogene **7**:1749-1755.

116. **Matsumoto, K., H. Shibata, J-I. Fujisawa, H. Inoue, A. Hakura, T. Tsukahara and F. Masahiro.** 1997. Human T cell leukemia virus type i tax protein transforms rat fibroblasts via two distince pathways. J.Virol. **71**:4445-4451.

117. **Mercurio, F., H. Zhu, B.W. Murray, A. Shevchenko, B.L. Bennett, J.W. Li, D.B. Young, M. Barbosa and M. Mann.** 1997. IKK-1 and IKK-2: cytokine-activated IκB kinases essential for NF-κB activation. Science **278**:860-866.

118. **Miyamoto, S., P.J. Chiao and I.M. Verma.** 1994. Enhanced IκBα degradation is responsible for constitutive NF-κB activity in mature murine B-cell lines. Mol.Cell Biol. **14**:3276-3282.

119. **Miyoshi, I., I. Kubonishi, S. Yoshimoto and Y. Shiraishi.** 1991. A T-cell line derived from normal human cord leukocytes by co-culturing with human leukemic T-cells. Gann. **72**:978-981.

120. **Mori, N., F. Kashanchi and D. Prager.** 1997. Repression of transcription from the human T-cell leukemia virus type I long terminal repeat and cellular gene promoters by wild-type p53. Blood **90**:4924-4932.

121. **Morin, P.J. and T.D. Gilmore.** 1992. The c-terminus of the NF-κB p50 precursor and an IκB isoform contain transcription activation domains. Nucl Acid Res **20**:2453-2455.

122. **Muchinik, G., N. Chamoles, I. Zapiola, A. Schenone, M.B. Bouzos, D. Gallo and C. Hanson.** 1993. HTLV-I/HTLV-II and multiple sclerosis in Buenos Aires. J.Acquir.Immune Defic.Syndr. **6**:326-327.

123. **Muller, C.W., F.A. Rey, M. Sodeoka, G.L. Verdine and S.C. Harrison.** 1995. Structure of the NF-κB p50 homodimer bound to DNA. Nature **373**:311-317.

124. **Murakami, T., H. Hirai, T. Suzuki, J-I. Fujisawa and M. Yoshida.** 1995. HTLV-I Tax enhances NF-κB2 expression and binds to the products p52 and p100, but does not suppress the inhibitory function of p100. Virol. **206**:1066-1074.

125. **Murphy, E.L., J.P. Figueroa, W.N. Gibbs, A. Brathwaite, M. Holding-Cobham, D. Waters, B. Cranston, B. Hanchard and W.A. Blattner.** 1989. Sexual transmission of human T-lymphotropic virus type I (HTLV-I). Ann.Int.Med. **111**:555-560.

126. **Nerenberg, M., S.H. Hinrichs, R.K. Reynolds, G. Khoury and G. Jay.** 1987. The *tat* gene of human T-lymphotropic virus type I induces mesenchymol tumors in transgenic mice. Science **237**:1324-1329.

127. **Neri, A., C.-C. Chang, L. Lombardi, M. Salina, P. Corradini, A.T. Maiolo, R.S.K. Chaganti and R. Dalla-Favera.** 1991. B cell lymphoma-associated chromosomal translocation involves candidate oncogene *lyt*-10, homologous to NF-κB p50. Cell **67**:1075-1087.

128. **Newbound, G.C., J.M. Andrews, J.P. O'Rouke, J.N. Brady and M.D. Lairmore.** 1996. Human T cell lymphotropic virus typel tax mediates enhanced transcription in $CD4^+$ T lymphocytes. J.Virol. **70**:2101-2106.

129. **Newman, G.W., T.G. Kelley, H. Gan, O. Kandil, M.J. Newman, P. Pinkston, R.M. Rose and H.G. Remold.** 1993. Concurrent infection of human macrophages with HIV-1 and *Mycobacterium avium* results in decreased cell viability, increased *M. avium* multiplication and altered cytokine production. J.Immunol. **151**:2261-2272.

130. **Nguyen, H., J. Hiscott and P.M. Pitha.** 1997. The growing family of IRF transcription factors. Cyt.Growth Fact.Rev. **8**:293-312.

131. **Nolan, G.P., S. Ghosh, H.-C. Liou, P. Tempst and D. Baltimore.** 1991. DNA binding and IκB inhibition of the cloned p65 subunit of NF-κB, a *rel*-related polypeptide. Cell **64**:961-969.

132. **Ohno, H., G. Takimoto and T.W. McKeithan.** 1990. The candidate proto-oncogene *bcl*-3 is related to genes implicated in cell lineage determination and cell-cycle control. Cell **60**:991-997.

133. **Okada, K., Y. Koyanagi, N. Kobayashi, Y. Tanaka, M. Nakai, K. Sano, K. Takeuchi, Y. Hinuma, M. Hatanaka and N. Yamamoto.** 1984. In vitro infection of human B lymphocytes with adult T-cell leukemia virus. Cancer lett **22**:11-21.

134. **Osame, M., K. Osuku, S. Izumo, N. Ijichi, H. Amitani, A. Igata, M. Matsumoto and M. Tara.** 1986. HTLV-I associated myelopathy: a new clinical entity. Lancet **1**:1031-1032.

135. **Osame, M., K. Usuku, S. Izumo, N. Ijichi, H. Amitani, A. Igata, M. Matsumoto and M. Tara.** 1986. HTLV-I associated myelopathy, a new clinical entity [letter]. Lancet **1**:1031-1032.

136. **Pepin, N., A. Roulston, J. Lacoste, R. Lin and J. Hiscott.** 1994. Subcellular redistribution of HTLV-1-Tax protein by NF-κB/Rel transcription factors. Virol. **204**:706-716.

137. **Perkel, J.M. and M.L. Atchison.** 1998. A two-step mechanism for recruitment of Pip by PU.1. J.Immunol. **160**:241-252.

138. **Perkins, N.D., R.M. Schmid, C.S. Duckett, K. Leung, N.R. Rice and G.J. Nabel.** 1992. Distinct combinations of NF-κB subunits determine the specificity of transcriptional activation. Proc.Natl.Acad.Sci.USA **89**:1529-1533.

139. **Petropoulos, L., R. Lin and J. Hiscott.** 1996. Human T cell leukemia virus type 1 Tax protein increases NF-κB dimer formation and antagonizes the inhibitory activity of the IκBα regulatory protein. Virol. **225**:52-64.

140. **Pique, C., F. Connan, J-P. Levilain, J. Chopin and M-C. Dokhelar.** 1996. Among all human T cell leukemia virus type 1 proteins, tax, polymerase, and envelope proteins are predicted as preferential targets for the HLA-A2-restricted cytotoxic T cell response. J.Virol. **70**:4919-4926.

141. **Pise-Masison, C.A., K.S. Choi, M. Radonovich, J. Dittmer, S.J. Kim and J.N. Brady.** 1998. Inhibition of p53 transactivation function by the human T cell lymphotropic virus type 1 Tax protein. J.Virol. **72**:1165-1170.

142. **Poiez, B.F., F.W. Ruscetti, P.A. Gazadar, P.A. Bunn, J.D. Minna and R.C. Gallo.** 1980. Detection and isolation of type C retrovirus particles from fresh cultured lymphocytes of a patient with cutaneous T-cell lymphoma. Proc.Natl.Acad.Sci.USA **77**:7415-7419.

143. **Rechsteiner, M. and S.W. Rogers.** 1996. PEST sequences and regulation by proteolysis. Trends Biochem.Sc. **21**:267-271.

144. **Richardson, J.H., A.J. Edwards, J.K. Cruickshank, P. Rudge and A.G. Dalgleish.** 1990. In vivo cellular tropism of human T-cell leukemia virus type I. J.Virol. **64**:5682-5687.

145. **Rodriguez, M.S., I. Michalopoulos, F. Arenzana-Seisdedos and R.T. Hay.** 1995. Inducible degradation of IκBα *in vitro* and *in vivo* requires the acidic C-terminal domain of the protein. Mol.Cell.Biol. **15**:2413-2419.

146. **Roulston, A., R. Lin, P. Beauparlant, M.A. Wainberg and J. Hiscott.** 1995. Regulation of HIV-1 and cytokine gene expression in myeloid cells by NF-κB/Rel transcription factors. Microbiol.Rev. **59**:481-505.

147. **Rousset, R., C. Desbois, F. Bantignies and P. Jalinot.** 1996. Effects on NF-κB1/p105 processing of the interaction between the HTLV-1 transactivator Tax and the proteasome. Nature **381**:328-331.

148. **Sachdev, S., A. Hoffmann and M. Hannink.** 1998. Nuclear localization of IκBα is mediated by the second ankyrin repeat: the IκBα ankyrin repeats define a novel class of cis-acting nuclear import sequences. Mol.Cell.Biol. **18**:2524-2534.

149. **Sakashita, A., T. Hattori, C.W. Miller, H. Suzushima, N. Asou, K. Takatsuki and H.P. Koeffler.** 1992. Mutations of the p53 gene in adult T-cell leukemia. Blood **79**:477-480.

150. **Sakurai, H., N. Kondo, C. Mikuni, H. Ikeda, A. Wakisaka and T. Yoshiki.** 1992. Molecular analysis of HTLV-IpX defective human adult T-cell leukemia. Leukemia Research **16**:941-946.

151. **Salahuddin, S.Z., R.M. Rose, J.E. Groopman, P.D. Markham and R.C. Gallo.** 1986. Human T-lymphotrophic virus type III infection of human alveolar macrophages. Blood **68**:281-284.

152. **Sanada, I., R. Tanaka, E. Kumagai, H. Tsuda, H. Nishimura, K. Yamaguchi, F. Kawano, H. Fujiwara and K. Takatsuki.** 1985. Chromosomal aberrations in adult T-cell leukemia: relationship to the clinical severity. Blood **65**:649-654.

153. **Scherer, D.C., J.A. Brockman, Z. Chen, T. Maniatis and D.W. Ballard.** 1995. Signal-induced degradation of IκBα requires site-specific ubiquitination. Proc.Natl.Acad.Sci.USA **92**:11259-11263.

154. **Schmid, R.M., N.D. Perkins, C.S. Duckett, P.C. Andrews and G.J. Nabel.** 1991. Cloning of an NF-κB subunit which stimulates HIV transcription in synergy with p65. Nature **352**:733-736.

155. **Schreck, R., P. Rieber and P.A. Baeuerle.** 1991. Reactive oxygen intermediates as apparently widely used messengers in the activation of the NF-kappa B transcription factor and HIV-1. EMBO J. **10**:2247-2258.

156. **Scott, E.W., M.C. Simon, J. Anastasi and H. Singh.** 1994. Requirement of transcription factor PU.1 in the development of multiple hematopoietic lineages. Science **265**:1573-1575.

157. **Semmes, O.J. and K-T. Jeang.** 1995. Definition of a Minimal Activation Domain in Human T-Cell Leukemia Virus Type I Tax. J.Virol. **69(3)**:1827-1833.

158. **Semmes, O.J. and K.-T. Jeang.** 1992. Mutational analysis of human T-cell leukemia virus type I Tax: regions necessary for function determined with 47 mutant proteins. J.Virol. **66**:7183-7192.

159. **Shimoyama, M.** 1991. Diagonostic criteria and classification of clinical subtypes of adult T-cell leukemia-lymphoma. A report from the Lymphoma Study Group (1984-87). Br.J.Haematol. **79**:428-437.

160. **Smith, M.R. and W.C. Greene.** 1990. Identification of HTLV-I *tax trans*-activator mutants exhibiting novel transcriptional phenotypes. Genes and Devel. **4**:1875-1885.

161. **Sodroski, J.** 1992. The human T-cell leukemia virus (HTLV) transactivator (Tax) protein. Biochim.Biophys.Acta. **1114**:19-29.

162. **Sonoda, S., T. Fujiyoshi and S. Yashiki.** 1996. . J.Acquir.Immune Defic.Syndr. **13(suppl. 1)**:119-123.

163. **Sonoda, S., S. Yashiki, T. Fujiyoshi and et al..** 1992. Immunogenetic factors involved in the pathogenesis of adult T-cell leukemia and HTLV-I associated myelopathy. Gann. **39**:81-93.

164. **Sun, S-C., J. Elwood, C. Beraud and W.C. Greene.** 1994. Human T-cell leukemia virus type I Tax activation of NF-κB/Rel involves phosphorylation and degradation of IκBα and RelA(p65)-mediated induction of the *c-rel* gene. Mol.Cell Biol. **14**:7377-7384.

165. **Sun, S.-C, J. Elwood and W.C. Greene.** 1996. Both amino- and carboxyl-terminal sequences within IκBα regulate its inducible degradation. Mol.Cell Biol. **16**:1058-1065.

166. **Sun, S.-C., P.A. Ganchi, D.W. Ballard and W.C. Greene.** 1993. NF-κB controls expression of inhibitor IκBα: evidence for an inducible autoregulatory pathway. Science **259**:1912-1915.

167. **Sun, S.-C., P.A. Ganchi, C. Béraud, D.W. Ballard and W.C. Greene.** 1994. Autoregulation of the NF-κB transactivator RelA (p65) by multiple cytoplasmic inhibitors containing ankyrin motifs. Proc.Natl.Acad.Sci.USA **91**:1346-1350.

168. **Suzuki, T., J-I. Fujisawa, M. Toita and M. Yoshida.** 1993. The trans-activator Tax of human T-cell leukemia virus type 1 (HTLV-1) interacts with cAMP-responsive element (CRE) binding and CRE modulator proteins that bind to the 21-base-pair enhancer of HTLV-1. Proc.Natl.Acad.Sci. **90**:610-614.

169. **Suzuki, T., H. Hirai, J-I. Fujisawa, T. Fujita and M. Yoshida.** 1993. A trans-activator Tax of human T-cell leukemia virus type 1 binds to NF-κB p50 and serum response factor (SRF) and associates with enhancer DNAs of the NF-κB site and CArG box. Oncogene **8**:2391-2397.

170. **Suzuki, T., H. Hirai, T. Murakami and M. Yoshida.** 1995. Tax protein of HTLV-I destabilizes the complexes of NF-κB and IκBα and induces nuclear translocation of NF-κB for transcriptional activation. Oncogene **10**:1199-1207.

171. **Suzuki, T., H. Hirai and M. Yoshida.** 1994. Tax protein of HTLV-I interacts with the Rel homology domain of NF-κB binding p65 and c-Rel proteins bound to the NF-κB binding site and activates transcription. Oncogene **9**:3099-3105.

172. **Suzuki, T., S. Kiato, H. Matsushime and M. Yoshida.** 1996. HTLV-1 tax protein interacts with cyclin-dependent kinase inhibitor p16INK4A and counteracts its inhibitory activity towards CDK4. EMBO J. **15**:1607-1614.

173. **Tanaka, A., C. Takahashi, S. Yamaoka, T. Nosaka, M. Maki and M. Hatanaka.** 1990. Oncogenic transformation by the *tax* gene of human T-cell leukemia virus type I *in vitro*. Proc.Natl.Acad.Sci. **87**:1071-1075.

174. **Ten, R.M., C.V. Paya, N. Israël, O. Le Bail, M.-G. Mattel, J.-L. Virelizier, P. Kourilsky and A. Israël.** 1992. The characterization of the promoter of the gene encoding the p50 subunit of NF-κB indicates that it participates in its own regulation. EMBO J. **11**:195-203.

175. **Thompson, J.E., R.J. Phillips, H. Erdjument-Bromage, P. Tempst and S. Ghosh.** 1995. IκB-β regulates the persistent response in a biphasic activation of NF-κB. Cell **80**:573-582.

176. **Tie, F., N. Adaya, W.C. Greene and C-Z. Giam.** 1996. Interaction of the human T-lymphotropic virus type 1 Tax dimer with CREB and the viral 21basepair repeat. J.Virol. **70**:8368-8374.

177. **Toledano, M.B., D. Ghosh, F. Trinh and W.J. Leonard.** 1993. N-terminal DNA-binding domains contribute to differential DNA-binding specificities of NF-κB p50 and p65. Mol.Cell Biol. **13**:852-860.

178. **Traenckner, E.B., H.L. Phal, T. Henkel, N.K. Schmidt, S. Wilk and P.A. Baeuerle.** 1995. Phosphorylation of human IκBα on serines 32 and 36 controls IκBα proteolysis and NF-κB activation in response to diverse stimuli. EMBO J. **14**:2876-2883.

179. **Traenckner, E.B.-M., S. Wilk and P.A. Baeuerle.** 1994. A proteasome inhibitor prevents activation of NF-κB and stabilizes a newly phosphorylated form of IκB-α that is still bound to NF-κB. EMBO J. **13**:5433-5441.

180. **Tsuchiya, H., M. Fujii, Y. Tanaka, H. Tozawa and M. Seiki.** 1994. Two distinct regions form a functional activation domain of the HTLV-1 trans-activator Tax1. Oncogene **9**:337-340.

181. **Uchiyama, T., J. Yodi, K. Sagawa, K. Takatsuki and H. Uchino.** 1977. Adult T cell leukemia: clinical and hematological features of 16 cases. Blood **50**:481-491.

182. **Urban, M.B. and P.A. Baeuerle.** 1990. The 65-kD subunit of NF-κB is a receptor for IκB and a modulator of DNA-binding specificity. Genes and Devel. **4**:1975-1984.

183. **Usuku, K., S. Sonada, M. Osame, S. Yashiki, S. Takahashi, M. Matsumoto, T. Sawada, K. Tsuji, M. Tara and A. Igata.** 1988. HLA haplotype-linked high immune responsiveness agaisnt HTLV-I in HTLV-I associated lymphoma. . Ann.Neurol. **suppl.**:S143-S150.

184. **Wagner, S. and M.R. Green.** 1993. HTLV-I Tax protein stimulation of DNA binding of bZIP proteins by enhancing dimerization. Science **262**:395-399.

185. **Watanabe, M., M. Muramatsu, H. Hirai, T. Suzuki, J-I. Fujisawa, M. Yoshida, K-I. Arai and N. Arai.** 1993. HTLV-I encoded Tax in association with NF-κB precursor p105 enhances nuclear localization of NF-κB p50 and p65 in transfected cells. Oncogene **8**:2949-2958.

186. **Whiteside, S.T., J. Epinat, N.R. Rice and A. Israel.** 1997. I kappa B epsilon, a novel member of the IκB family, controls RelA and cRel NF-κB activity. EMBO J. **16**:1413-1426.

187. **Whiteside, S.T., M.K. Ernst, O. LeBail, C. Laurent-Winter, N. Rice and A. Israel.** 1995. N- and C-terminal sequences control degradation of MAD3/IκBα in response to inducers of NF-κB activity. Mol.Cell Biol. **15**:5339-5345.

188. **Wood, L.D. and A. Richmond.** 1995. Constitutive and cytokine-induced expression of the melanoma growth stimulatory activity/GROα requires both NF-κB and novel constitutive factors. J.Biol.Chem. **270**:30619-30626.

189. **Woronicz, J.D., X. Gao, Z. Cao, M. Rothe and D.V. Goeddel.** 1997. IκB kinase-β: NF-κB activation and complex formation with IκB kinase-α and NIK. Science **278**:866-869.

190. **Wulczyn, F.G., M. Naumann and C. Scheidereit.** 1992. Candidate proto-oncogene *bcl-3* encodes a subunit-specific inhibitor of transcription factor NF-κB. Nature **358**:597-599.

191. **Yamagata, T., J. Nishida, T. Tanaka, R. Sakai, K. Mitani, M. Yoshida, T. Taniguchi, Y. Yazaki and H. Hirai.** 1996. A novel interferon regulatory factor family transcription factor, ICSAT/Pip/LSIRF, that negatively regulates the activity of interferon-regulated genes. Mol.Cell Biol. **16**:1283-1294.

192. **Yamaguchi, K., T. Kiyokawa, K. Nakada, LS. Yul, N. Asou, T. Ishii, I. Sanada, M. Seiki, M. Yoshida, E. Matutes and et al.** 1988. Polyclonal integration of HTLV-I proviral DNA in lymphocytes from HTLV-I seropositive individuals: an intermediate state between the healthy carrier state and smouldering ATL. Br.J.Haematol. **68**:169-174.

193. **Yamaoka, S., H. Inoue, M. Sakurai, T. Sugiyama, M. Hazama, T. Yamada and M. Hatanaka.** 1996. Constitutive activation of NF-κB is essential for transformation of rat fibroblasts by the human T-cell leukemia virus type 1 Tax protein. EMBO J. **15**:873-887.

194. **Yaron, A., H. Gonen, I. Alkalay, A. Hatzubai, S. Jung, S. Beyth, F. Mercurio, A.M. Manning, A. Ciechanover and Y. Ben-Neriah.** 1997. Inhibition of NF-κB cellular function via specific targeting of the IκB-ubiquitin ligase. EMBO J. **21**:6486-6494.

195. **Yin, M-J., L.B. Christerson, Y. Yamamoto, Y-T. Kwak, S. Xu, F. Mercurio, M. Barbosa, M.H. Cobb and R.B. Gaynor.** 1998. HTLV-I Tax protein binds to MEKK1 to stimulate IκB kinase activity and NF-κB activation. Cell **93**:875-884.

196. **Yin, M-J. and R.B. Gaynor.** 1996. Complex formation between CREB and Tax enhances the binding affinity of CREB for the human T-cell leukemia virus type 1 21-base-pair repeats. Mol.Cell Biol. **16**:3156-3168.

197. **Yin, M-J., E. Paulssen, J. Seeler and R.B. Gaynor.** 1995. Chimeric proteins composed of Jun and CREB define domains required for interaction with the human T cell leukemia virus type 1 Tax protein. . J.Virol. **69**:6209-6218.

198. **Yoshida, M.** 1993. HTLV-1 tax: regulation of gene expression and disease. Trends in Microbiology **1**:131-135.

199. **Zandi, E., D.M. Rothwarf, M. Delhase, M. Hayakawa and M. Karin.** 1997. The IkappaB kinase complex (IKK) contains two kinase subunits, IKKalpha and IKKbeta, necessary for IkappaB phosphorylation and NF-kappaB activation. Cell **91**:243-252.

200. **Zhao, L.J. and C.Z. Giam.** 1992. Human T cell lymphotropic virus type 1 (HTLV-1) transcriptional activator, Tax enhances CREB binding to HTLV-1 21 base pair repeats by protein-protein interaction. Proc.Natl.Acad.Sci.USA **89**:7070-7074.